CENTRO POLITÉCNICO SUPERIOR
UNIVERSIDAD DE ZARAGOZA

DESIGN AND MEASUREMENT OF MICROSTRIP PATCH ANTENNAS FOR THEIR USE IN AN ACC (ADAPTIVE CRUISE CONTROL) RADAR SYSTEM FOR AUTOMOBILES

TOMO 2/2 (ANEXOS)

AUTOR: JULIO MODREGO GIL

DIRECTOR: DR. ING. THOMAS BINZER

PONENTE: JESÚS DE MINGO SANZ

DEPARTAMENTO DE INGENIERÍA ELECTRÓNICA Y COMUNICACIONES

INGENIERÍA SUPERIOR DE TELECOMUNICACIONES

ESPECIALIDAD COMUNICACIONES

CURSO 2010-2011

FECHA: 03.04.2011

A mi madre, Rosa,
Por su infinita paciencia.
Nunca te lo agradeceré lo suficiente.

ÍNDICE GENERAL

ÍNDICE DE FIGURAS Y TABLAS

DESCRIPCIÓN **PÁG.**

TABLAS

6. ANEXOS

6.1 ANNEX 1: GRAPHICS

This annex contains all the graphical results mentioned in this Project.

6.1.1 Results of a single rectangular patch

Simulation results obtained with FEKO of the gain (azimuth and elevation) of a single rectangular patch antenna. The *".pre"* FEKO file used to generate this figure is included in 6.2 “ANNEX 2: PROGRAMS AND CODE”, point 6.2.2.

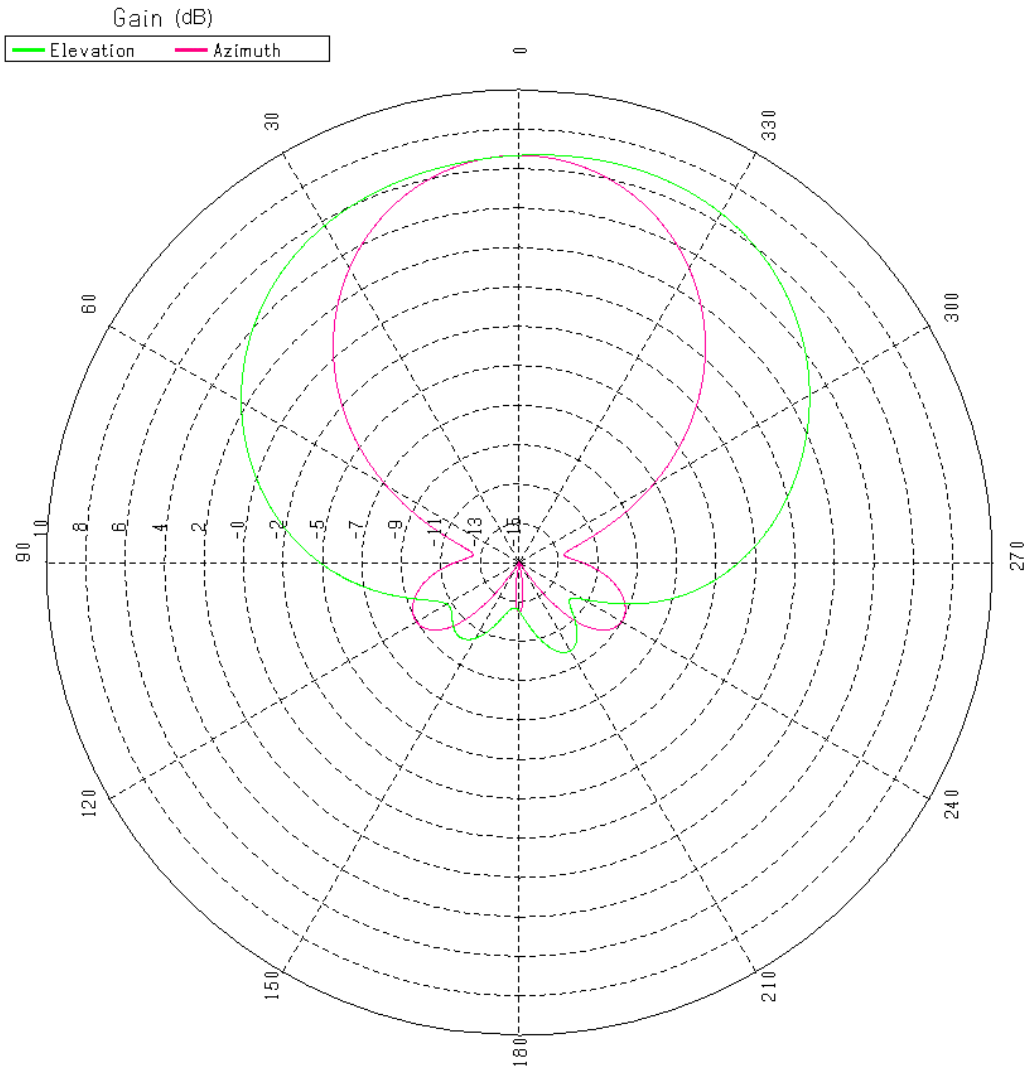

Figura 6-1 Gain (elevation and azimuth) of a single rectangular patch antenna

6.1.2 Theoretical results of the 1x16 array

Simulation results of the 1x16 array obtained with FEKO. The preFEKO file used to define the geometry and the field calculations to be made can be consulted in point 6.2.3 of annex 6.2 “ANNEX 2: PROGRAMS AND CODE”.

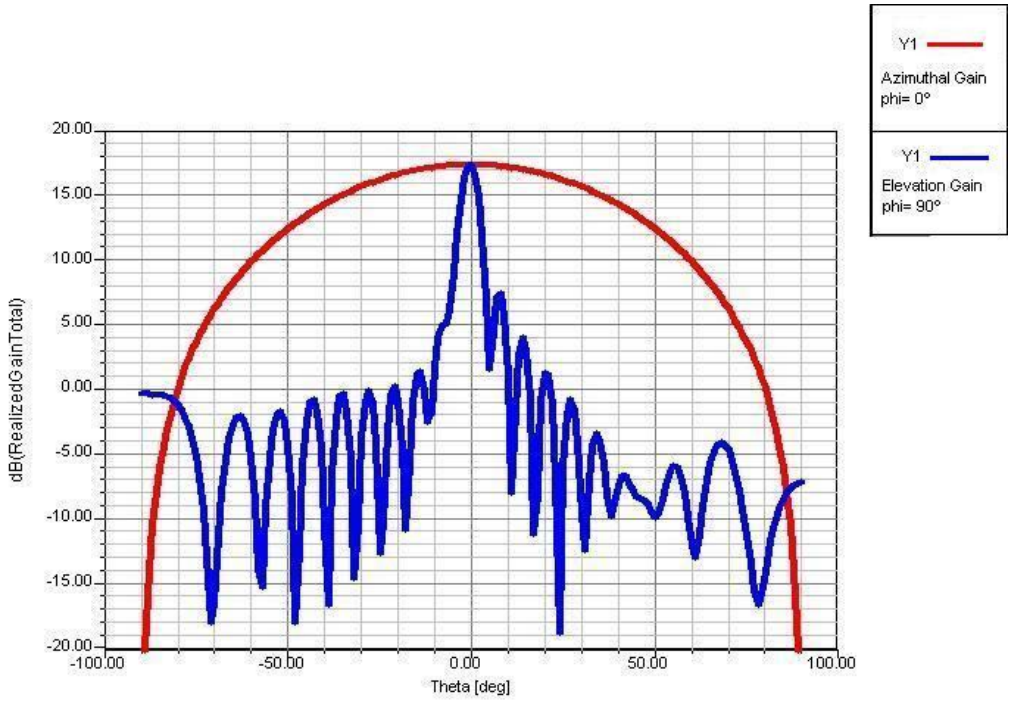

Figura 6-2 Azimuth and Elevation gain of the 1x16 array of rectangular patches over the Y-axe

6.1.3 Experimental results of the 1x16 array

Experimental measures obtained in anechoic chamber for the 1x16 array pattern. These results belong to BOSCH GROUP GmbH internal documentation, so the conditions in which they were made cannot be mentioned here. It's shown only to appreciate the gain pattern of the array at the work frequency of the system (76.5 GHz).

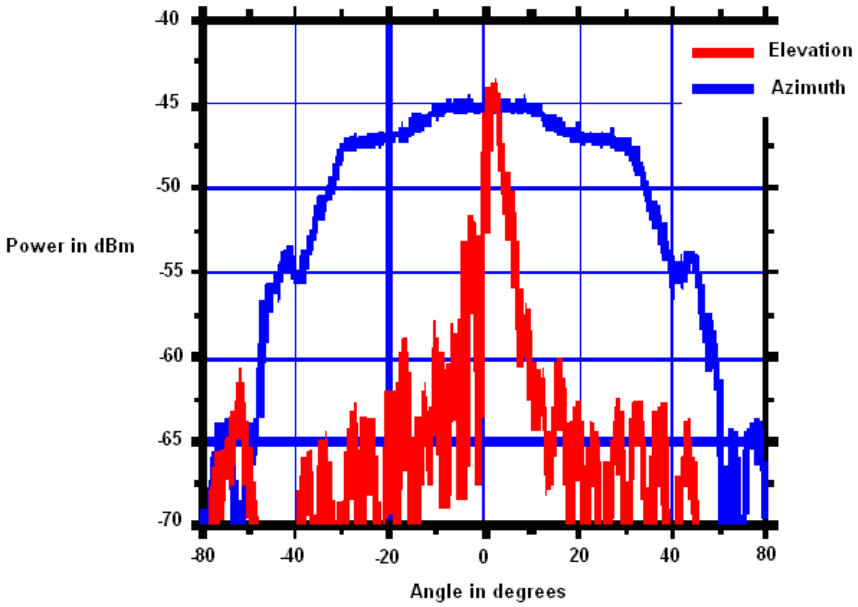

Figura 6-3 Real measured gain (azimuth and elevation) of the 1x16 array

6.1.4 Simulation results of the 20x16 and 24x16 arrays

Simulation measures of the azimuth and elevation gain of the arrays of 20x16 and 24x16 patches. The "*.pre" FEKO files created to obtain these results are included in points 6.2.4 (array 20x16) and 6.2.5 (array 24x16) of the annex 6.2 "ANNEX 2: PROGRAMS AND CODE".

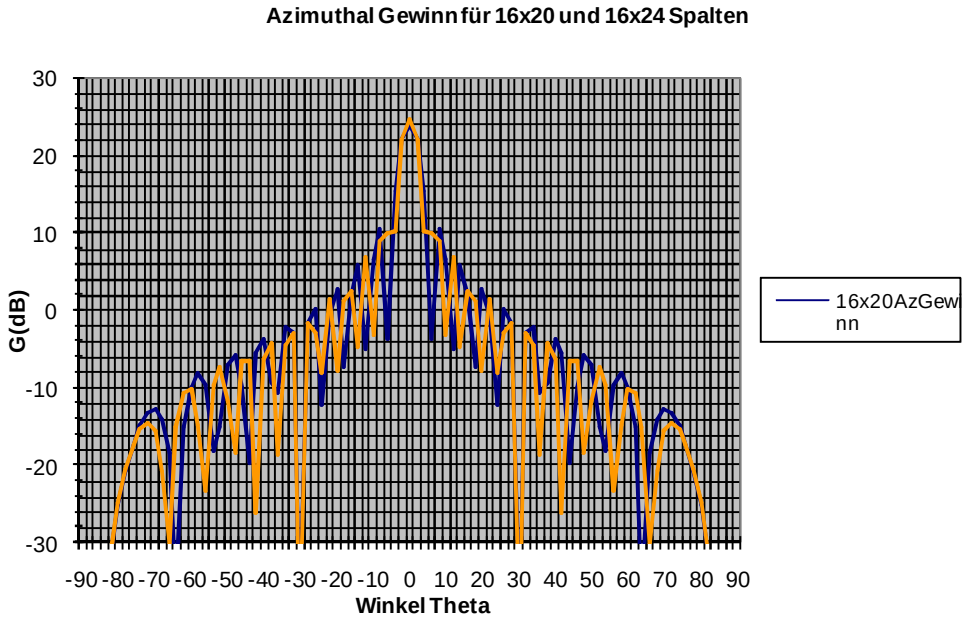

Figura 6-4 Gain in azimuth of the 20x16 and 24x16 arrays

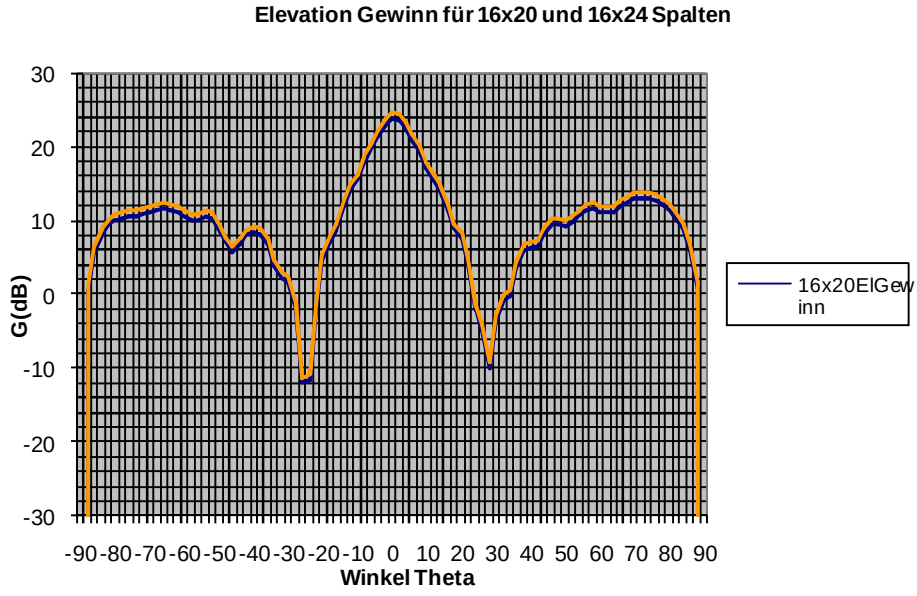

Figura 6-5 Gain in elevation of the 20x16 and 24x16 arrays

6.1.5 Effect of an electromagnetic lens

This point illustrates the effect of an aplanatic lens placed over an antenna. The lens deflects incoming radiation from the antenna, making it converge to a determined focal point. The total effect is a reduction in the diagram of radiation, which becomes narrower.

A more detailed explanation about the subjacent theory of the dielectric lenses can be consulted in reference **[11]** of the Bibliography.

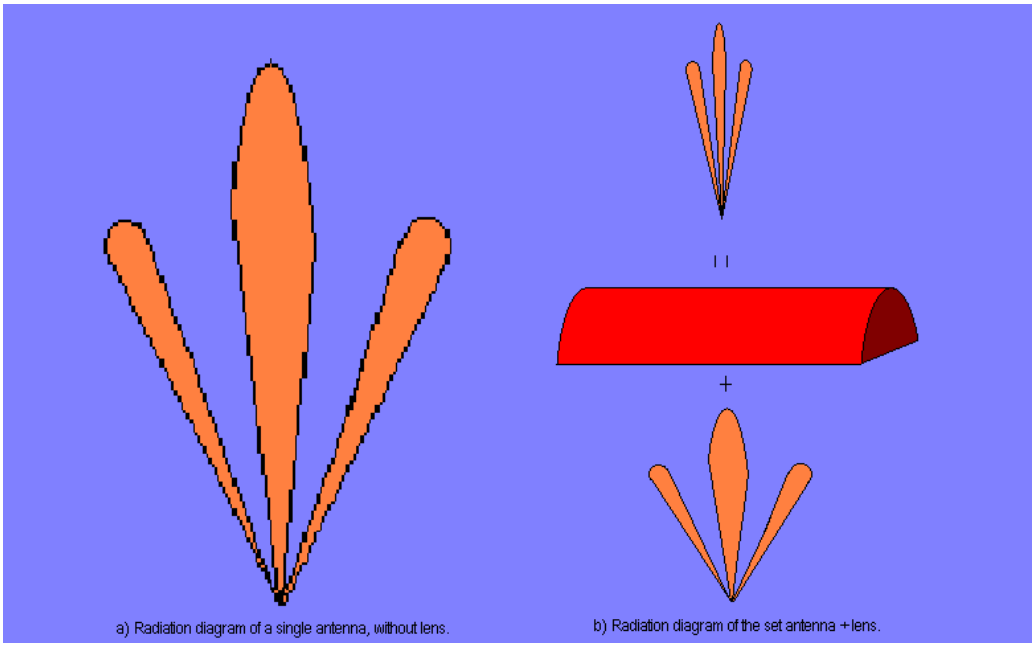

Figura 6-6 Effect of an electromagnetic lens: a) Radiation diagram of an antenna without lens. b) Effect of the lens: The whole radiation of the antenna experiments a compression in angle, not in amplitude

6.1.6 Results of the 1x3 array with uniform power supply

Azimuth and elevation gain reached by the 1x3 array when the three patches are fed with the same amplitude of voltage and phase (Voltages $V_1 = V_2 = V_3 = 1$, and phases $\Delta\varphi_{1-2} = \Delta\varphi_{2-3} = 0^o$). Results obtained with the "*.pre" FEKO file included in point 6.2.6. of annex 6.2 "ANNEX 2: PROGRAMS AND CODE".

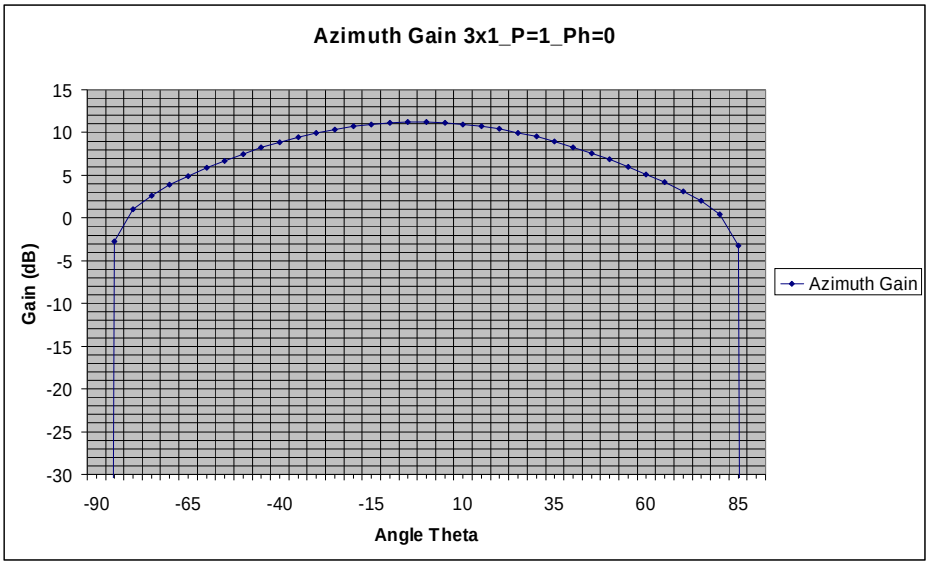

Figura 6-7 Azimuth gain of the 1x3 array with uniform power supply

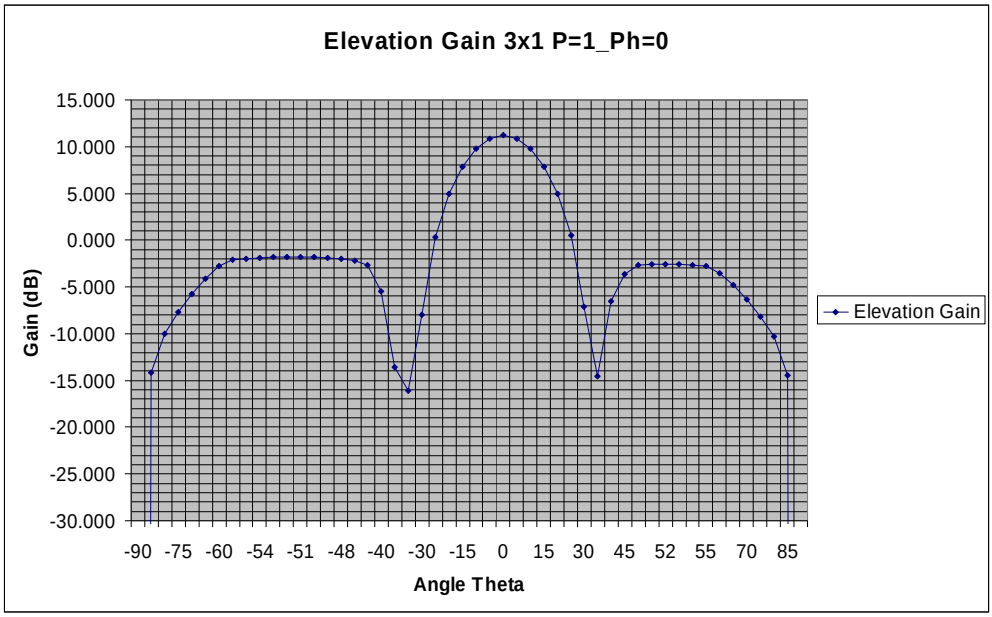

Figura 6-8 Elevation gain of the 1x3 array with uniform feeding in all the patches

6.1.7 Results of the 1x3 Array with different amplitudes

Comparison of the azimuth and elevation gain for the 1x3 array is done, when the patches have different amplitudes in power supply. In the diagram of the azimuth, not all the configurations checked have been included, as all of them are quite similar and don't provide more information. In the elevation diagram, all the tested circuits have been included.

These results were obtained with the "*.pre" FEKO file of the point 6.2.7 of annex 6.2 ANNEX 2: PROGRAMS AND CODE" and making small variations on it, as it is described in the mentioned point.

Notation: The different arrangements have been named following the next considerations:

Patch_3x1_X-XX_Y_Z-ZZ

- *"Patch_3x1_": Common part identifying the simulated array.*
- *"X-XX": Voltage amplitude at the input of the upper patch of the array. That is, the patch with a greater value for y. All the digits after the dash correspond to decimal values. (For example: 0-75 is 0.75; 0-2 is 0.2; etc.)*
- *"Y": Voltage amplitude at the input of the central patch of the array. It will always have a value of 1.*
- *"Z-ZZ": Voltage amplitude at the input of the lower patch of the array. That is, that one with lower value of y. The digits after the dash correspond to decimal values.*

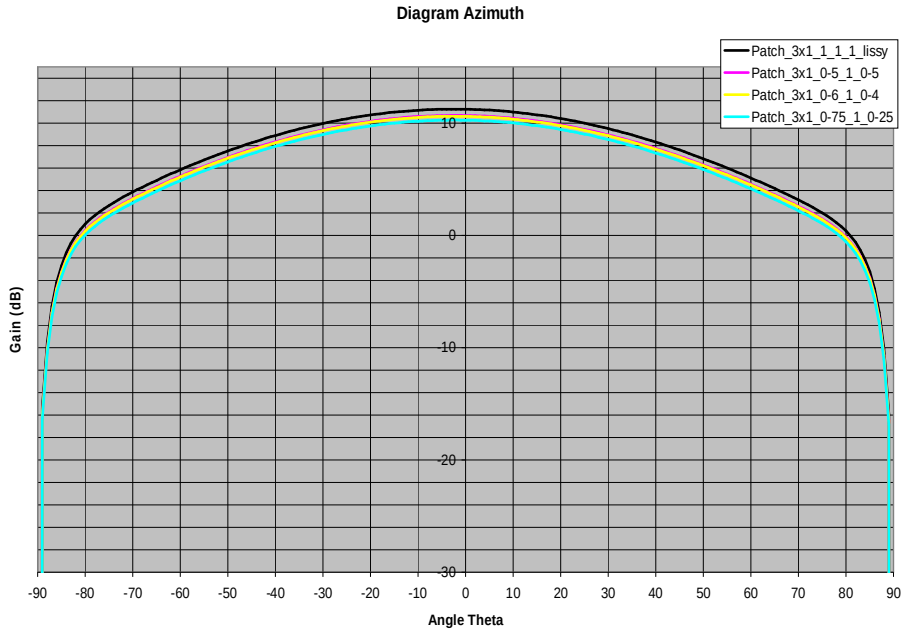

Figura 6-9 Azimuth gain of the 1x3 array with different amplitudes in the patches

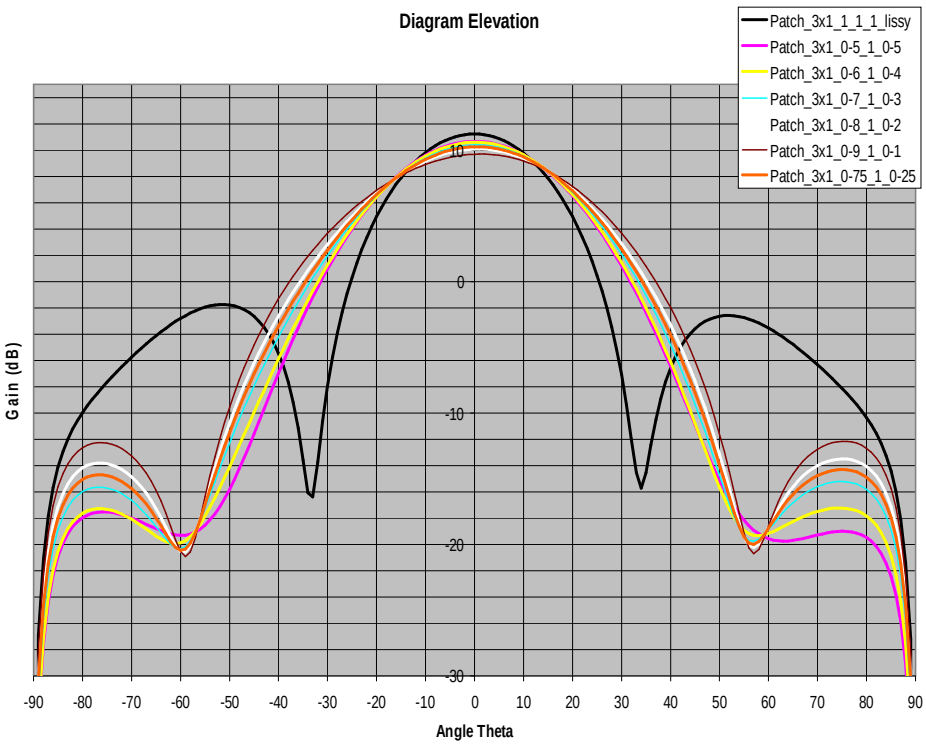

Figura 6-10 Elevation gain of the 1x3 array with different amplitudes feeding the patches

6.1.8 Results of the 1x3 array with different amplitudes and phases

The figures included in this point capture the differences in the radiation patterns of the 1x3 array with supply amplitudes $V_{y\uparrow} = 0.5\,V_{middle} = V_{y\downarrow}$ when phase gaps between the signals getting into the patches are introduced.

All the results obtained here are derived from the "*.pre" FEKO file included in point 6.2.8 of annex 6.2 "ANNEX 2: PROGRAMS AND CODE".

The central patch is considered as the phase reference for the gaps introduced, and the notation has the following structure:

Patch_3x1_0-5_1_0-5_PX-XX_Y-YY

- *"Patch_3x1_0-5_1_0-5_P": Common part identifying the simulated array.*
- *"X-XX": Phase shift with respect to the central patch of the upper patch of the array. That is, the patch with a greater value for y. All the digits after the dash correspond to decimal values. (For example: 12-5 is 12.5; etc.)*
- *"Y-YY": Phase shift with respect to the central patch of the lower patch of the array. That is, that one with lower value of y. Again, the digits after the dash correspond to decimal values.*

A negative value in the phase shift will indicate that the phase is lower than that at the central patch of the array. A positive value, in contrary, will indicate a bigger value with respect to the central patch of the array.

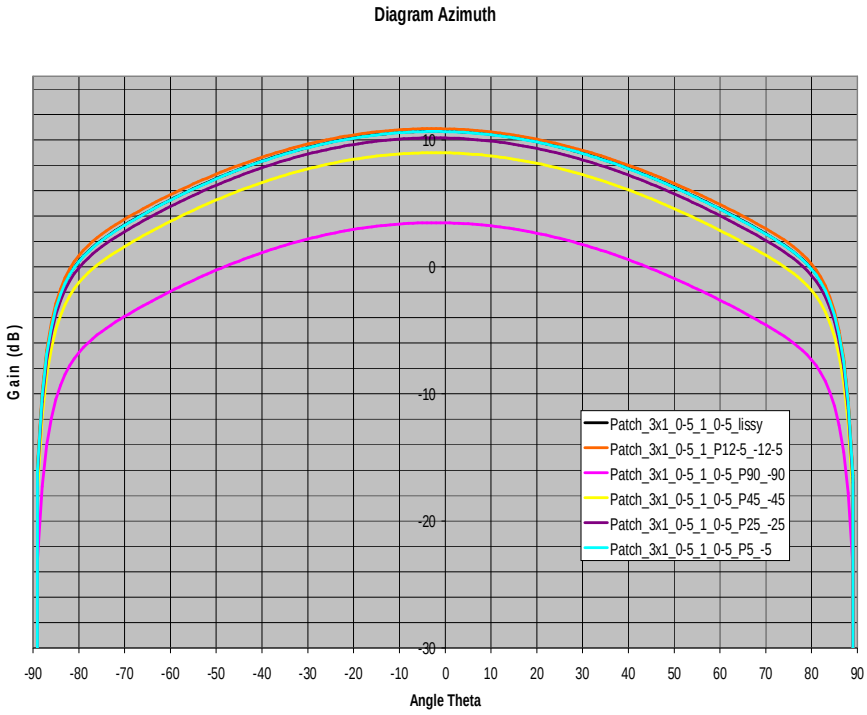

Figura 6-11 Azimuth gain of the 1x3 array with amplitudes $V_{y\uparrow} = 0.5\,V_{middle} = V_{y\downarrow}$ and different phase gaps

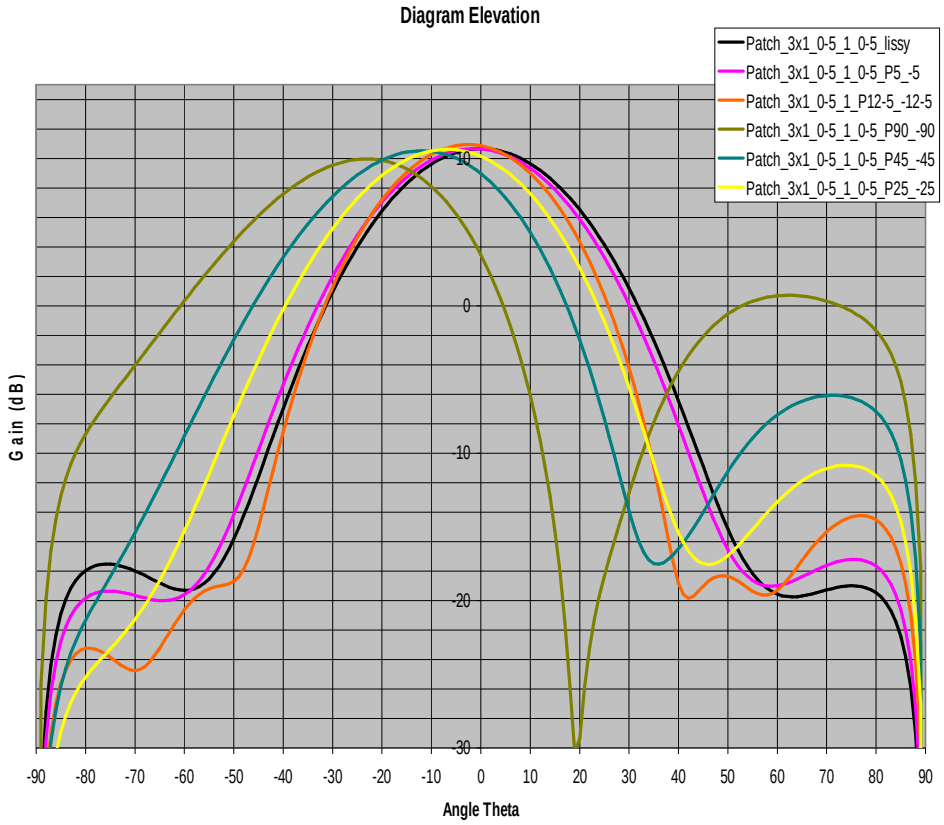

Figura 6-12 Elevation gain of the 1x3 array with amplitudes $V_{y\uparrow} = 0.5\,V_{middle} = V_{y\downarrow}$ and different phase gaps among the patches

The best results for the 1x3 array are obtained with the following supply:

- $V_{y\uparrow} = 0.5\,V_{middle} = V_{y\downarrow}$
- $\Delta\varphi_{y\uparrow-middle} = 12.5^{\circ} = -\Delta\varphi_{middle-y\downarrow}$

From now on, the 1x3 array with this arrangement of amplitudes and phase shifts in supply will be referred as the “1x3 array”.

6.1.9 Results of the 1x3 array (with different amplitudes and phases) with lens

In this point the azimuth and elevation gain of the 1x3 array (Amplitudes=0,5-1-0,5; Phase Shifts= 12,5º-0º-(-12,5º)) with lens are shown. As it could be expected, the results improve a lot with the use of the lens, increasing the directivity of the whole set.

These results are obtained using the "*.ffe" files obtained with FEKO from the "*.pre" FEKO file of point 6.2.8 as input for the program LISSY. The "*.pre" FEKO file defining the geometry of the lens and the far field calculations of the set "array 1x3 with lens" is included in point 6.2.9 of annex 6.2 "ANNEX 2: PROGRAMS AND CODE".

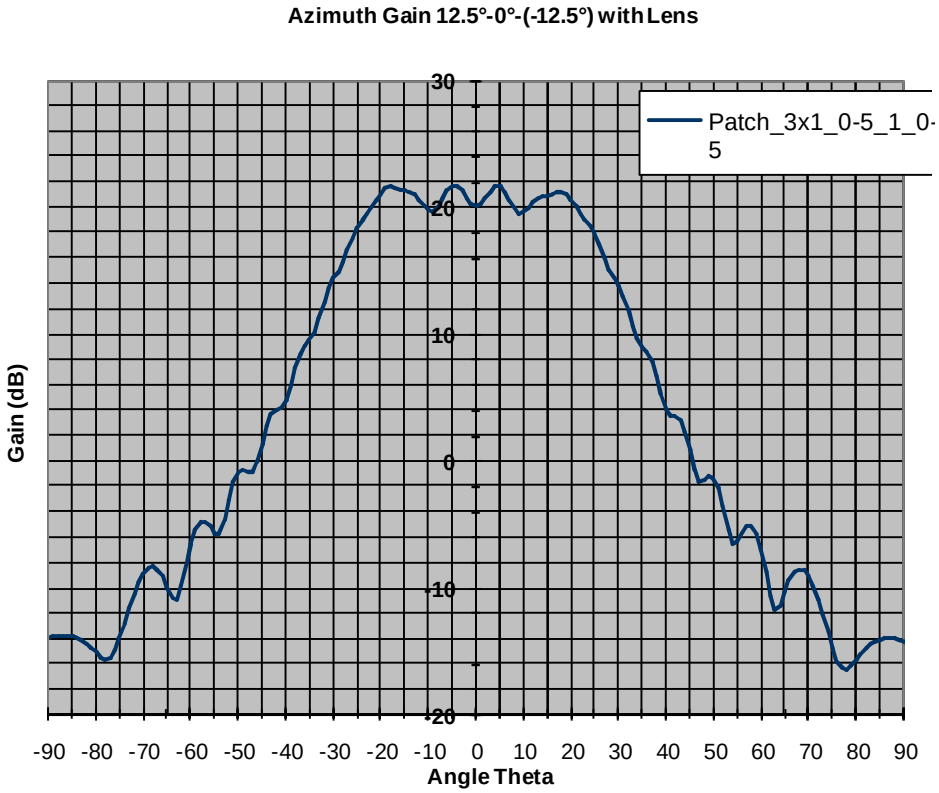

Figura 6-13 Gain in azimuth of the 1x3 array with a superimposed lens

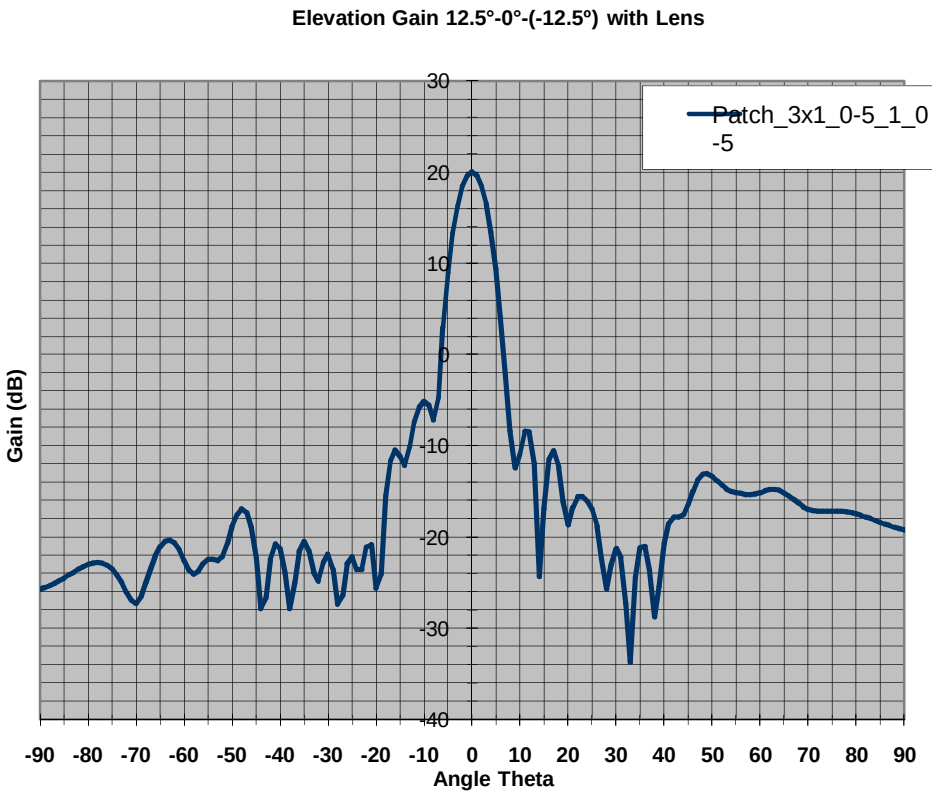

Figura 6-14 Elevation gain of the 1x3 array with a lens

6.1.10 Results of the 20x3 and the 24x3 arrays with lens

The next figures show the azimuth and elevation diagrams comparing the results obtained with a set of 20 copies and a set of 24 copies of the “1x3 array” equally spaced along the x-axe.

From now on, these configurations will be designated as “20x3 array” and “24x3 array”.

The “*.pre” FEKO files with whom these results have been obtained are included in points 6.2.10 (array 20x3) and 6.2.11 (array 24x3) of the annex 6.2 “ANNEX 2: PROGRAMS AND CODE”.

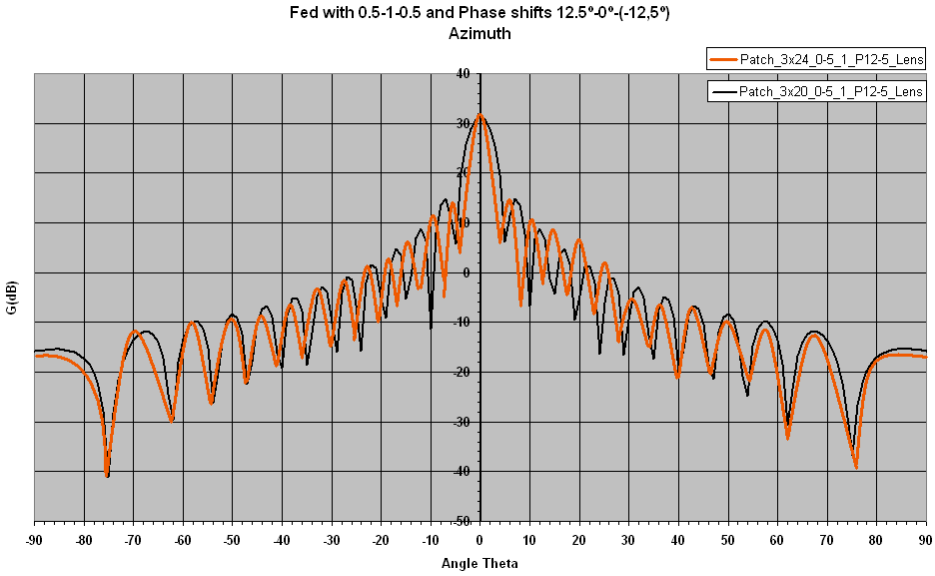

Figura 6-15 Azimuth gains of the 20x3 and 24x3 arrays with lens

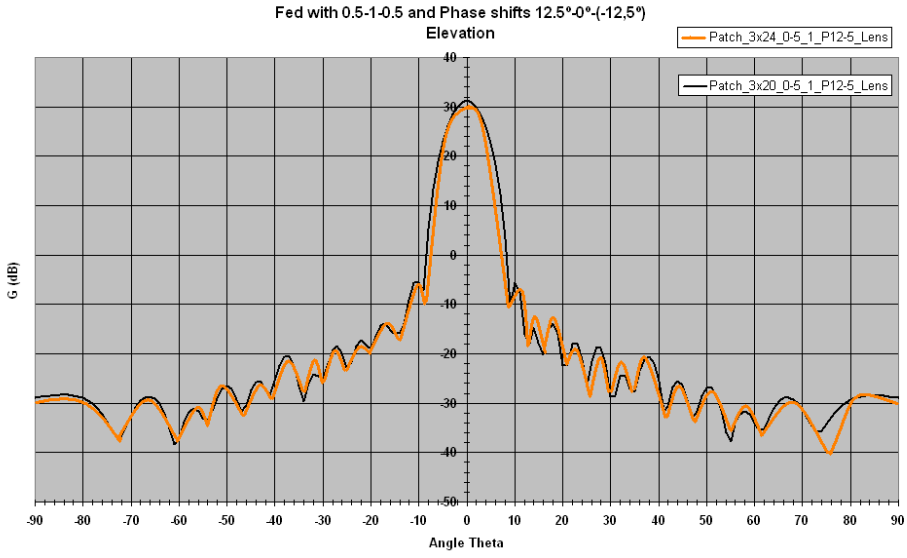

Figura 6-16 Elevation gains of the arrays of 20x3 and 24x3 patches with lens

6.1.11 The 20x16 array versus the 20x3 array with lens

This point compares the results obtained with the two solutions proposed in chapter 1: The array of 20x16 patches without lens, and the array of 20x3 patches (with different amplitudes and phase shifts at the input of each patch of the 1x3 array) used with a cylindrical lens.

The results exhibited here have been taken from the previous points (6.1.4 and 6.1.10) of this annex.

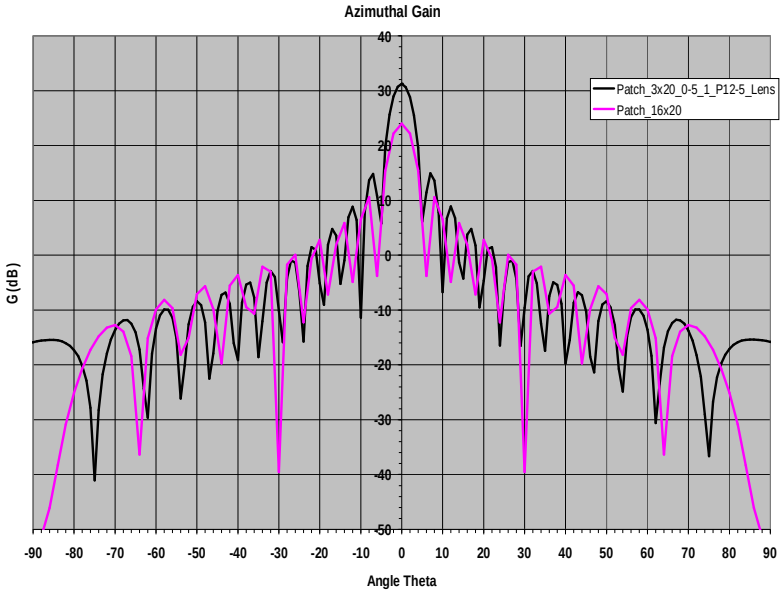

Figura 6-17 Comparison of the azimuth gain of the 20x16 array and the 20x3 array with lens

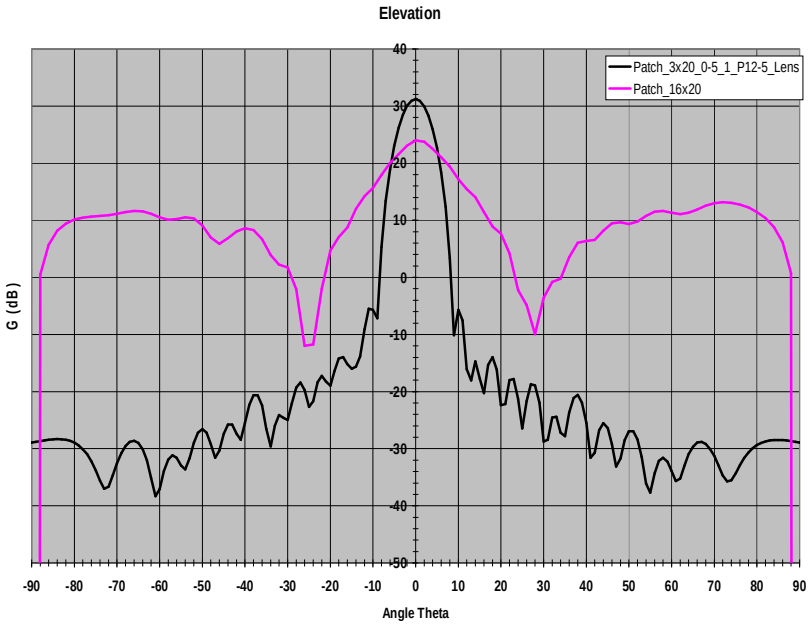

Figura 6-18 Comparison in elevation of the 20x16 array and the 20x3 array with lens

6.1.12 Supply Circuit for the 1x3 array without phase shifts among patches

The circuit that obtains the best results for the power distribution in the 1x3 array without phase shifts is shown in Figura 6-19. In Figura 6-20 appear the results obtained for the most relevant S-Parameters. And Figura 6-21 depicts the phase shifts among the different patches, despite of the fact that they haven't been modified yet.

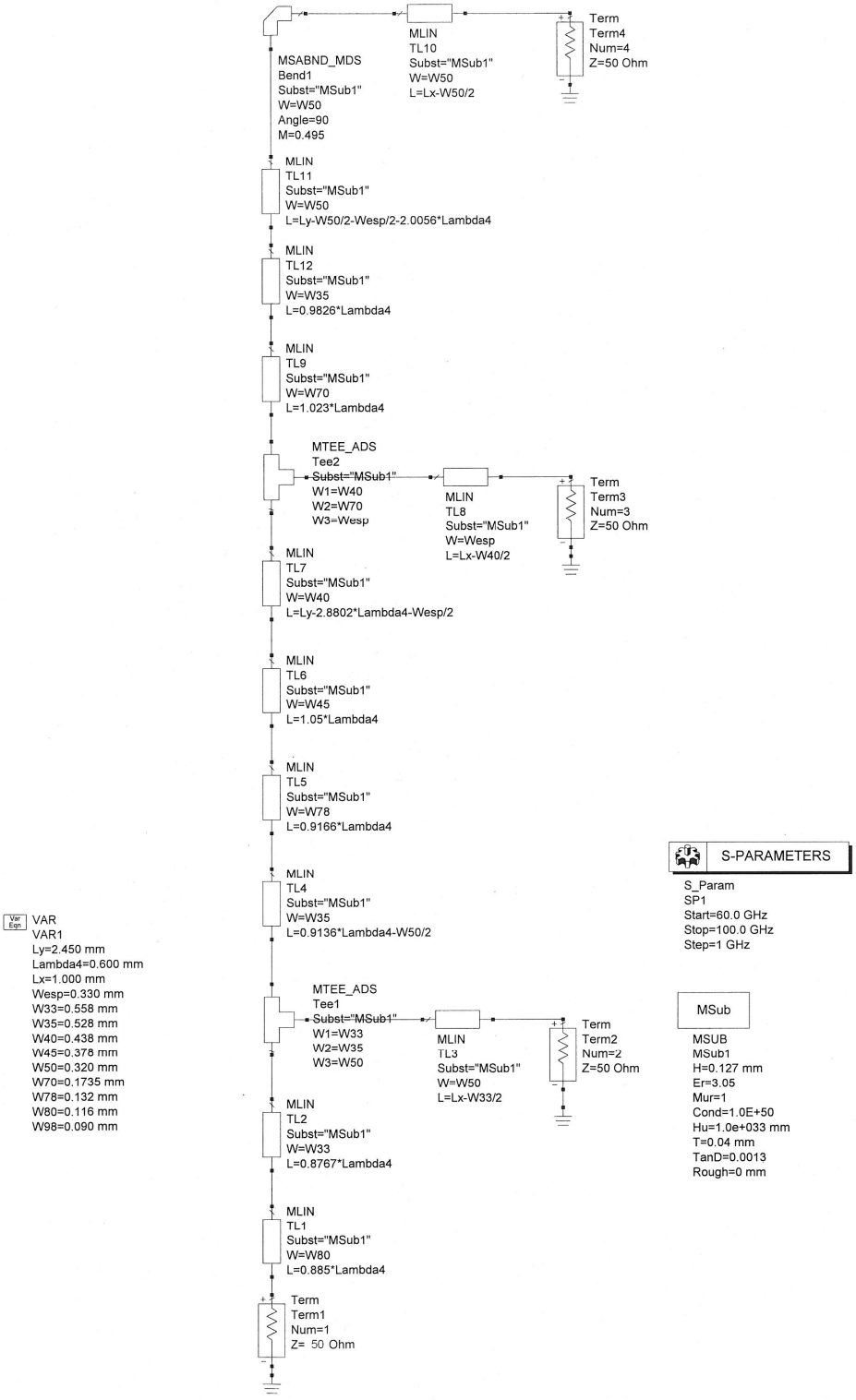

Figura 6-19 Description of the supply circuit of the 1x3 array without phase shifts among patches

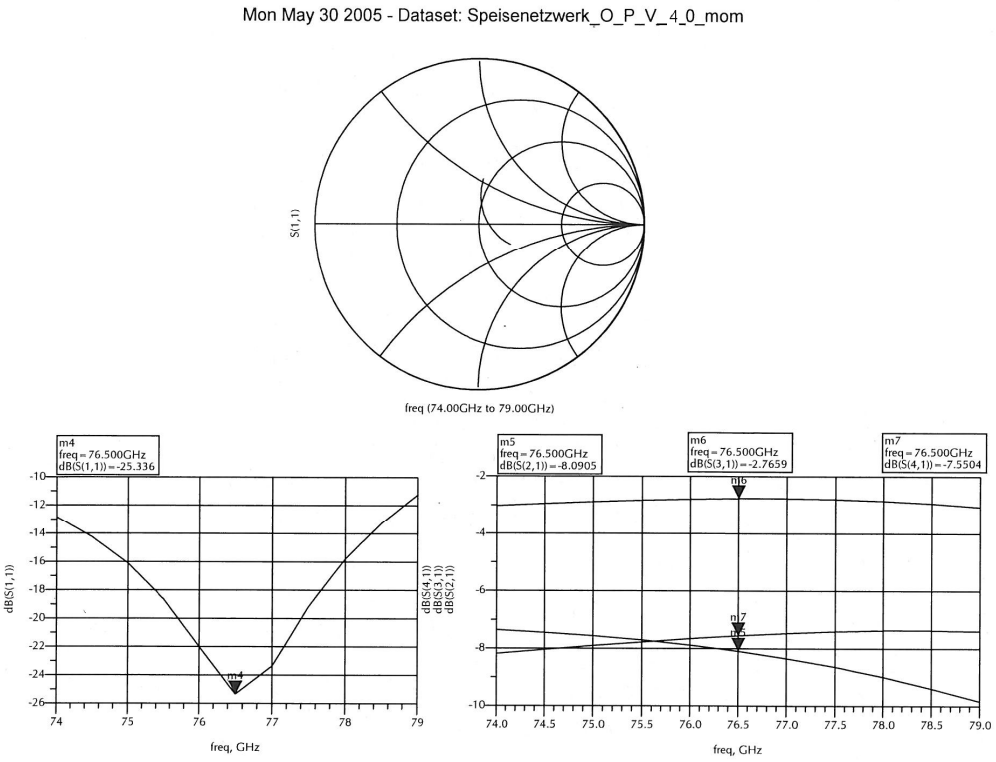

Figura 6-20 Main S Parameters of the circuit

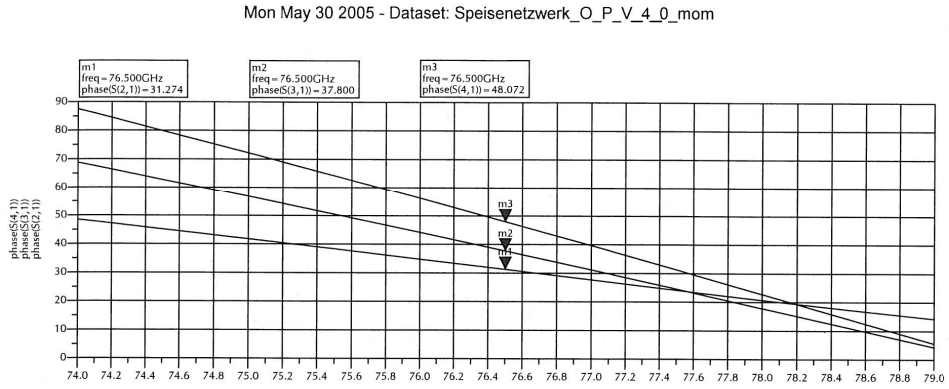

Figura 6-21 Phase shifts among patches of the circuit

6.1.13 Supply circuit for the "1x3 array"

The circuit "Speisenetzwerk_MPV_Def.dsn" is introduced in Figura 6-23. It is the responsible of feeding the 1x3 array with the suitable phase and amplitude at every patch. The results obtained for the S-Parameters and the phase shifts are depicted in Figura 6-22.

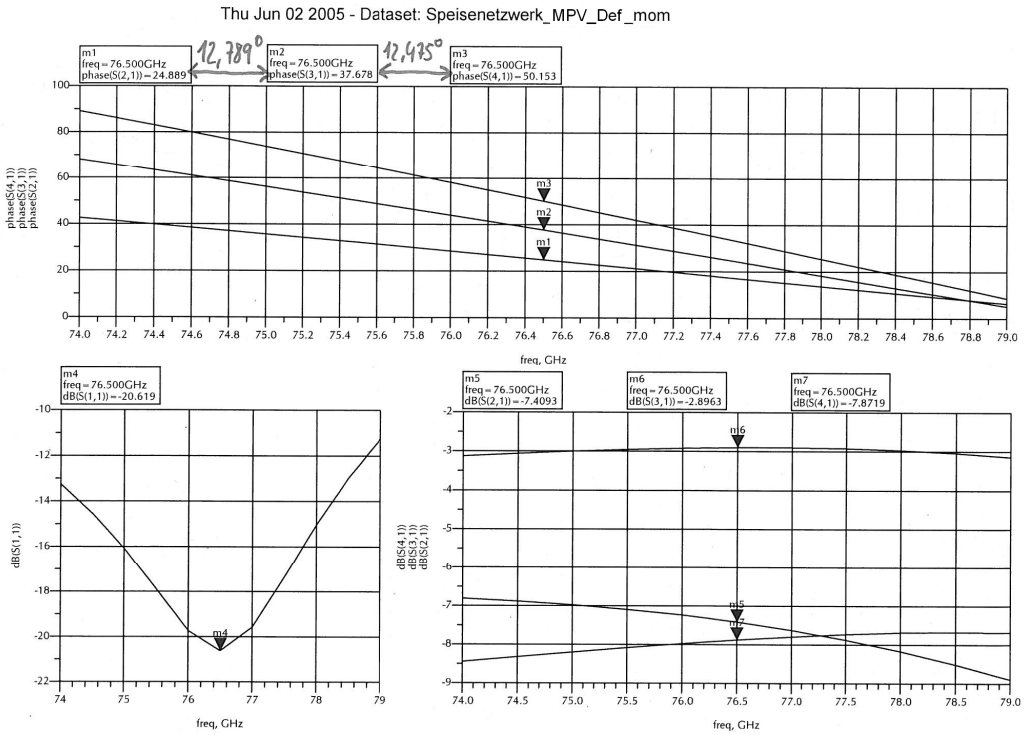

Figura 6-22 Phase shifts among patches (upper part of the figure) and main S Parameters obtained with the circuit of Figura 6-23 (S_{11} at the left, and S_{21}, S_{31}, S_{41} at the right of the lower part)

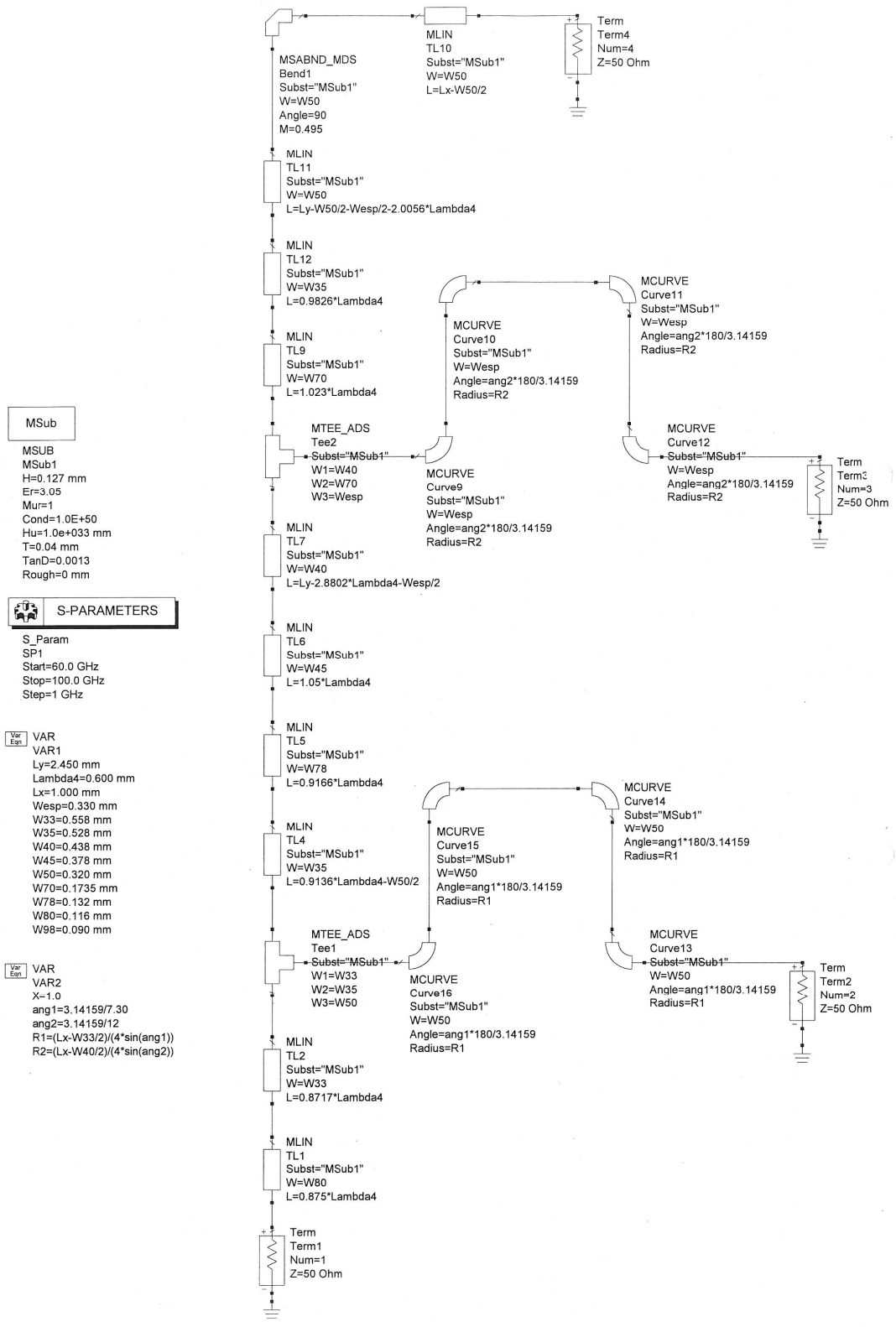

Figura 6-23 Description of the supply circuit of the 1x3 array with phase shifts among patches

6.1.14 Supply circuit of the 20x3 array: common part

Figura 6-24 shows the circuit that delivers the same amplitude and phase to 4 groups of 5 arrays 1x3. Figura 6-25 shows the results obtained for the relevant S-Parameters and the phase shifts among terminals of the circuit.

As it can be seen in Figura 6-25, all the terminals have more or less the same phase respecting terminal 5 (power supply). And the S Parameters present a value about 6 dB in each terminal, as it was expected. For the S_{55} parameter, the result is -15,171 dB. A very good value that indicates a good impedance matching with the power supply.

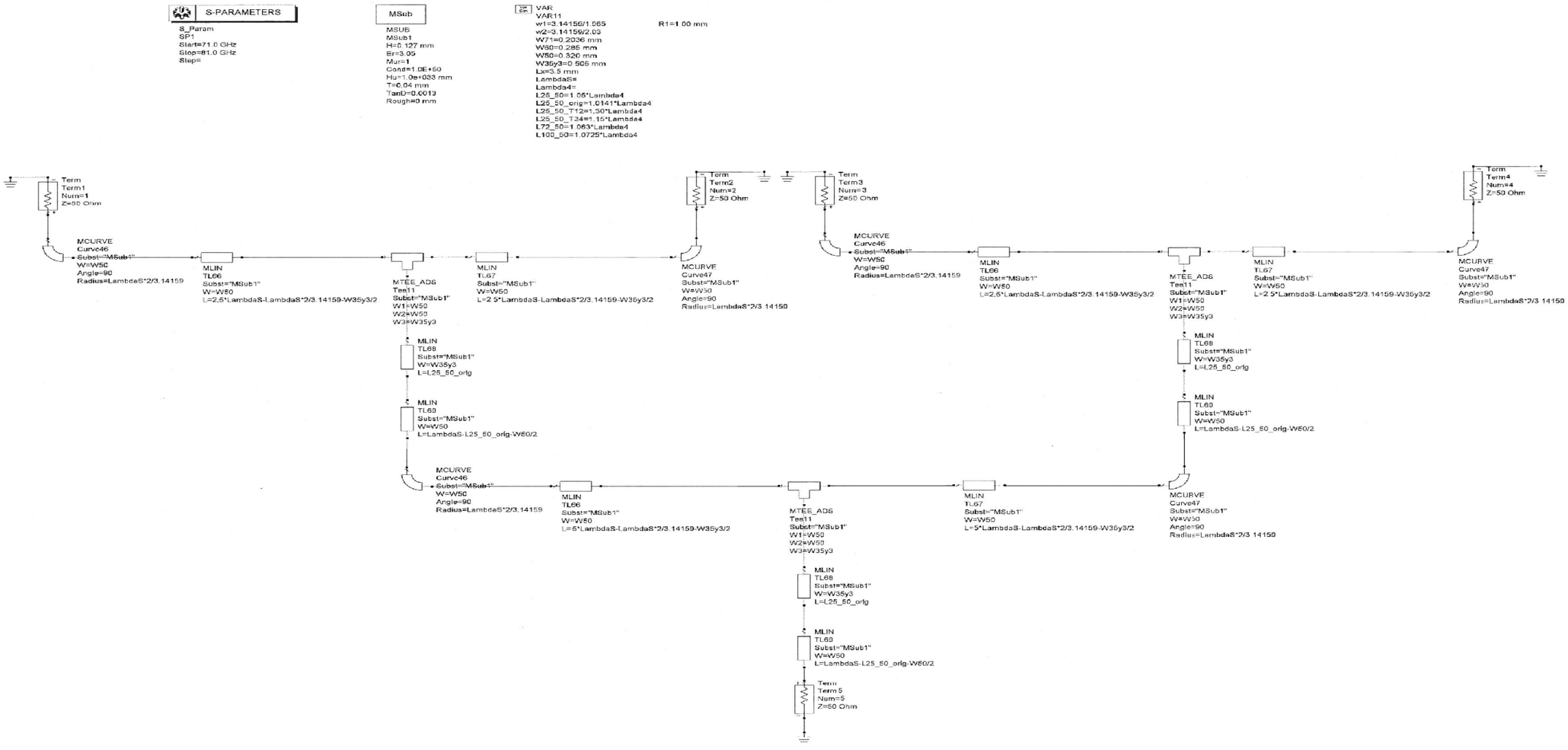

Figura 6-24 Supply circuit providing the same amplitude and phase to the 4 groups of 5 arrays 1x3

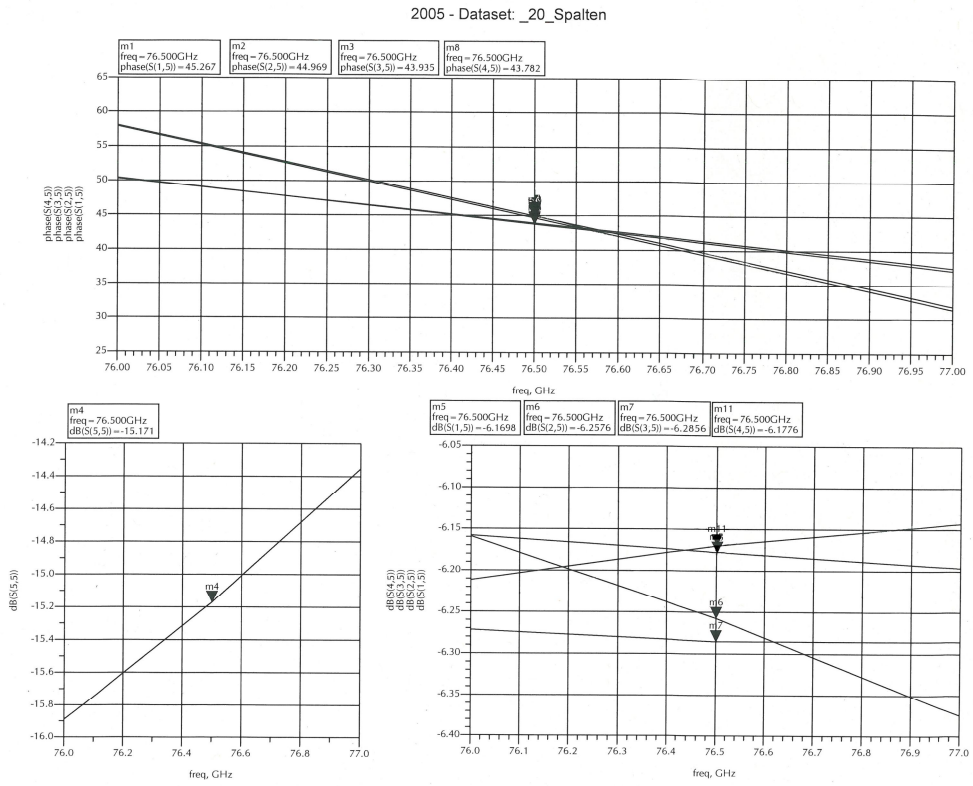

Figura 6-25 Phase shifts and main S-Parameters of the circuit depicted in Figura 6-24

6.1.15 Supply circuit of the 20x3 array: the group of 5 copies of the 1x3 array

Figura 6-27 shows the circuit that must survey 5 arrays of 1x3 rectangular patches with the same amplitude and phase. Figura 6-26 reveals the results obtained.

As a consequence of these results, the 20x3 circuit was fabricated to be tested in laboratory. This circuit was constructed by joining the circuits of points 6.1.14 and 6.1.15.

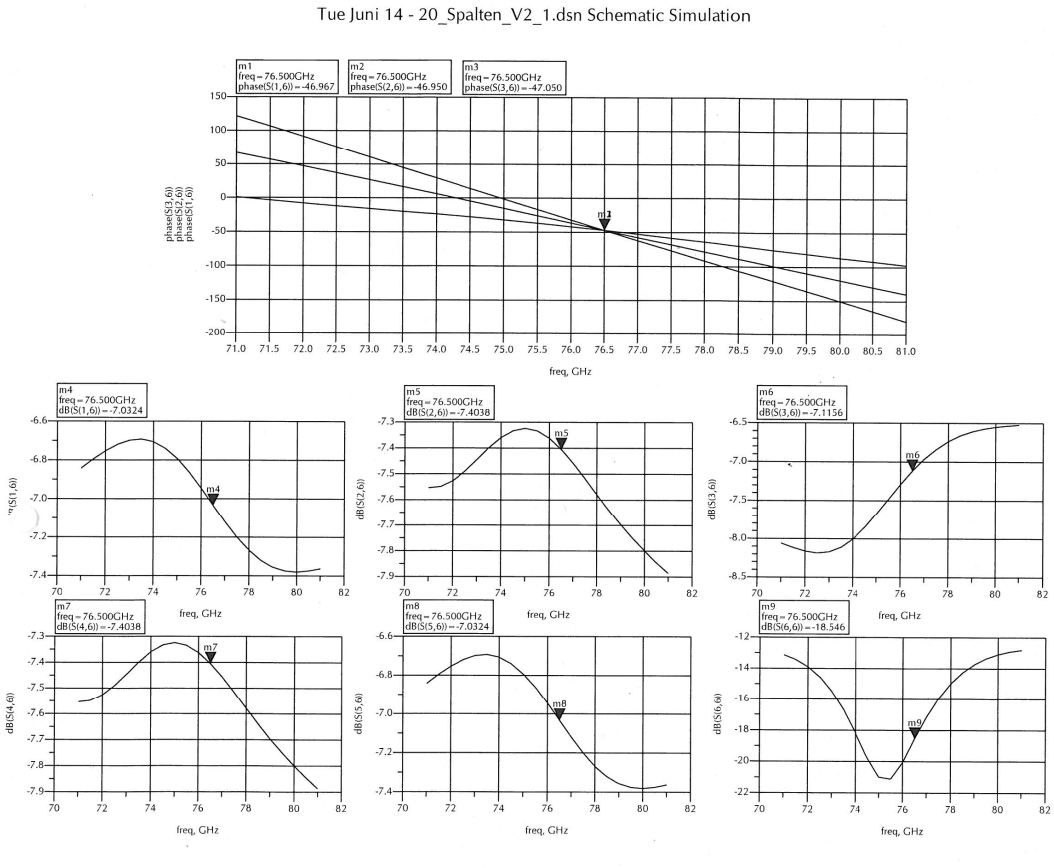

Figura 6-26 Phase shifts (upper part) and main S Parameters of the circuit providing same amplitude and phase to the 5 copies of the 1x3 array

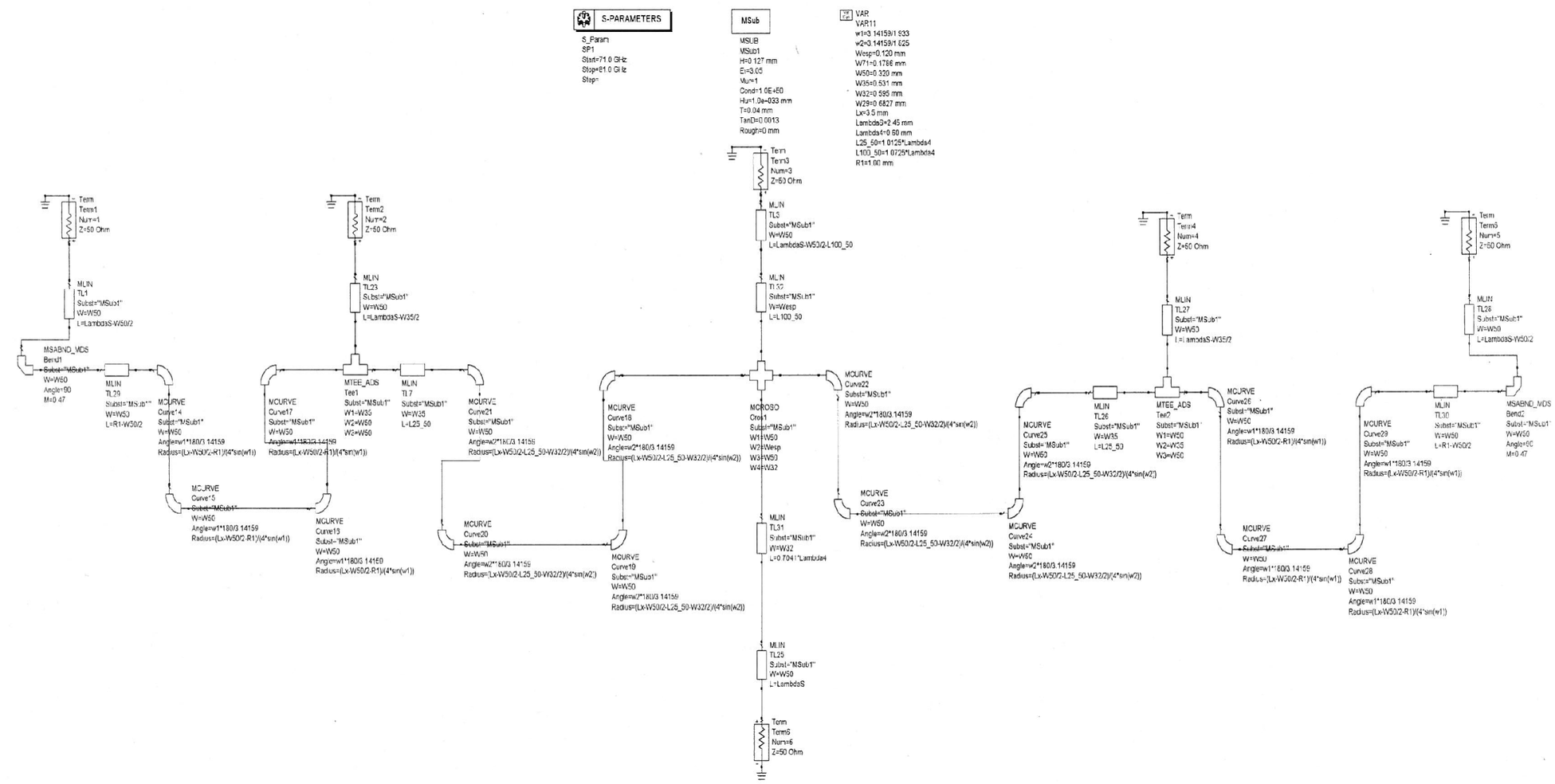

Figura 6-27 Description of the circuit providing the same amplitude and phase to the 5 copies of the 1x3 array

6.1.16 Supply circuit of the 24x3 array: common part

Figura 6-28 shows the circuit that supplies the same amplitude and phase to the 4 groups of 6 copies of the “1x3 array”.

Figura 6-29 shows the results obtained for the phase shifts among terminals of the circuit, and also the most important S Parameters. Regarding the phase shifts, all of them are very similar as it was desired. With the S Parameters, a value close to 6 dB is reached in all the terminals. This is the value expected, as the power coming from the supply must be divided equally in the 4 branches of the circuit.

The S_{55} parameter reaches a value of -15,334 dB. It can be considered as good enough accordingly to the requisites of the system.

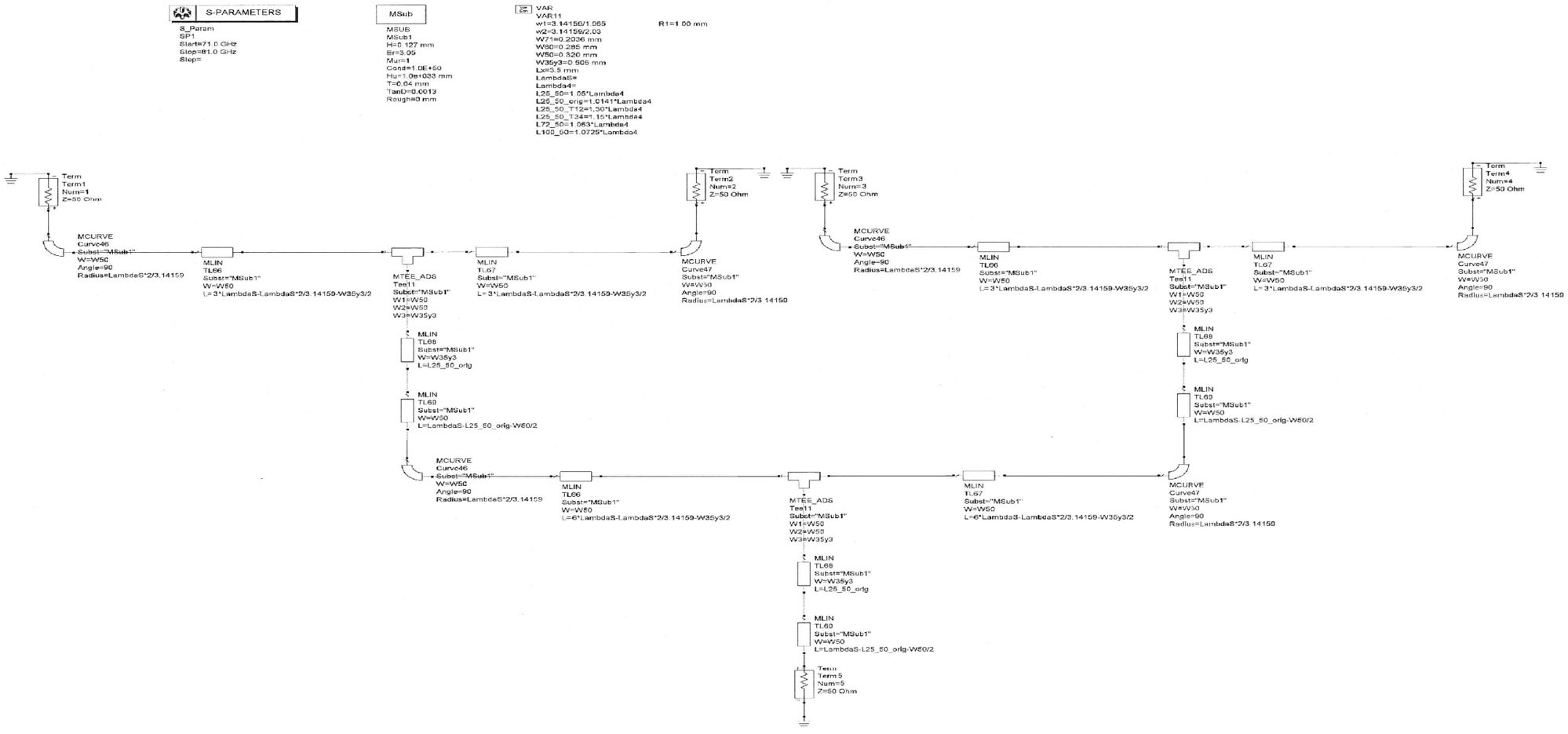

Figura 6-28 Supply circuit providing the same amplitude and phase to the 4 groups of 6 arrays 1x3

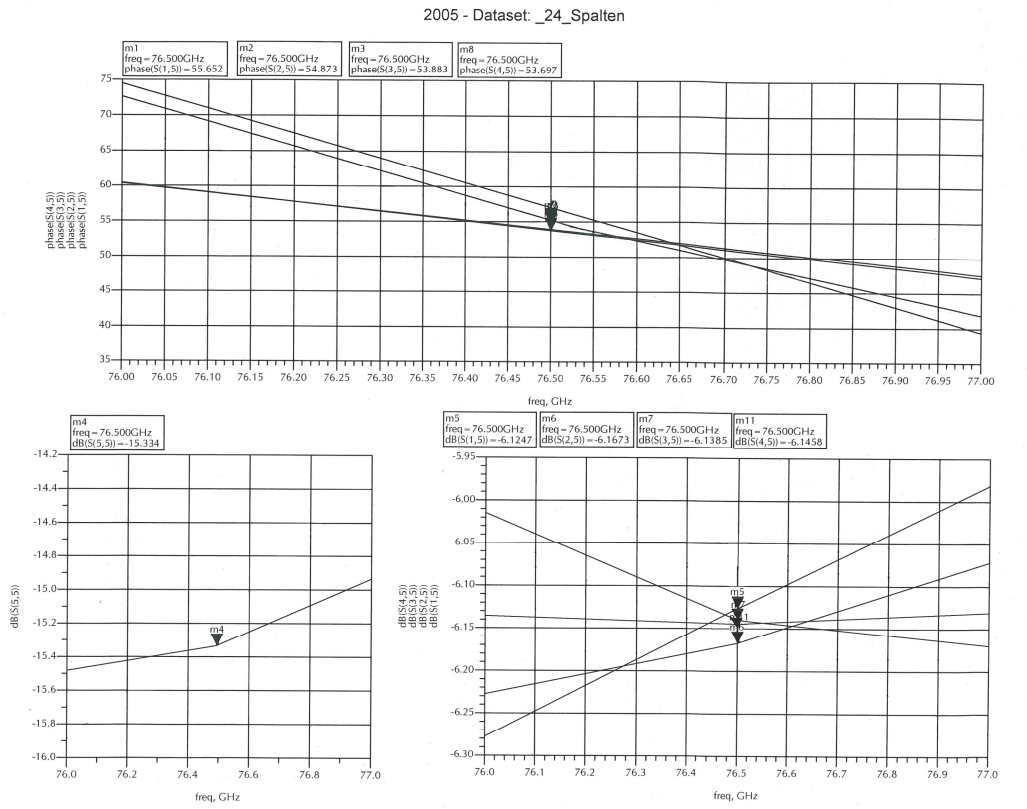

Figura 6-29 Results for the phase shifts (upper part) and the main S Parameters for the circuit of Figura 6-28

6.1.17 Supply circuit of the 24x3 array: the group of 6 copies of the 1x3 array

Figura 6-31 shows the supply circuit that provides the same amplitude and phase to the 6 copies of the 1x3 array. In Figura 6-30 the phase shifts among them, and the main S Parameters are depicted.

As a consequence of these results, the 24x3 circuit was fabricated to be tested in laboratory. This circuit was constructed by joining the circuits of points 6.1.16 and 6.1.17.

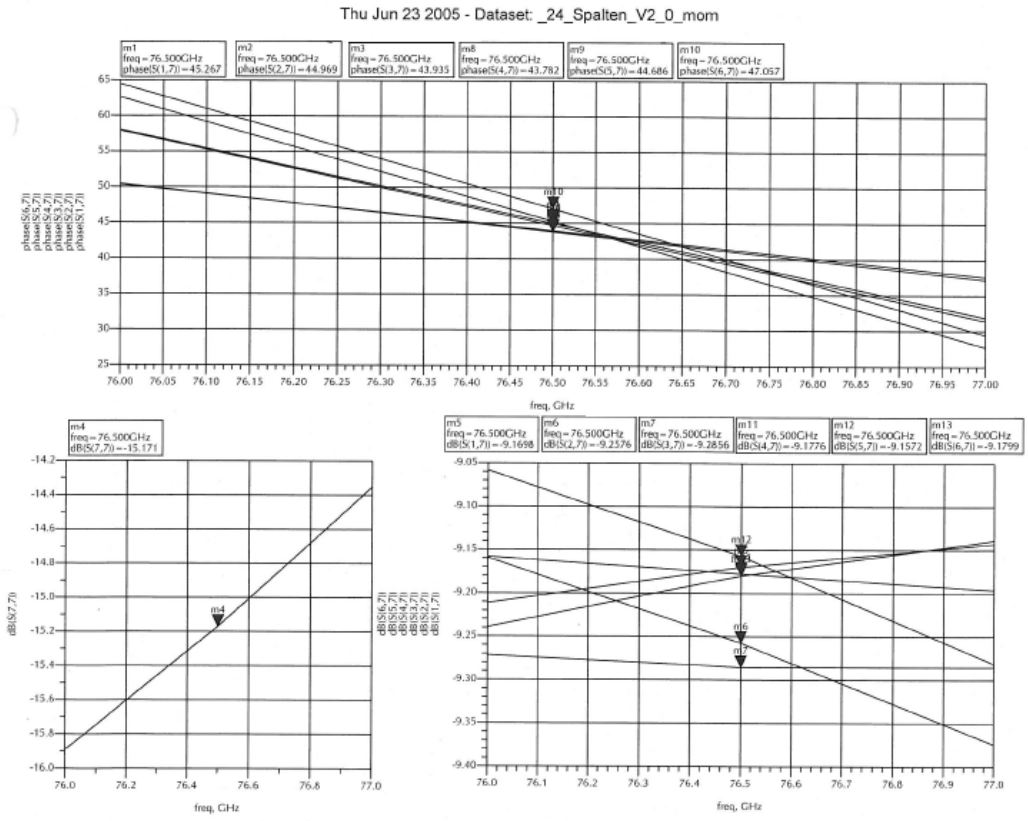

Figura 6-30 Phase shifts (upper part) and main S Parameters of the circuit providing the same amplitude and phase to the 6 copies of the 1x3 array

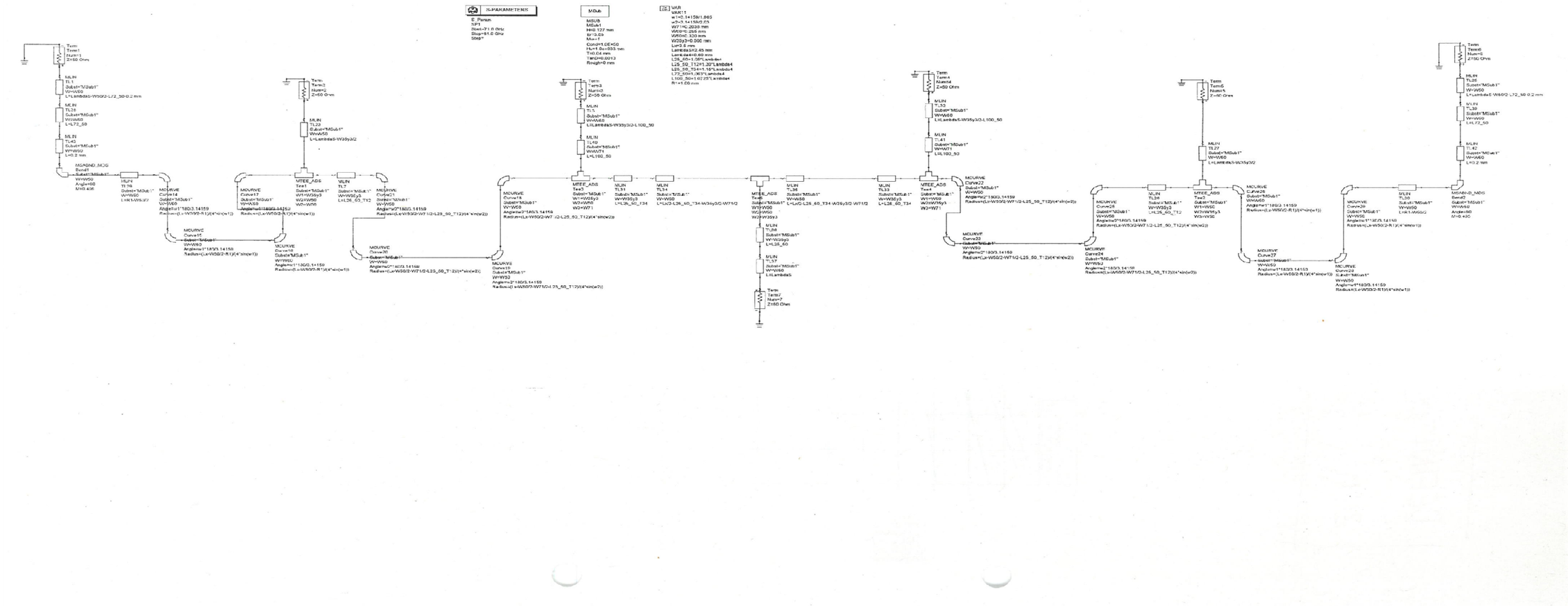

Figura 6-31 Supply circuit providing the same amplitude and phase to the 6 copies of the 1x3 array

6.1.18 Fabricated Circuits

In this point, photographs of all the circuits tested in laboratory are included. These circuits are the shown in Tabla 6-1.

Section	Circuit included
6.1.18.1	1x3 patch array with the power supply specified in Ec. 6-20 a) (only Amplitude).
6.1.18.2	1x3 patch array with the power supply specified in Ec. 6-20 a) y b) (Amplitude and Phase shift).
6.1.18.3	Array of 20 copies of the 1x3 patch array (amplitude and phase) with whom "Schematic" from ADS obtains the best results.
6.1.18.4	Array of 24 copies of the 1x3 patch array (amplitude and phase) with whom "Momentum" from ADS obtains the best results.

Tabla 6-1 Circuits tested in anechoic chamber

From each one, two different modifications will be constructed: One for the measurement of the Antenna Parameters of the array (basically directivity and gain). Another for the measurement of the S-Parameters of the array (basically S_{11}).

The reason why two different circuits are needed in order to determine the different parameters (Antenna and Scattering) of the circuits is that the feeding technique will differ depending on the parameters to test.

When measuring the S Parameters of the circuit, the Coplanar Waveguide Technique will be used. It is fully described in reference **[10]** of the bibliography. And it is shown in Figura 6-32. In every circuit fed with this technique, there will appear three calibration ports in the left lower corner of the board. They are used for obtaining S_{11} of the circuit by means of a comparison with the values obtained in them, which are known. The feeding point appears in the upper side of Figura 6-32, in the center of the picture, and connected to the circuit under study.

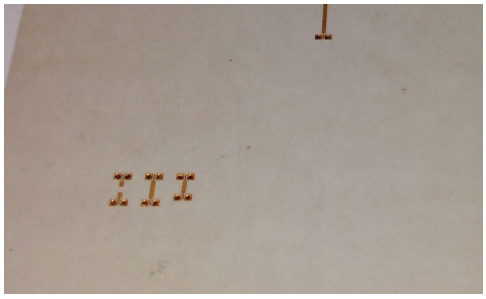

Figura 6-32 Calibration ports for the calculation of S_{11}

On the other hand, when Antenna Parameters are to be measured, the Microstrip Line Technique will be used instead. It is described in reference **[5]** and also in **[10]** of the bibliography, and also in chapter 2.2 "TÉCNICA DE ALIMENTACIÓN" of this document. Figura 6-33 describes this technique, in which a special connector is used to insert the signal to the microstrip line. The installation of this connector requires a cut in the board, removing the conductor plane and the dielectric. So the connector is placed directly below the conductor of the microstrip line with the help of a microscope. Figura 6-34

shows the cutting edge before the installation of the connector. And Figura 6-35 shows the connector already installed.

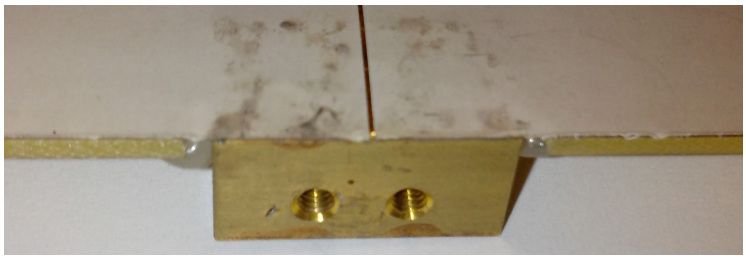

Figura 6-33 Special connector used to insert the signal to the microstrip line of the feeding circuit

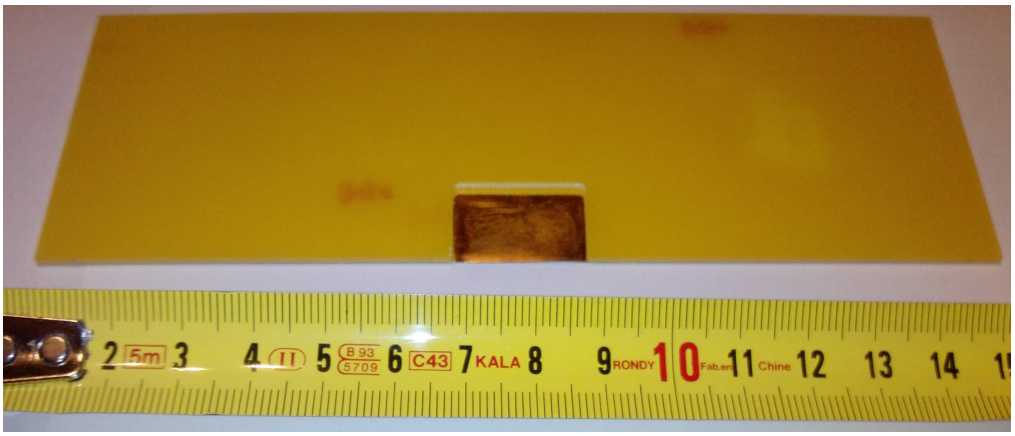

Figura 6-34 Detail on the cut for the installation of the special connector of the Microstrip Line Technique

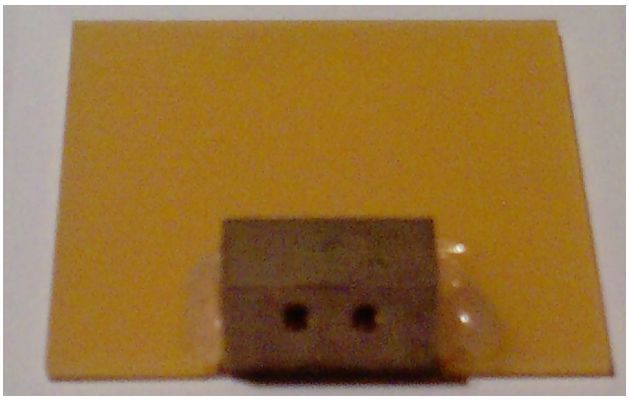

Figura 6-35 Connector for the measurement of the Antenna Parameters already installed

In the following subsections, the different circuits measured will be presented.

6.1.18.1 1x3 Patch Array without Phase Shifts among patches

In this point, the circuits to characterize the properties of the 1x3 Patch Array without Phase Shifts among patches are shown. The following pictures don't need any comment.

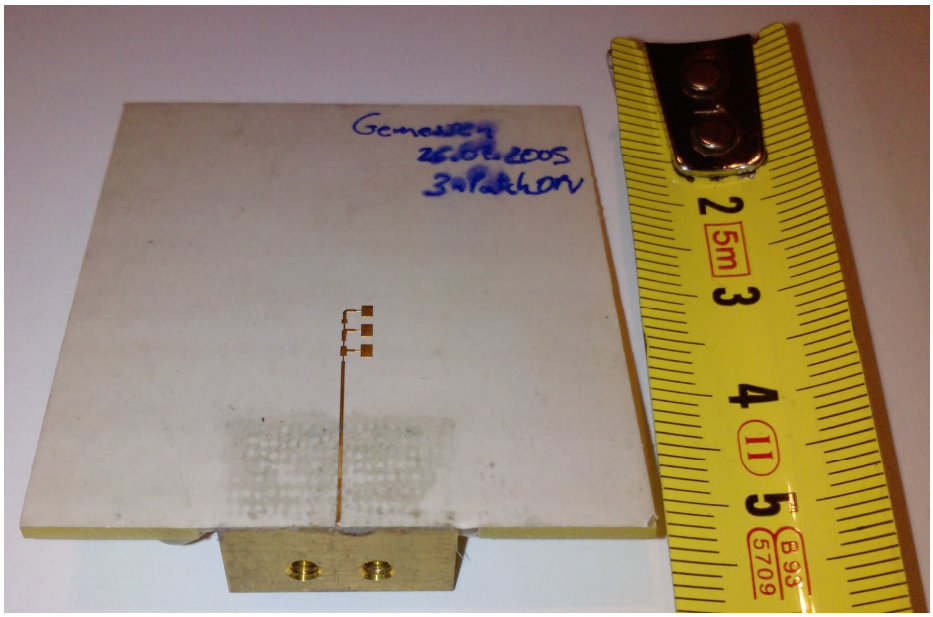

Figura 6-36 Circuit measuring the Antenna Parameters of the 1x3 Patch Array without Phase Shifts

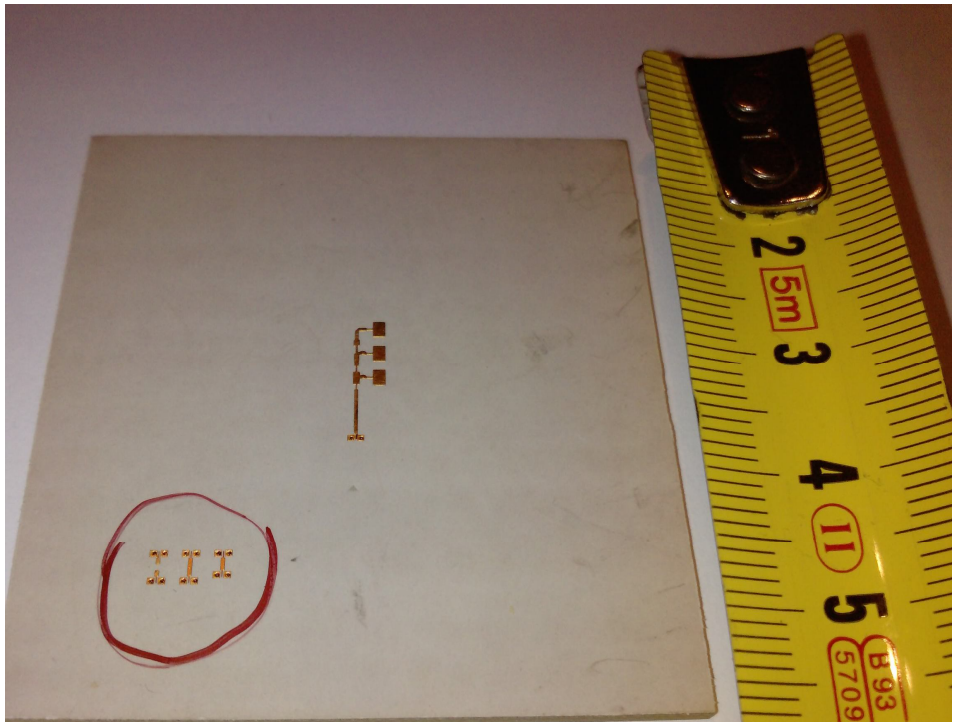

Figura 6-37 Circuit measuring the S-Parameters of the 1x3 Patch Array without Phase Shifts

6.1.18.2 1x3 Patch Array (with phase shifts among patches)

In this point, the circuits to characterize the properties of the 1x3 Patch Array, fed accordingly to Ec. 6-20 a) and b) (right amplitudes and phases at the input of every patch) are shown.

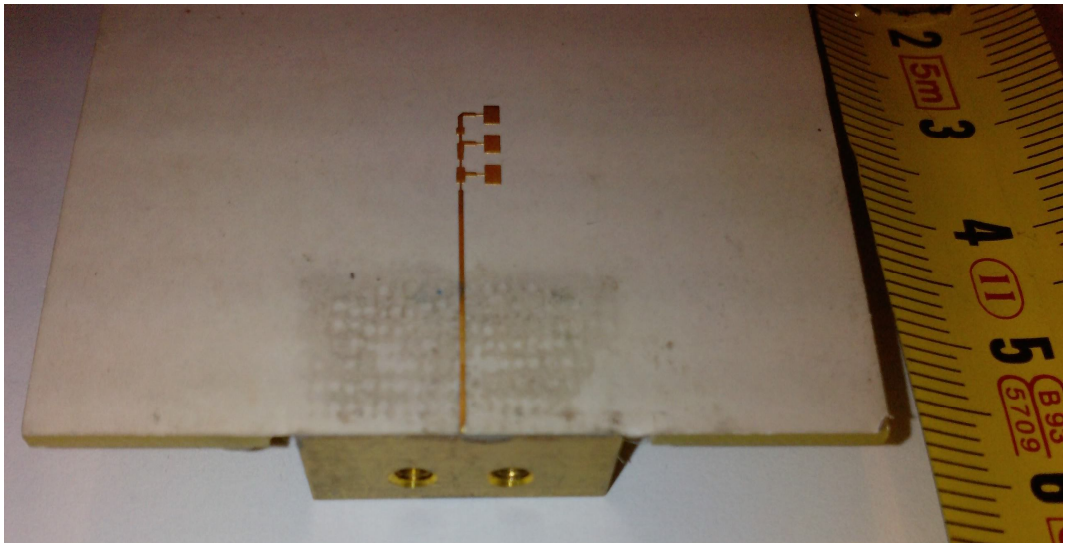

Figura 6-38 Circuit measuring the Antenna Parameters of the 1x3 array (amplitude and phase)

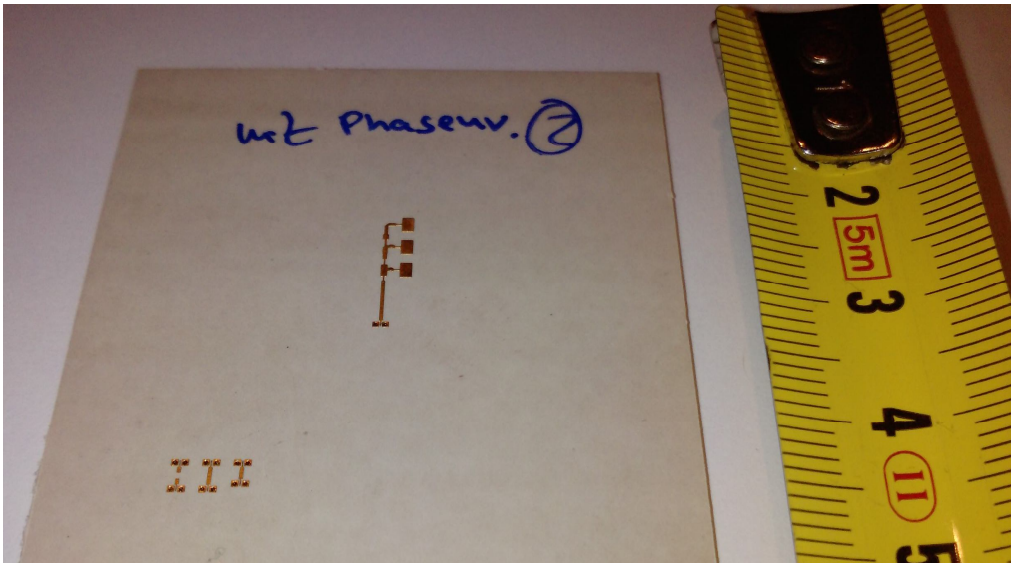

Figura 6-39 Circuit measuring the S Parameters of the 1x3 Patch Array

6.1.18.3 Array 20x3

In this point, the circuits used to characterize the properties of the 20x1x3 Array are shown.

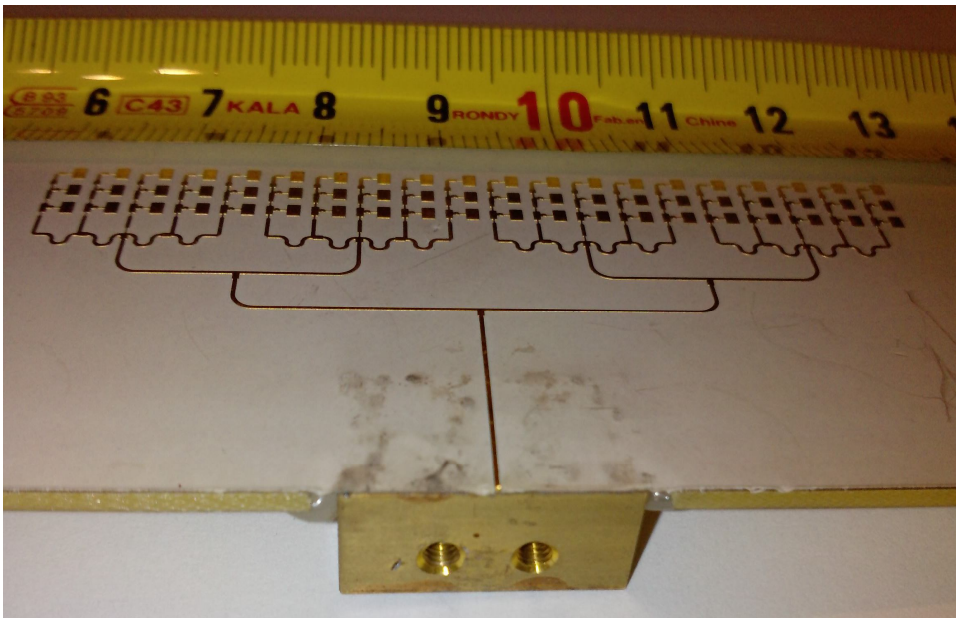

Figura 6-40 Circuit measuring the Antenna Parameters of the 20x3 array

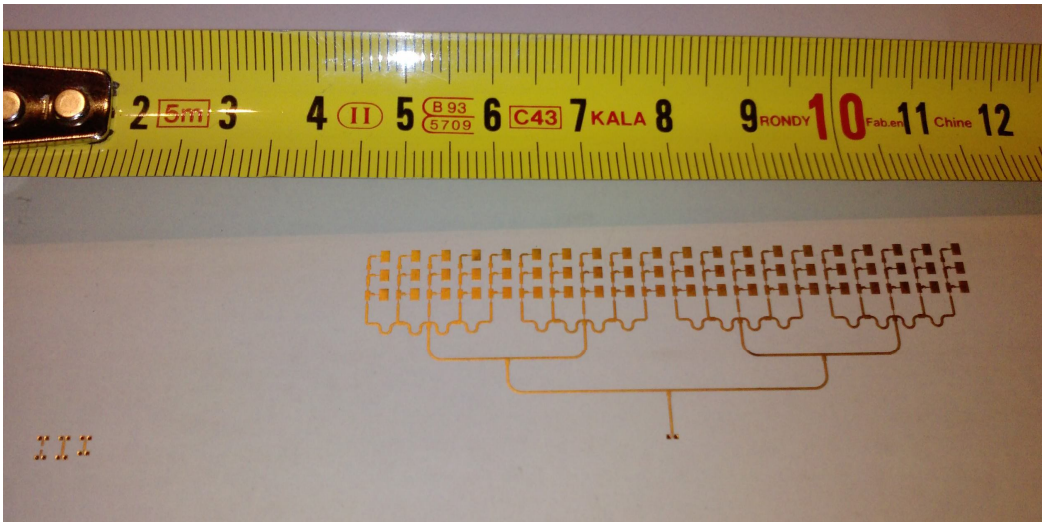

Figura 6-41 Circuit measuring the S-Parameters of the 20x3 array

6.1.18.4 Array 24x3

In this point, the circuits used to characterize the properties of the 24x1x3 Array are shown.

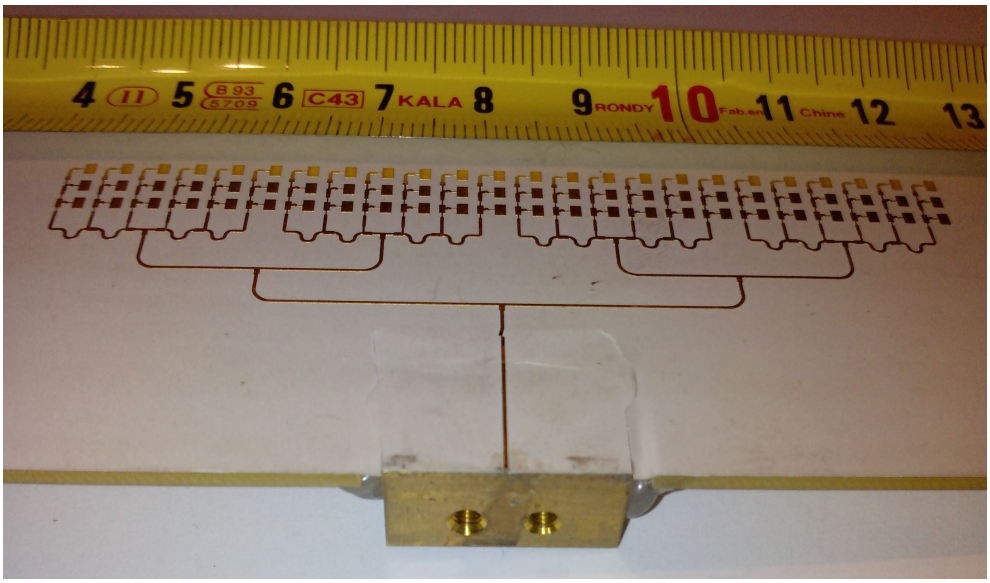

Figura 6-42 Circuit measuring the Antenna Parameters of the 24x3 array

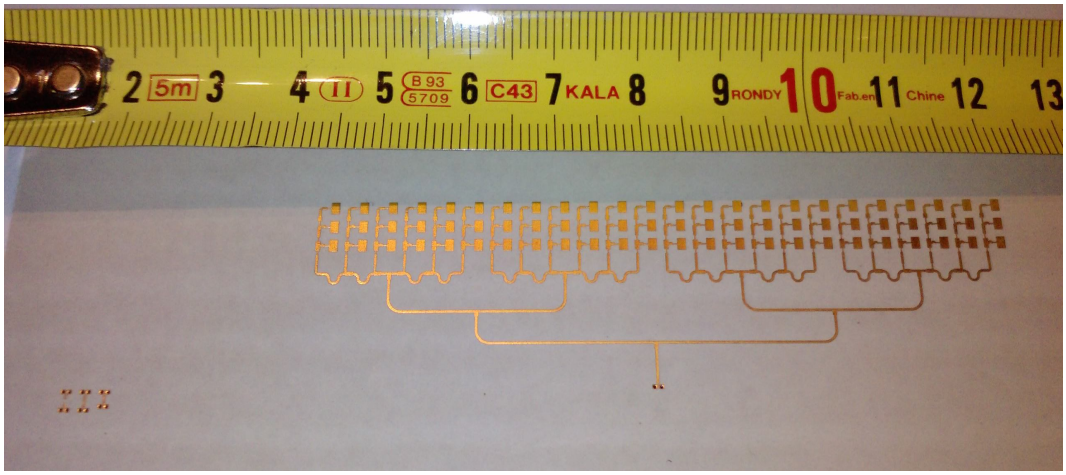

Figura 6-43 Circuit measuring the S-Parameters of the 24x3 array

6.2 ANNEX 2: PROGRAMS AND CODE

6.2.1 Simulation Programs Used

Before including any source code, it would be interesting to mention the simulation programs used, introducing their main characteristics. Despite of their differences, all of them have the same purpose: to solve the electromagnetic wave equation in problems with different geometries and boundary conditions.

6.2.1.1 FEKO (FEldberechnung bei Körpern mit beliebiger Oberfläche)

FEKO is an abbreviation derived from the German phrase mentioned above, whose meaning is: Field computations involving bodies of arbitrary shape. As its name suggests, it can be used for the analysis of electromagnetic fields involving objects of any shape. Its simplicity of use was the key point in choosing this program.

The geometry of the problem can be easily introduced in two ways. The first one, called EditFEKO, consists of a text editor where different “cards” (a card is a command of the FEKO language) are used to describe the location of the different components of the system to simulate. As result of this edition a “.pre” FEKO file is created. This file also contains information about the fields to calculate, the feeding powers, etc.

The second one, FEMAP, makes use of a graphic environment, permitting us to create the description of the system with a 3D CAD/mesher tool. It is preferred for very complex geometries or for importing data from other CAD packages.

As the geometry of our problem is not very complicated, we are going to use EditFEKO files to describe it. Once the geometry is fully depicted, we use the card “EG” (End of Geometry) to indicate this fact to FEKO. Afterwards, we indicate the program how will be the feeding like, which fields have to be calculated and with how many points, etc. A whole description of all FEKO features and their application can be found in ***[6]***.

All the *".pre"* FEKO files generated in order to obtain different simulation results mentioned in this work can be found in this annex.

6.2.1.2 Advanced Design System (ADS)

This program is a very complete application for the design of microstrip line circuits. With its help we can work out the transmission characteristics of the circuit (S-Parameters, impedances, losses, etc.), and we can obtain standardized sketches of the design that can be sent directly to the manufacturer.

That’s why it has been used to test the behaviour of the final designs, containing the radiating elements and the feeding circuit. A quick reference about all its abilities can be consulted in ***[8]***.

6.2.1.3 LISSY

This is an application created by Dr. Eng. Thomas Binzer, director of this project, which allows the calculation of the effect of a lens over a radiating structure.

This program was designed to work jointly with FEKO, as it uses a FEKO ".ffe" file as input. Accordingly, the way in which geometry and properties of a lens are defined in LISSY is completely analogous to that one from EditFEKO. That is, the lens is fully characterized by means of different commands or "cards" introduced in a simple text document with ".pre" extension. Among these "cards", there is an "AF" card to establish the feeding of the lens. With this card, a file with ".ffe" extension containing the results for the far field calculations of a radiating structure obtained with FEKO is used to feed the lens.

Finally, LISSY produces an output file with ".out" extension as FEKO does. This file can be examined with a text editor, and contains the far field results from the combination of the radiating element from FEKO and the lens from LISSY.

For further details about the performance of LISSY, the original version in German of its manuals can be consulted in annex 4 of this project.

6.2.2 Single rectangular patch

The following document represents the EditFEKO file that allows simulate and calculate the far field components of a single rectangular patch antenna placed on the plane z=0.

```
** Default PRE file for radiation problems

** Patch Antenne (Erster Versuch)
** Creator of file: Julio Modrego Gil
** Date created: 10.2.2005
** Date last edited: 15.2.2005


** Variables

** Dimensions of Patch
#patch_W = **e-3        ** Breite des Patches
#patch_L = ***e-3       ** Länge des Patches

** Dimensions lines of transmision
#linie1_W = ****e-3       ** Breite Linienelementtrafo
#linie1_L = 0.600e-3      ** Länge Linienelementtrafo

#linie2_W = *********e-3                  ** Breite Linie Art 2
#linie2_L = #linie1_L + #Schnitt_L       ** Länge Linie Art 2

#linie3_W = ***e-3       ** Breite Mikrostreifenleitung
#linie3_L = 0.63e-3      ** Länge Mikrostreifenleitung


** Substrate parameters
#h = 0.127e-3            ** Height
#epsrSub = 3.05          ** Relative permitivity
#tanSub = 0.0013         ** Dämpfung Tangent
#epsEff = 2.470
** The substrate is an infinite plane in the plane z=0 *************

** Frequency and wavelength
#freq = 76.5e9          ** frequency in Hertz
#lam0 = #c0/#freq       ** wavelength in metre.
#lam_eff = #lam0 / sqrt(#epsEff)

** Dimensions of the Lambda/4 Trafo
#Trafo_W = **e-3        ** Breite des Trafos
#Trafo_L = 0.600e-3       **#lam_eff * 1.2 / 4    **0.600e-3        ** Länge des Trafos


** Segmentation parameters ****************************************
```

**#tri_len = #lam0 /4
#fine_tri = min(#lam0/2,2*#h)
#segl = #lam0/10
#segr = #lam0/500
IP #segr #fine_tri #segl #fine_tri

** Geometrical dimensions **********
** Wir wollen einen Patch mit seinem 2 Teilen (1/2 der #feed_L) des
** Anpasstrafos machen. Wir schaffen es mit der Karte PM (Polygon mesh
** into triangles). Wir skizieren die Punkte des Polygons
**
**
**
**
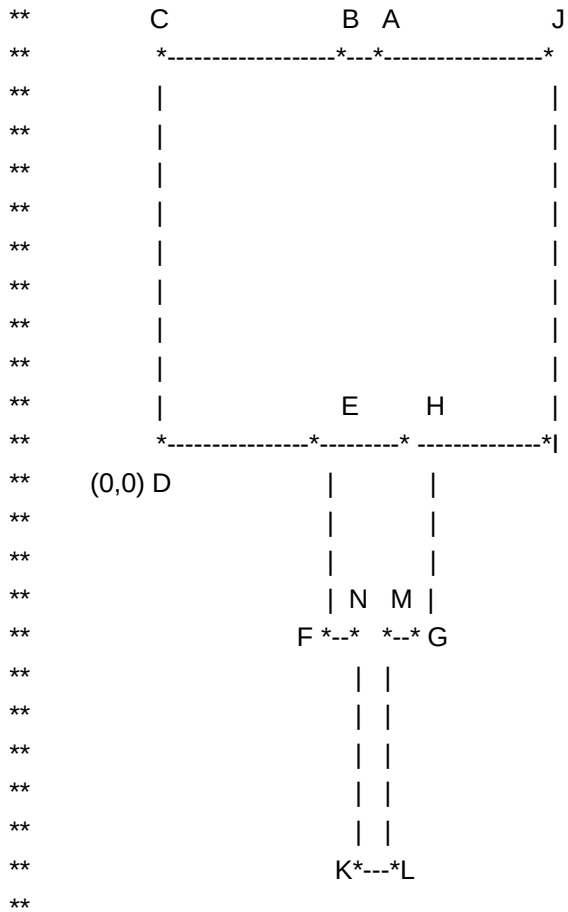

**

** 1.Definition des ersten Patches **********

** 1.a) Definition der Variablen der Pünkte **********
#A2x = #patch_W/2 + #linie3_W/2
#A2y = #patch_L
** z=0 für alle Punkte!!
#B2x = #patch_W/2 - #linie3_W/2
#B2y = #patch_L

```
#C2x = 0
#C2y = #patch_L

#D2x = 0
#D2y = 0

#E2x = #patch_W/2 - #linie1_W/2
#E2y = 0

#F2x = #patch_W/2 - #linie1_W/2
#F2y = -#linie1_L

#G2x = #patch_W/2 + #linie1_W/2
#G2y = -#linie1_L

#H2x = #patch_W/2 + #linie1_W/2
#H2y = 0

#I2x = #patch_W
#I2y = 0

#J2x = #patch_W
#J2y = #patch_L

#K2x = #F2x+#linie1_W/2-#linie3_W/2
#K2y = #F2y-#linie3_L

#L2x = #G2x-#linie1_W/2+#linie3_W/2
#L2y = #G2y-#linie3_L

#M2x = #G2x-#linie1_W/2+#linie3_W/2
#M2y = #G2y

#N2x = #F2x+#linie1_W/2-#linie3_W/2
#N2y = #F2y


** 1.b) Definition der Punkte (mit Hilfe der Variablen) *********
DP   A2                  #A2x     #A2y     0
DP   B2                  #B2x     #B2y     0
DP   C2                  #C2x     #C2y     0
DP   D2                  #D2x     #D2y     0
DP   E2                  #E2x     #E2y     0
DP   F2                  #F2x     #F2y     0
DP   G2                  #G2x     #G2y     0
DP   H2                  #H2x     #H2y     0
DP   I2                  #I2x     #I2y     0
DP   J2                  #J2x     #J2y     0
DP   K2                  #K2x     #K2y     0
```

```
DP   L2                  #L2x     #L2y     0
DP   M2                   #M2x     #M2y     0
DP   N2                   #N2x     #N2y     0


** 1.c) Definition der Fläche (triangulierte Fläche) ************
** Diese Struktur hat Label 2
LA   2
PM   A2   B2   C2   D2       E2       H2       I2       J2
PM   E2   F2   N2   K2       L2       M2       G2       H2


** 2. Definition der Anpassungstrafo (lambda/4) ***********************

** 2.a) Definition der Variablen der Punkte *********************
#A1x = #patch_W/2 - #linie3_W/2
#A1y = -(#linie1_L +#linie3_L)
                              ** z=0 für alle Punkte!!
#B1x = #patch_W/2 - #linie3_W/2
#B1y = -1.75 * (#linie1_L +#linie3_L)

#C1x = #patch_W/2 - #Trafo_W/2
#C1y = -1.75 * (#linie1_L +#linie3_L)

#D1x = #patch_W/2 - #Trafo_W/2
#D1y = -1.75 * (#linie1_L +#linie3_L) - #Trafo_L

#E1x = #patch_W/2
#E1y = -1.75 * (#linie1_L +#linie3_L) - #Trafo_L

#F1x = #patch_W/2 + #Trafo_W/2
#F1y = -1.75 * (#linie1_L +#linie3_L) - #Trafo_L

#G1x = #patch_W/2 + #Trafo_W/2
#G1y = -1.75 * (#linie1_L +#linie3_L)

#H1x = #patch_W/2 + #linie3_W/2
#H1y = -1.75 * (#linie1_L +#linie3_L)

#I1x = #patch_W/2 + #linie3_W/2
#I1y = -(#linie1_L +#linie3_L)


** 2.b) Definition der Punkte ***********************************
DP   A1                  #A1x     #A1y     0
DP   B1                  #B1x     #B1y     0
DP   C1                  #C1x     #C1y     0
DP   D1                  #D1x     #D1y     0
DP   E1                  #E1x     #E1y     0
```

```
DP   F1                  #F1x     #F1y     0
DP   G1                  #G1x     #G1y     0
DP   H1                  #H1x     #H1y     0
DP   I1                  #I1x     #I1y     0


** 2.c) Definition der triangulierte Fläche des Trafos **********
** Diese Struktur hat Label 1
LA   1
PM   A1   B1   C1   D1       E1       F1       G1       H1       I1


** End of geometry
**EG   1    0    0        0    1.0e-7                                                    1
EG   1    0    0        0                                                    1

*************************************************************************

** ** Wir definieren unser planare Multilayer Substrate ******************
**
GF   10   1            0            1        1              0        0
                      #h        2.85      1              0.0013

** We set the frequency of the circuit
FR   21   0              70E9             80E9


** We have to feed the circuit (AE Card):
AE   0    D1   F1   3        1        0        50


** Calculation of the Gain of the Antenna:
FF   1    91   9    1        -90      0        1        45


** ** Calculation of the S-Parameters:
SP                       50



** End
EN
```

6.2.3 Array 1x16

The present code defines the geometry, the feeding and the way in which far field calculations are made for the array of 16 x 1 patches along the Y-axe.

```
** Default PRE file for radiation problems

** Patch Antenne
** Creator of file: Julio Modrego Gil
** Date created: 10.2.2005
** Date last edited: 23.2.2005

** Variables*****************************************************************

** Dimensions of Patch
#patch_W = **e-3        ** Breite des Patches
#patch_L = **e-3        ** Längre des Patches

** Dimensions of the Cut of the 16th Patch
#Schnitt_W = **e-3      ** Breite des Schnitts
#Schnitt_L = **e-3      ** Länge des Schnitts

** Dimensions lines of transmision
#linie1_W = **e-3       ** Breite Linie Art 1
#linie1_L = 1.230e-3      ** Länge Linie Art 1 (0.974 für opt)

#linie2_W = **e-3                ** Breite Linie Art 2
#linie2_L = #linie1_L + #Schnitt_L       ** Länge Linie Art 2

** Distances for the displacements with TG Card
#d_y_Achse = #patch_L + #linie1_L   ** Fahrtabstand über y-Achse
#d_x_Achse = **e-3              ** Fahrtabstand über x-Achse

** Substrate parameters
#h = 0.127e-3           ** Height
#epsrSub = 3.05          ** Relative permitivity
#tanSub = 0.0013         ** Dämpfung Tangent
#epsEff = 2.470
** The substrate an infinite plane in the plane z=0 *************

**   Frequency and wavelength
#freq = 76.5e9          ** frequency in Hertz
#lam0 = #c0/#freq       ** wavelength in metre.
#lam_eff = #lam0 / sqrt(#epsEff)

** Dimensions of the Lambda/4 Trafo
#Ent_Tr = 1.75 * #linie1_L
```

```
#Trafo_W = **e-3        ** Breite des Trafos
#Trafo_L = 0.600e-3       **#lam_eff * 1.2 / 4    **0.600e-3        ** Länge des Trafos


** Segmentation parameters ********************************************

**#tri_len = #lam0 /4
#fine_tri = min(#lam0/2,2*#h)
#segl = #lam0/10
#segr = #lam0/500
IP                      #segr     #fine_tri #segl     #fine_tri


** Geometrical dimensions *********************************************
** Wir wollen einen Patch mit seinem 2 Teilen (1/2 der #feed_L) des
** Anpasstrafos machen. Wir schaffen es mit der Karte PM (Polygon mesh
** into triangles). Wir skizieren die Punkte des Polygons
**
**
**
**             C       B          A       J
**              *------*---------*------*
**              |                       |
**              |                       |
**              |                       |
**              |                       |
**              |                       |
**              |                       |
**              |                       |
**              |                       |
**              |       E          H      |
**              *------*---------*------*
**             D        |          |        I
**                      |          |
**                      |          |
**                      |          |
**                     *---------*
**                      F          G
**
**


** 1.Definition des ersten Patches ************************************

** 1.a) Definition der Variablen der Pünkte *********************

#A2x = #patch_W/2 + #linie1_W/2
#A2y = #patch_L
                              ** z=0 für alle Punkte!!
```

```
#B2x = #patch_W/2 - #linie1_W/2
#B2y = #patch_L

#C2x = 0
#C2y = #patch_L

#D2x = 0
#D2y = 0

#E2x = #patch_W/2 - #linie1_W/2
#E2y = 0

#F2x = #patch_W/2 - #linie1_W/2
#F2y = -#linie1_L

#G2x = #patch_W/2 + #linie1_W/2
#G2y = -#linie1_L

#H2x = #patch_W/2 + #linie1_W/2
#H2y = 0

#I2x = #patch_W
#I2y = 0

#J2x = #patch_W
#J2y = #patch_L


** 1.b) Definition der Punkte (mit Hilfe der Variablen) *********
DP   A2                  #A2x     #A2y     0
DP   B2                  #B2x     #B2y     0
DP   C2                  #C2x     #C2y     0
DP   D2                  #D2x     #D2y     0
DP   E2                  #E2x     #E2y     0
DP   F2                  #F2x     #F2y     0
DP   G2                  #G2x     #G2y     0
DP   H2                  #H2x     #H2y     0
DP   I2                  #I2x     #I2y     0
DP   J2                  #J2x     #J2y     0


** 1.c) Definition der Fläche (triangulierte Fläche) ************
** Diese Struktur hat Label 2
LA   2
PM   A2   B2   C2   D2       E2       F2       G2       H2       I2       J2


** 2. Definition der Anpassungstrafo (lambda/4) ***********************
** 2.a) Definition der Variablen der Punkte *********************
```

```
#A1x = #patch_W/2 - #linie1_W/2
#A1y = -#linie1_L
                                ** z=0 für alle Punkte!!
#B1x = #patch_W/2 - #linie1_W/2
#B1y = -#Ent_Tr

#C1x = #patch_W/2 - #Trafo_W/2
#C1y = -#Ent_Tr

#D1x = #patch_W/2 - #Trafo_W/2
#D1y = -#Ent_Tr - #Trafo_L

#E1x = #patch_W/2
#E1y = -#Ent_Tr - #Trafo_L

#F1x = #patch_W/2 + #Trafo_W/2
#F1y = -#Ent_Tr - #Trafo_L

#G1x = #patch_W/2 + #Trafo_W/2
#G1y = -#Ent_Tr

#H1x = #patch_W/2 + #linie1_W/2
#H1y = -#Ent_Tr

#I1x = #patch_W/2 + #linie1_W/2
#I1y = -#linie1_L

** 2.b) Definition der Punkte ***********************************
DP   A1                  #A1x     #A1y     0
DP   B1                  #B1x     #B1y     0
DP   C1                  #C1x     #C1y     0
DP   D1                  #D1x     #D1y     0
DP   E1                  #E1x     #E1y     0
DP   F1                  #F1x     #F1y     0
DP   G1                  #G1x     #G1y     0
DP   H1                  #H1x     #H1y     0
DP   I1                 #I1x     #I1y     0


** 2.c) Definition der triangulierte Fläche des Trafos **********

** Diese Struktur hat Label 1
LA   1
PM   A1   B1   C1   D1       E1       F1       G1       H1       I1


** 3. Wir kopieren die elementare Struktur 13mal **********************
TG   14   2    2    1    0    0        0        0        0        #d_y_Achse0
** Nach allen diesen Sachen haben wir 14 Patches über dem Y-Achse
```

```
** 4. Wir machen den 16. Element (16. Patch) **************************

** 4.a) Definition der Variablen der Punkte **********************

#Abst_y = 14 * #linie1_L + 15 * #patch_L
** Abstand wir sollen unser Struktur über den y-Achse bewegen

#A16x = #patch_W
#A16y = #Abst_y + #linie1_L
                              ** z=0 für alle Punkte!!
#B16x = #patch_W
#B16y = #patch_L + #linie1_L + #Abst_y

#C16x = 0
#C16y = #patch_L + #linie1_L + #Abst_y

#D16x = 0
#D16y = #linie1_L + #Abst_y

#E16x = #patch_W/2 - #linie2_W/2 - #Schnitt_W
#E16y = #linie1_L + #Abst_y

#F16x = #patch_W/2 - #linie2_W/2 - #Schnitt_W
#F16y = #linie2_L + #Abst_y

#G16x = #patch_W/2 - #linie2_W/2
#G16y = #linie2_L + #Abst_y

#H16x = #patch_W/2 - #linie2_W/2
#H16y = #Abst_y

#I16x = #patch_W/2 + #linie2_W/2
#I16y = #Abst_y

#J16x = #patch_W/2 + #linie2_W/2
#J16y = #linie2_L + #Abst_y

#K16x = #patch_W/2 + #linie2_W/2 + #Schnitt_W
#K16y = #linie2_L + #Abst_y

#L16x = #patch_W/2 + #linie2_W/2 + #Schnitt_W
#L16y = #linie1_L + #Abst_y


** 6.b) Definition der Punkte des 16. Patches ********************

DP   A16                  #A16x     #A16y     0
```

```
DP   B16                #B16x     #B16y     0
DP   C16                #C16x     #C16y     0
DP   D16                #D16x     #D16y     0
DP   E16                #E16x     #E16y     0
DP   F16                #F16x     #F16y     0
DP   G16                #G16x     #G16y     0
DP   H16                #H16x     #H16y     0
DP   I16                #I16x     #I16y     0
DP   J16                #J16x     #J16y     0
DP   K16                #K16x     #K16y     0
DP   L16                #L16x     #L16y     0


** 6.c) Definition der Fläche des 16. Patches ******************

** Dieser Patch het Label 17
LA   17
PM   A16  B16  C16  D16      E16      F16      G16      H16      I16      J16      K16
L16


** 7. Definition of the segments of feeding ***************************

** These segments go from a point over the ground plane to the point 1
DP   FEED1               #E1x      #E1y      -#h

** Definition of the feeding segments (Label 18):
LA   18
BL   FEED1E1


****************************************************************************
** End of geometry
EG   1    0    0        0                                                  1
****************************************************************************

** ** Wir definieren unser planare Multilayer Substrate ******************
**

GF   10   1            0            1        1                      0
                      #h        2.85      1              0.004

** We set the frequency of the circuit *********************************

FR   5    0              #freq-2e9 1e9


** We have to feed the circuit (A1 card): ****************************
** First we assume that the voltage source is going to be in one side
```

```
** of the first patch. This point is the point E1. In this point we
** to define a segment or group of segments!!

A1   0    18              0.5      0                          50


** Source of power with no internal impedance ************************

** PW   2    0               1        50       0


** Calculation of the Gain of the Antenna: ****************************

FF   1    91   9    1        -90      0        2        45


** Calculation of the S-Parameters: ***********************************

SP                      50


** End ****************************************************************

EN
```

6.2.4 Array 20x16

The following code implements the array of 20x16 patches. It has been constructed using the symmetry card SY of FEKO. FEKO presents three possible symmetry modes: Geometrical, magnetical and electrical. The one used here is geometrical, as no magnetic or electric walls can be used to obtain the symmetry.

```
** Default PRE file for radiation problems

** Patch Antenne
** Creator of file: Julio Modrego Gil
** Date created: 10.2.2005
** Date last edited: 21.3.2005

** Variables**********************************************************************
#npuf = 100

** Dimensions of Patch
#patch_W = **e-3        ** Breite des Patches
#patch_L = **e-3        ** Längre des Patches

** Dimensions of the Cut of the 16th Patch
#Schnitt_W = **e-3     ** Breite des Schnitts
#Schnitt_L = **e-3              ** Länge des Schnitts

** Dimensions lines of transmision
#linie1_W = **e-3       ** Breite Linienelementtrafo
#linie1_L = 0.600e-3       ** Länge Linienelementtrafo

#linie2_W = **e-3                    ** Breite Linie Art 2
#linie2_L = #linie1_L + #Schnitt_L        ** Länge Linie Art 2

#linie3_W = **e-3       ** Breite Mikrostreifenleitung
#linie3_L = 0.600e-3       ** Länge Mikrostreifenleitung

** Distances for the displacements with TG Card
#d_y = #patch_L + #linie1_L  +#linie3_L  ** Fahrtabstand über y-Achse
#d_x = **e-3                        ** Fahrtabstand über x-Achse
#d_x_1 = -#patch_W/2
#d_x_2 = #d_x/2

** Substrate parameters
#h = 0.127e-3            ** Height
#epsrSub = 3.05          ** Relative permitivity
#tanSub = 0.0013         ** Dämpfung Tangent
** The substrate is an infinite plane in the plane z=0 *************

** Frequency and wavelength
```

```
#freq = 76.5e9          ** frequency in Hertz
#lam0 = #c0/#freq       ** wavelength in metre.

** Dimensions of the Lambda/4 Trafo
#Ent_Tr = 1.75 * (#linie1_L + #linie3_L)   ** Entfernung zwischen Trafo und 1. Patch
#Trafo_W = **e-3        ** Breite des Trafos
#Trafo_L = 0.600e-3       ** Länge des Trafos

** Segmentation parameters ********************************************

**#tri_len = #lam0 /4
#fine_tri = min(#lam0/2,3*#h)
#segl = #lam0/10
#segr = #lam0/500
IP                      #segr     #fine_tri #segl     #fine_tri
** Geometrical dimensions ********************************************
** Wir wollen einen Patch mit seinem 2 Teilen (1/2 der #feed_L) des
** Anpasstrafos machen. Wir schaffen es mit der Karte PM (Polygon mesh
** into triangles). Wir skizieren die Punkte des Polygons
**
**
**
**            C          B    A          J
**             *---------*---*---------*
**             |                       |
**             |                       |
**             |                       |
**             |                       |
**             |                       |
**             |                       |
**             |                       |
**             |                       |
**             |       E         H     |
**             *------*---------*------*
**             D      |         |       I
**                    |         |
**                    |         |
**                    | N   M   |
**                 F *--*   *--* G
**                      |   |
**                      |   |
**                      |   |
**                      |   |
**                      |   |
**                    K*---*L
**
```

```
** 1.Definition des ersten Patches ************************************

** 1.a) Definition der Variablen der Pünkte **********************

#A2x = #patch_W/2 + #linie3_W/2
#A2y = #patch_L
                                ** z=0 für alle Punkte!!
#B2x = #patch_W/2 - #linie3_W/2
#B2y = #patch_L

#C2x = 0
#C2y = #patch_L

#D2ax = 0
#D2ay = 0

#E2ax = #patch_W/2 - #linie1_W/2
#E2ay = 0

#F2ax = #patch_W/2 - #linie1_W/2
#F2ay = -#linie1_L

#G2x = #patch_W/2 + #linie1_W/2
#G2y = -#linie1_L

#H2x = #patch_W/2 + #linie1_W/2
#H2y = 0

#I2x = #patch_W
#I2y = 0

#J2x = #patch_W
#J2y = #patch_L

#K2x = #F2ax + #linie1_W/2 - #linie3_W/2
#K2y = #F2ay - #linie3_L

#L2x = #G2x - #linie1_W/2 + #linie3_W/2
#L2y = #G2y - #linie3_L

#M2x = #G2x - #linie1_W/2 + #linie3_W/2
#M2y = #G2y

#N2x = #F2ax + #linie1_W/2 - #linie3_W/2
#N2y = #F2ay


** 1.b) Definition der Punkte (mit Hilfe der Variablen) *********
```

```
** Diese Struktur hat Label 1002
LA   1002

DP   A2                  #A2x      #A2y      0
DP   B2                  #B2x      #B2y      0
DP   C2                  #C2x      #C2y      0
DP   D2a                 #D2ax     #D2ay     0
DP   E2a                 #E2ax     #E2ay     0
DP   F2a                 #F2ax     #F2ay     0
DP   G2                  #G2x      #G2y      0
DP   H2                  #H2x      #H2y      0
DP   I2                  #I2x      #I2y      0
DP   J2                  #J2x      #J2y      0
DP   K2                  #K2x      #K2y      0
DP   L2                  #L2x      #L2y      0
DP   M2                  #M2x      #M2y      0
DP   N2                  #N2x      #N2y      0


** 1.c) Definition der Fläche (triangulierte Fläche) ************

PM   A2   B2   C2   D2a      E2a      H2       I2       J2
PM   E2a  F2a  N2   K2       L2       M2       G2       H2


** 2. Definition der Anpassungstrafo (lambda/4) ************************

** 2.a) Definition der Variablen der Punkte **********************

#A1x = #patch_W/2 - #linie3_W/2
#A1y = -(#linie1_L +#linie3_L)
                                ** z=0 für alle Punkte!!
#B1x = #patch_W/2 - #linie3_W/2
#B1y = -#Ent_Tr

#C1x = #patch_W/2 - #Trafo_W/2
#C1y = -#Ent_Tr

#D1x = #patch_W/2 - #Trafo_W/2
#D1y = -#Ent_Tr  - #Trafo_L

** #E1x = #patch_W/2
** #E1y = -#Ent_Tr  - #Trafo_L

#F1x = #patch_W/2 + #Trafo_W/2
#F1y = -#Ent_Tr  - #Trafo_L

#G1x = #patch_W/2 + #Trafo_W/2
#G1y = -#Ent_Tr
```

```
#H1x = #patch_W/2 + #linie3_W/2
#H1y = -#Ent_Tr

#I1x = #patch_W/2 + #linie3_W/2
#I1y = -(#linie1_L +#linie3_L)


** 2.b) Definition der Punkte ***********************************

** Diese Struktur hat Label 1001

LA   1001

DP   A1                #A1x     #A1y     0
DP   B1                #B1x     #B1y     0
DP   C1                #C1x     #C1y     0

** Diese Punkte werden die Struktur Speisen. Label 100
LA   100

DP   D1                #D1x     #D1y     0
** DP   E1                #E1x     #E1y     0
DP   F1                #F1x     #F1y     0

** Die andere Punkte haben das gleich Label as früher (Label 1001)
LA   1001

DP   G1                #G1x     #G1y     0
DP   H1                #H1x     #H1y     0
DP   I1                #I1x     #I1y     0


** Wir kopieren diese Punkte 19 mal um alle Spalten zu speisen ********

LA   200
DP   D2                #D1x     #D1y     0
** DP   E2                #E1x     #E1y     0
DP   F2                #F1x     #F1y     0

LA   300
DP   D3                #D1x     #D1y     0
** DP   E3                #E1x     #E1y     0
DP   F3                #F1x     #F1y     0

LA   400
DP   D4                #D1x     #D1y     0
** DP   E4                #E1x     #E1y     0
DP   F4                #F1x     #F1y     0
```

```
LA   500
DP   D5              #D1x     #D1y     0
** DP   E5            #E1x     #E1y     0
DP   F5              #F1x     #F1y     0

LA   600
DP   D6              #D1x     #D1y     0
** DP   E6            #E1x     #E1y     0
DP   F6              #F1x     #F1y     0

LA   700
DP   D7              #D1x     #D1y     0
** DP   E7            #E1x     #E1y     0
DP   F7              #F1x     #F1y     0

LA   800
DP   D8              #D1x     #D1y     0
** DP   E8            #E1x     #E1y     0
DP   F8              #F1x     #F1y     0

LA   900
DP   D9              #D1x     #D1y     0
** DP   E9            #E1x     #E1y     0
DP   F9              #F1x     #F1y     0

LA   1000
DP   D10             #D1x     #D1y     0
** DP   E10           #E1x     #E1y     0
DP   F10             #F1x     #F1y     0

LA   1100
DP   D11             #D1x     #D1y     0
** DP   E11           #E1x     #E1y     0
DP   F11             #F1x     #F1y     0

LA   1200
DP   D12             #D1x     #D1y     0
** DP   E12           #E1x     #E1y     0
DP   F12             #F1x     #F1y     0

LA   1300
DP   D13             #D1x     #D1y     0
** DP   E13           #E1x     #E1y     0
DP   F13             #F1x     #F1y     0

LA   1400
DP   D14             #D1x     #D1y     0
** DP   E14           #E1x     #E1y     0
```

```
DP   F14                #F1x     #F1y     0

LA   1500
DP   D15                #D1x     #D1y     0
** DP   E15                #E1x     #E1y     0
DP   F15                #F1x     #F1y     0

LA   1600
DP   D16                #D1x     #D1y     0
** DP   E16                #E1x     #E1y     0
DP   F16                #F1x     #F1y     0

LA   1700
DP   D17                #D1x     #D1y     0
** DP   E17                #E1x     #E1y     0
DP   F17                #F1x     #F1y     0

LA   1800
DP   D18                #D1x     #D1y     0
** DP   E18                #E1x     #E1y     0
DP   F18                #F1x     #F1y     0

LA   1900
DP   D19                #D1x     #D1y     0
** DP   E19                #E1x     #E1y     0
DP   F19                #F1x     #F1y     0

LA   2000
DP   D20                #D1x     #D1y     0
** DP   E20                #E1x     #E1y     0
DP   F20                #F1x     #F1y     0

** Ende der Definition der Speisenpunkte ******************************


** 2.c) Definition der triangulierte Fläche des Trafos **********
** Diese Struktur hat Label 1001
LA   1001
PM   A1   B1   C1   D1       F1       G1       H1       I1


** 3. Wir kopieren die elementare Struktur 14mal **********************
TG   14   1002 1002 1    0                                   #d_y
** Nach allen diesen Sachen haben wir 14 Patches über dem Y-Achse


** 4. Wir machen den 16. Element (16. Patch) **************************

** 4.a) Definition der Variablen der Punkte **********************
```

```
#Abst_y = 14 * (#linie1_L +#linie3_L) + 15 * #patch_L
** Abstand wir sollen unser Struktur über den y-Achse bewegen

#A16x = #patch_W
#A16y = #Abst_y + (#linie1_L +#linie3_L)
                                ** z=0 für alle Punkte!!
#B16x = #patch_W
#B16y = #patch_L + (#linie1_L +#linie3_L) + #Abst_y

#C16x = 0
#C16y = #patch_L + (#linie1_L +#linie3_L) + #Abst_y

#D16ax = 0
#D16ay = (#linie1_L +#linie3_L) + #Abst_y

#E16ax = #patch_W/2 - #Schnitt_W/2
#E16ay = (#linie1_L +#linie3_L) + #Abst_y

#F16ax = #patch_W/2 - #Schnitt_W/2
#F16ay = (#linie2_L +#linie3_L) + #Abst_y

#G16x = #patch_W/2 - #linie3_W/2
#G16y = (#linie2_L +#linie3_L) + #Abst_y

#H16x = #patch_W/2 - #linie3_W/2
#H16y = #Abst_y

#I16x = #patch_W/2 + #linie3_W/2
#I16y = #Abst_y

#J16x = #patch_W/2 + #linie3_W/2
#J16y = (#linie2_L +#linie3_L) + #Abst_y

#K16x = #patch_W/2 + #Schnitt_W/2
#K16y = (#linie2_L +#linie3_L) + #Abst_y

#L16x = #patch_W/2 + #Schnitt_W/2
#L16y = (#linie1_L +#linie3_L) + #Abst_y


** 4.b) Definition der Punkte des 16. Patches ******************
** Dieser Patch het Label 1017
LA   1017
DP   A16              #A16x    #A16y    0
DP   B16              #B16x    #B16y    0
DP   C16              #C16x    #C16y    0
DP   D16a              #D16ax    #D16ay    0
DP   E16a              #E16ax    #E16ay    0
DP   F16a              #F16ax    #F16ay    0
```

```
DP   G16                #G16x     #G16y     0
DP   H16                #H16x     #H16y     0
DP   I16                #I16x     #I16y     0
DP   J16                #J16x     #J16y     0
DP   K16                #K16x     #K16y     0
DP   L16                #L16x     #L16y     0


** 4.c) Definition der Fläche des 16. Patches ******************

PM   A16  B16  C16  D16a      E16a      F16a      G16       H16       I16       J16
K16       L16


** 5. Wir repetieren diese Struktur  9mal in der x-Richtung ***********
#Tr_x = #d_x_1 + #d_x_2

** Am Anfang verschieben wir den Sturuktur Achse auf den y-Achse
TG   0    1001 1017 0    0                          #Tr_x

** Am Ende kopieren wir alles 9 mal in der x-achse Richtung
TG   9    1001 1017 1000 0                           #d_x


** 6. Nutzung von Simetry Karte ************************************

SY   1    1    0    0    10000


** 7. Verschiebung der Speisenpunkte der Spalten **********************

** Verschiebung der Speisenpunkte ************************************

** 1. Spalte
#Tr_x = #d_x_1 + #d_x_2
TP       100  100  0                              #Tr_x
** 2. Spalte
#Tr_x = #d_x + #d_x_1 + #d_x_2
TP       200  200  0                              #Tr_x
** 3. Spalte
#Tr_x = #Tr_x + #d_x
TP       300  300  0                              #Tr_x
** 4. Spalte
#Tr_x = #Tr_x + #d_x
TP       400  400  0                              #Tr_x
** 5. Spalte
#Tr_x = #Tr_x + #d_x
TP       500  500  0                              #Tr_x
```

```
** 6. Spalte
#Tr_x = #Tr_x + #d_x
TP       600  600  0                          #Tr_x
** 7. Spalte
#Tr_x = #Tr_x + #d_x
TP       700  700  0                          #Tr_x
** 8. Spalte
#Tr_x = #Tr_x + #d_x
TP       800  800  0                          #Tr_x
** 9. Spalte
#Tr_x = #Tr_x + #d_x
TP       900  900  0                          #Tr_x
** 10. Spalte
#Tr_x = #Tr_x + #d_x
TP       1000 1000 0                           #Tr_x
** -11. Spalte (die am rechsten des y-Achses liegt)
#Tr_x = #d_x_1 - #d_x_2
TP       1100 1100 0                           #Tr_x
** -12. Spalte
#Tr_x = #Tr_x - #d_x
TP       1200 1200 0                           #Tr_x
** -13. Spalte
#Tr_x = #Tr_x - #d_x
TP       1300 1300 0                           #Tr_x
** -14. Spalte
#Tr_x = #Tr_x - #d_x
TP       1400 1400 0                           #Tr_x
** -15. Spalte
#Tr_x = #Tr_x - #d_x
TP       1500 1500 0                           #Tr_x
** -16. Spalte
#Tr_x = #Tr_x - #d_x
TP       1600 1600 0                           #Tr_x
** -17. Spalte
#Tr_x = #Tr_x - #d_x
TP       1700 1700 0                           #Tr_x
** -18. Spalte
#Tr_x = #Tr_x - #d_x
TP       1800 1800 0                           #Tr_x
** -19. Spalte
#Tr_x = #Tr_x - #d_x
TP       1900 1900 0                           #Tr_x
** -20. Spalte
#Tr_x = #Tr_x - #d_x
TP       2000 2000 0                           #Tr_x


************************************************************************
** End of geometry ******************************************************
```

```
EG  1   0   0       0                                                   1

***************************************************************************


** Wir definieren unser planare Multilayer Substrate ******************

GF  10  1           0           1       1               0       0
                    #h      #epsrSub    1               #tanSub

** We set the frequency of the circuit *********************************
FR  2   0               71E9    5.5E9

** We have to feed the circuit (20mal AE card) ************************

AE  0   D1  F1  3       1       0       50
AE  1   D2  F2  3       1       0       50
AE  1   D3  F3  3       1       0       50
AE  1   D4  F4  3       1       0       50
AE  1   D5  F5  3       1       0       50
AE  1   D6  F6  3       1       0       50
AE  1   D7  F7  3       1       0       50
AE  1   D8  F8  3       1       0       50
AE  1   D9  F9  3       1       0       50
AE  1   D10 F10 3       1       0       50
AE  1   D11 F11 3       1       0       50
AE  1   D12 F12 3       1       0       50
AE  1   D13 F13 3       1       0       50
AE  1   D14 F14 3       1       0       50
AE  1   D15 F15 3       1       0       50
AE  1   D16 F16 3       1       0       50
AE  1   D17 F17 3       1       0       50
AE  1   D18 F18 3       1       0       50
AE  1   D19 F19 3       1       0       50
AE  1   D20 F20 3       1       0       50


** Calculation of the Gain of the Antenna:
FF  1   181 2   1       -45     0       0.5     90


** Calculation of the S-Parameters:
SP                      50


** End
EN
```

6.2.5 Array 24x16

In this point, the ".pre" FEKO file defining the 24x16 array is presented. Again, we have made use of the symmetry card SY to save time and usage of memory during computation.

```
** Default PRE file for radiation problems


** Patch Antenne
** Creator of file: Julio Modrego Gil
** Date created: 10.2.2005
** Date last edited: 21.3.2005


** Variables
#npuf = 100

** Dimensions of Patch
#patch_W = xxxe-3        ** Breite des Patches
#patch_L = xxxe-3        ** Längre des Patches

** Dimensions of the Cut of the 16th Patch
#Schnitt_W = xxxe-3 + yyye-3     ** Breite des Schnitts
#Schnitt_L = xxxe-3              ** Länge des Schnitts

** Dimensions lines of transmision
#linie1_W = xxxe-3       ** Breite Linienelementtrafo
#linie1_L = 0.600e-3      ** Länge Linienelementtrafo

#linie2_W = xxxe-3                  ** Breite Linie Art 2
#linie2_L = #linie1_L + #Schnitt_L       ** Länge Linie Art 2

#linie3_W = xxxe-3       ** Breite Mikrostreifenleitung
#linie3_L = 0.600e-3      ** Länge Mikrostreifenleitung

** Distances for the displacements with TG Card
#d_y = #patch_L + #linie1_L  +#linie3_L  ** Fahrtabstand über y-Achse
#d_x = xxxe-3                       ** Fahrtabstand über x-Achse
#d_x_1 = -#patch_W/2
#d_x_2 = #d_x/2

** Substrate parameters
#h = 0.127e-3            ** Height
#epsrSub = 3.05           ** Relative permitivity
#tanSub = 0.0013          ** Dämpfung Tangent
** The substrate an infinite plane in the plane z=0 *************
```

```
** Frequency and wavelength
#freq = 76.5e9          ** frequency in Hertz
#lam0 = #c0/#freq       ** wavelength in metre.

** Dimensions of the Lambda/4 Trafo
#Ent_Tr = 1.75 * (#linie1_L + #linie3_L)  ** Entfernung zwischen Trafo und 1. Patch
#Trafo_W = 0.190e-3       ** Breite des Trafos
#Trafo_L = 0.600e-3       ** Länge des Trafos


** Segmentation parameters ******************************************
**#tri_len = #lam0 /4
#fine_tri = min(#lam0/2,3*#h)
#segl = #lam0/10
#segr = #lam0/500
IP                      #segr     #fine_tri #segl     #fine_tri


** Geometrical dimensions *******************************************
** Wir wollen einen Patch mit seinem 2 Teilen (1/2 der #feed_L) des
** Anpasstrafos machen. Wir schaffen es mit der Karte PM (Polygon mesh
** into triangles). Wir skizieren die Punkte des Polygons
**
**
**
**            C          B   A          J
**             *---------*---*---------*
**             |                       |
**             |                              |
**             |                       |
**             |                       |
**             |                       |
**             |                       |
**             |                       |
**             |                       |
**             |       E          H    |
**             *------*---------*------*
**             D       |          |      I
**                     |          |
**                     |          |
**                     | N   M    |
**                  F *--*   *--* G
**                       |   |
**                       |   |
**                       |   |
**                       |   |
**                       |   |
**                     K*---*L
```

```
**


** 1.Definition des ersten Patches ************************************
** 1.a) Definition der Variablen der Pünkte **********************
#A2x = #patch_W/2 + #linie3_W/2
#A2y = #patch_L
                                    ** z=0 für alle Punkte!!
#B2x = #patch_W/2 - #linie3_W/2
#B2y = #patch_L

#C2x = 0
#C2y = #patch_L

#D2ax = 0
#D2ay = 0

#E2ax = #patch_W/2 - #linie1_W/2
#E2ay = 0

#F2ax = #patch_W/2 - #linie1_W/2
#F2ay = -#linie1_L

#G2x = #patch_W/2 + #linie1_W/2
#G2y = -#linie1_L

#H2x = #patch_W/2 + #linie1_W/2
#H2y = 0

#I2x = #patch_W
#I2y = 0

#J2x = #patch_W
#J2y = #patch_L

#K2x = #F2ax + #linie1_W/2 - #linie3_W/2
#K2y = #F2ay - #linie3_L

#L2x = #G2x - #linie1_W/2 + #linie3_W/2
#L2y = #G2y - #linie3_L

#M2x = #G2x - #linie1_W/2 + #linie3_W/2
#M2y = #G2y

#N2x = #F2ax + #linie1_W/2 - #linie3_W/2
#N2y = #F2ay


** 1.b) Definition der Punkte (mit Hilfe der Variablen) *********
```

```
** Diese Struktur hat Label 1002
LA   1002
DP   A2                  #A2x      #A2y      0
DP   B2                  #B2x      #B2y      0
DP   C2                  #C2x      #C2y      0
DP   D2a                  #D2ax     #D2ay     0
DP   E2a                  #E2ax     #E2ay     0
DP   F2a                  #F2ax     #F2ay     0
DP   G2                  #G2x      #G2y      0
DP   H2                  #H2x      #H2y      0
DP   I2                 #I2x      #I2y      0
DP   J2                  #J2x      #J2y      0
DP   K2                  #K2x      #K2y      0
DP   L2                 #L2x      #L2y      0
DP   M2                  #M2x      #M2y      0
DP   N2                  #N2x      #N2y      0


** 1.c) Definition der Fläche (triangulierte Fläche) ************
PM   A2   B2   C2   D2a       E2a       H2        I2        J2
PM   E2a  F2a  N2   K2        L2        M2        G2        H2


** 2. Definition der Anpassungstrafo (lambda/4) ************************
** 2.a) Definition der Variablen der Punkte *********************
#A1x = #patch_W/2 - #linie3_W/2
#A1y = -(#linie1_L +#linie3_L)
                              ** z=0 für alle Punkte!!
#B1x = #patch_W/2 - #linie3_W/2
#B1y = -#Ent_Tr

#C1x = #patch_W/2 - #Trafo_W/2
#C1y = -#Ent_Tr

#D1x = #patch_W/2 - #Trafo_W/2
#D1y = -#Ent_Tr  - #Trafo_L

** #E1x = #patch_W/2
** #E1y = -#Ent_Tr  - #Trafo_L

#F1x = #patch_W/2 + #Trafo_W/2
#F1y = -#Ent_Tr  - #Trafo_L

#G1x = #patch_W/2 + #Trafo_W/2
#G1y = -#Ent_Tr

#H1x = #patch_W/2 + #linie3_W/2
#H1y = -#Ent_Tr
```

```
#I1x = #patch_W/2 + #linie3_W/2
#I1y = -(#linie1_L +#linie3_L)


** 2.b) Definition der Punkte ***********************************
** Diese Struktur hat Label 1001
LA   1001
DP   A1                #A1x     #A1y     0
DP   B1                #B1x     #B1y     0
DP   C1                #C1x     #C1y     0

** Diese Punkte werden die Struktur Speisen. Label 100
LA   100
DP   D1                #D1x     #D1y     0
** DP   E1               #E1x     #E1y     0
DP   F1                #F1x     #F1y     0

** Die andere Punkte haben das gleich Label as früher (Label 1001)
LA   1001
DP   G1                #G1x     #G1y     0
DP   H1                #H1x     #H1y     0
DP   I1                #I1x     #I1y     0


** Wir kopieren diese Punkte 23 mal um alle Spalten zu speisen ********
LA   200
DP   D2                #D1x     #D1y     0
** DP   E2               #E1x     #E1y     0
DP   F2                #F1x     #F1y     0

LA   300
DP   D3                #D1x     #D1y     0
** DP   E3               #E1x     #E1y     0
DP   F3                #F1x     #F1y     0

LA   400
DP   D4                #D1x     #D1y     0
** DP   E4               #E1x     #E1y     0
DP   F4                #F1x     #F1y     0

LA   500
DP   D5                #D1x     #D1y     0
** DP   E5               #E1x     #E1y     0
DP   F5                #F1x     #F1y     0
LA   600
DP   D6                #D1x     #D1y     0
** DP   E6               #E1x     #E1y     0
DP   F6                #F1x     #F1y     0
```

```
LA   700
DP   D7              #D1x     #D1y     0
** DP   E7            #E1x     #E1y     0
DP   F7              #F1x     #F1y     0

LA   800
DP   D8              #D1x     #D1y     0
** DP   E8            #E1x     #E1y     0
DP   F8              #F1x     #F1y     0

LA   900
DP   D9              #D1x     #D1y     0
** DP   E9            #E1x     #E1y     0
DP   F9              #F1x     #F1y     0

LA   1000
DP   D10             #D1x     #D1y     0
** DP   E10           #E1x     #E1y     0
DP   F10             #F1x     #F1y     0

LA   1100
DP   D11             #D1x     #D1y     0
** DP   E11           #E1x     #E1y     0
DP   F11             #F1x     #F1y     0

LA   1200
DP   D12             #D1x     #D1y     0
** DP   E12           #E1x     #E1y     0
DP   F12             #F1x     #F1y     0

LA   1300
DP   D13             #D1x     #D1y     0
** DP   E13           #E1x     #E1y     0
DP   F13             #F1x     #F1y     0

LA   1400
DP   D14             #D1x     #D1y     0
** DP   E14           #E1x     #E1y     0
DP   F14             #F1x     #F1y     0

LA   1500
DP   D15             #D1x     #D1y     0
** DP   E15           #E1x     #E1y     0
DP   F15             #F1x     #F1y     0

LA   1600
DP   D16             #D1x     #D1y     0
** DP   E16           #E1x     #E1y     0
DP   F16             #F1x     #F1y     0
```

```
LA   1700
DP   D17              #D1x     #D1y     0
** DP   E17             #E1x     #E1y     0
DP   F17              #F1x     #F1y     0

LA   1800
DP   D18              #D1x     #D1y     0
** DP   E18             #E1x     #E1y     0
DP   F18              #F1x     #F1y     0

LA   1900
DP   D19              #D1x     #D1y     0
** DP   E19             #E1x     #E1y     0
DP   F19              #F1x     #F1y     0

LA   2000
DP   D20              #D1x     #D1y     0
** DP   E20             #E1x     #E1y     0
DP   F20              #F1x     #F1y     0

LA   2100
DP   D21              #D1x     #D1y     0
** DP   E21             #E1x     #E1y     0
DP   F21              #F1x     #F1y     0

LA   2200
DP   D22              #D1x     #D1y     0
** DP   E22             #E1x     #E1y     0
DP   F22              #F1x     #F1y     0

LA   2300
DP   D23              #D1x     #D1y     0
** DP   E23             #E1x     #E1y     0
DP   F23              #F1x     #F1y     0

LA   2400
DP   D24              #D1x     #D1y     0
** DP   E24             #E1x     #E1y     0
DP   F24              #F1x     #F1y     0

** Ende der Definition der Speisenpunkte ******************************


** 2.c) Definition der triangulierte Fläche des Trafos **********
** Diese Struktur hat Label 1001
LA   1001
PM   A1   B1   C1   D1       F1       G1       H1       I1
```

```
** 3. Wir kopieren die elementare Struktur 14mal **********************
TG   14   1002 1002 1    0                                    #d_y
** Nach allen diesen Sachen haben wir 14 Patches über dem Y-Achse


** 4. Wir machen den 16. Element (16. Patch) **************************
** 4.a) Definition der Variablen der Punkte **********************

#Abst_y = 14 * (#linie1_L +#linie3_L) + 15 * #patch_L
** Abstand wir sollen unser Struktur über den y-Achse bewegen

#A16x = #patch_W
#A16y = #Abst_y + (#linie1_L +#linie3_L)
                          ** z=0 für alle Punkte!!
#B16x = #patch_W
#B16y = #patch_L + (#linie1_L +#linie3_L) + #Abst_y

#C16x = 0
#C16y = #patch_L + (#linie1_L +#linie3_L) + #Abst_y

#D16ax = 0
#D16ay = (#linie1_L +#linie3_L) + #Abst_y

#E16ax = #patch_W/2 - #Schnitt_W/2
#E16ay = (#linie1_L +#linie3_L) + #Abst_y

#F16ax = #patch_W/2 - #Schnitt_W/2
#F16ay = (#linie2_L +#linie3_L) + #Abst_y

#G16x = #patch_W/2 - #linie3_W/2
#G16y = (#linie2_L +#linie3_L) + #Abst_y

#H16x = #patch_W/2 - #linie3_W/2
#H16y = #Abst_y

#I16x = #patch_W/2 + #linie3_W/2
#I16y = #Abst_y

#J16x = #patch_W/2 + #linie3_W/2
#J16y = (#linie2_L +#linie3_L) + #Abst_y

#K16x = #patch_W/2 + #Schnitt_W/2
#K16y = (#linie2_L +#linie3_L) + #Abst_y

#L16x = #patch_W/2 + #Schnitt_W/2
#L16y = (#linie1_L +#linie3_L) + #Abst_y
```

```
** 4.b) Definition der Punkte des 16. Patches ********************
** Dieser Patch het Label 1017
LA   1017
DP   A16                  #A16x     #A16y     0
DP   B16                  #B16x     #B16y     0
DP   C16                  #C16x     #C16y     0
DP   D16a                 #D16ax    #D16ay    0
DP   E16a                 #E16ax    #E16ay    0
DP   F16a                 #F16ax    #F16ay    0
DP   G16                  #G16x     #G16y     0
DP   H16                  #H16x     #H16y     0
DP   I16                 #I16x     #I16y     0
DP   J16                  #J16x     #J16y     0
DP   K16                  #K16x     #K16y     0
DP   L16                  #L16x     #L16y     0


** 4.c) Definition der Fläche des 16. Patches ********************
PM   A16  B16  C16  D16a     E16a     F16a     G16      H16      I16      J16      K16
L16


** 5. Wir repetieren diese Struktur 11mal in der x-Richtung ***********
** #d_x = #d_x_Achse
** #d_x_1 = -#patch_W/2
** #d_x_2 = #d_x/2

#Tr_x = #d_x_1 + #d_x_2

** Am Anfang verschieben wir den Sturuktur Achse auf den y-Achse
TG   0    1001 1017 0    0                          #Tr_x

** Am Ende kopieren wir alles 11 mal in der x-achse Richtung
TG   11   1001 1017 1000 0                           #d_x


** 6. Nutzung von Simetry Karte ***************************************
SY   1    1    0    0    12000


** 7. Verschiebung der Speisenpunkte **********************************
** 1. Spalte
#Tr_x = #d_x_1 + #d_x_2
TP       100  100  0                              #Tr_x

** 2. Spalte
#Tr_x = #d_x + #d_x_1 + #d_x_2
TP       200  200  0                              #Tr_x
```

```
** 3. Spalte
#Tr_x = #Tr_x + #d_x
TP      300  300  0                    #Tr_x

** 4. Spalte
#Tr_x = #Tr_x + #d_x
TP      400  400  0                    #Tr_x

** 5. Spalte
#Tr_x = #Tr_x + #d_x
TP      500  500  0                    #Tr_x

** 6. Spalte
#Tr_x = #Tr_x + #d_x
TP      600  600  0                    #Tr_x

** 7. Spalte
#Tr_x = #Tr_x + #d_x
TP      700  700  0                    #Tr_x

** 8. Spalte
#Tr_x = #Tr_x + #d_x
TP      800  800  0                    #Tr_x

** 9. Spalte
#Tr_x = #Tr_x + #d_x
TP      900  900  0                    #Tr_x

** 10. Spalte
#Tr_x = #Tr_x + #d_x
TP      1000 1000 0                     #Tr_x

** 11. Spalte
#Tr_x = #Tr_x + #d_x
TP      1100 1100 0                     #Tr_x

** 12. Spalte
#Tr_x = #Tr_x + #d_x
TP      1200 1200 0                     #Tr_x

** -13. Spalte (die am rechsten des y-Achses liegt)
#Tr_x = #d_x_1 - #d_x_2
TP      1300 1300 0                     #Tr_x

** -14. Spalte
#Tr_x = #Tr_x - #d_x
TP      1400 1400 0                     #Tr_x

** -15. Spalte
```

```
#Tr_x = #Tr_x - #d_x
TP       1500 1500 0                        #Tr_x

** -16. Spalte
#Tr_x = #Tr_x - #d_x
TP       1600 1600 0                        #Tr_x

** -17. Spalte
#Tr_x = #Tr_x - #d_x
TP       1700 1700 0                        #Tr_x

** -18. Spalte
#Tr_x = #Tr_x - #d_x
TP       1800 1800 0                        #Tr_x

** -19. Spalte
#Tr_x = #Tr_x - #d_x
TP       1900 1900 0                        #Tr_x

** -20. Spalte
#Tr_x = #Tr_x - #d_x
TP       2000 2000 0                        #Tr_x

** -21. Spalte
#Tr_x = #Tr_x - #d_x
TP       2100 2100 0                        #Tr_x

** -22. Spalte
#Tr_x = #Tr_x - #d_x
TP       2200 2200 0                        #Tr_x

** -23. Spalte
#Tr_x = #Tr_x - #d_x
TP       2300 2300 0                        #Tr_x

** -24. Spalte
#Tr_x = #Tr_x - #d_x
TP       2400 2400 0                        #Tr_x



**********************************************************************
** End of geometry ****************************************************
EG   1    0    0        0                                              1
**********************************************************************

** Wir definieren unser planare Multilayer Substrate ******************

GF   10   1            0           1        1              0        0
```

```
                    #h      #epsrSub    1               #tanSub


** We set the frequency of the circuit *********************************
FR   2    0                71E9      5.5E9


** We have to feed the circuit (24mal AE card) ************************
AE   0    D1   F1   3        1        0        50
AE   1    D2   F2   3        1        0        50
AE   1    D3   F3   3        1        0        50
AE   1    D4   F4   3        1        0        50
AE   1    D5   F5   3        1        0        50
AE   1    D6   F6   3        1        0        50
AE   1    D7   F7   3        1        0        50
AE   1    D8   F8   3        1        0        50
AE   1    D9   F9   3        1        0        50
AE   1    D10  F10  3        1        0        50
AE   1    D11  F11  3        1        0        50
AE   1    D12  F12  3        1        0        50
AE   1    D13  F13  3        1        0        50
AE   1    D14  F14  3        1        0        50
AE   1    D15  F15  3        1        0        50
AE   1    D16  F16  3        1        0        50
AE   1    D17  F17  3        1        0        50
AE   1    D18  F18  3        1        0        50
AE   1    D19  F19  3        1        0        50
AE   1    D20  F20  3        1        0        50
AE   1    D21  F21  3        1        0        50
AE   1    D22  F22  3        1        0        50
AE   1    D23  F23  3        1        0        50
AE   1    D24  F24  3        1        0        50


** Calculation of the Gain of the Antenna:
FF   1    181  2    1        -45      0        0.5      90


** Calculation of the S-Parameters:
SP                           50


** End
EN
```

6.2.6 Array 1x3 with the same amplitude and phase in all patches

Code of the ".pre" FEKO file defining the geometry and the input signals for the 1x3 array when the amplitudes and phases are the same for the three patches (Uniform power supply).

```
** ACC 2 Antenne (Patche)
** Autor: ACC2 Gruppe
** Date created: **.**.****
** Modified by: Julio Modrego Gil (Diplomand)
** Date last modified: 1.3.2005


#MAXNV = 9  ** Max number of connection points between surfaces and wires
** Scaling factor since all dimensions below in mm
SF   1                    0.001


** Dimensions of Patch
#patch_W = ***
#patch_L = ***

** Dimensions Feedline
#feed_W = ** ** Breite Feedline
#feed_L = 0.522  ** Länge Feedline

** Dimensions Array
#d = 0

** Dimensions of the substrate
#gnd_x = 4 **4
#gnd_y = 2.31 **4

** Substrate parameters
#h = 0.127    ** Height
#epsrSub = 3.05 ** Relative permitivity
#tanSub = 0.0013

** Frequency (for the discretisation)
#freq = 76.5e9
#lam = 1000 * #c0 / #freq / sqrt(#epsrSub)    ** Wavelength in mm

** Segmentation parameters
**#tri_len = #lam /4
#fine_tri = min(#lam/2,#h)
#segl = #lam / 10
#segr = #lam/500
```

```
IP                      #segr     #fine_tri #segl    #fine_tri


** Berechnung der Punkte ***********************************************
** Patche
** 1. Patch
#alpha = -45/180*#pi
#pa_x =  #patch_L/2*cos(#alpha)-#patch_W/2*sin(#alpha)
#pa_y = -#patch_L/2*sin(#alpha) - #patch_W/2*cos(#alpha)+  1/2*#d
#pb_x =  #patch_L/2*cos(#alpha)+ #patch_W/2*sin(#alpha)
#pb_y = -#patch_L/2*sin(#alpha) + #patch_W/2*cos(#alpha)+  1/2*#d
#pc_x = -#patch_L/2*cos(#alpha)+ #patch_W/2*sin(#alpha)
#pc_y =  #patch_L/2*sin(#alpha) + #patch_W/2*cos(#alpha)+  1/2*#d
#pd_x = -#patch_L/2*cos(#alpha)-#patch_W/2*sin(#alpha)
#pd_y =  #patch_L/2*sin(#alpha) - #patch_W/2*cos(#alpha)+  1/2*#d


** Feedline 1.Patch
#fa_x =  (#patch_L/2+#feed_L)*cos(#alpha)-#feed_W/2*sin(#alpha)
#fa_y = -(#patch_L/2+#feed_L)*sin(#alpha) - #feed_W/2*cos(#alpha)+  1/2*#d
#fb_x = (#patch_L/2+#feed_L)*cos(#alpha)+ #feed_W/2*sin(#alpha)
#fb_y = -(#patch_L/2+#feed_L)*sin(#alpha) + #feed_W/2*cos(#alpha)+  1/2*#d
#fc_x = -(#patch_L/2-#patch_L)*cos(#alpha)+ #feed_W/2*sin(#alpha)
#fc_y =  (#patch_L/2-#patch_L)*sin(#alpha) + #feed_W/2*cos(#alpha)+  1/2*#d
#fd_x = - (#patch_L/2-#patch_L)*cos(#alpha)-#feed_W/2*sin(#alpha)
#fd_y =   (#patch_L/2-#patch_L)*sin(#alpha) - #feed_W/2*cos(#alpha)+  1/2*#d
#n1_x =   (#patch_L/2+#feed_L)*cos(#alpha)
#n1_y =   -(#patch_L/2+#feed_L)*sin(#alpha)+  1/2*#d


*** Definition der Punkte ********************************************
** Definition of the points of the Patch
DP   PA                 #pa_x     #pa_y     0
DP   PB                 #pb_x     #pb_y     0
DP   PC                 #pc_x     #pc_y     0
DP   PD                 #pd_x     #pd_y     0


** Definition of the points of the Feedline
DP   FA                 #fa_x     #fa_y     0
DP   FB                 #fb_x     #fb_y     0
DP   FC                 #fc_x     #fc_y     0
DP   FD                 #fd_x     #fd_y     0
DP   N1                 #n1_x     #n1_y     0
DP   N1H                 #n1_x     #n1_y     -#h  ** Zum Speisen!!


** Definition Objekte ************************************************
** Patch 1 (Label 1)
```

```
LA   1
PM   PA   FD   FC   PB   0    PC       PD

** Feedline (Label 2)
LA   2
PM   FD   FA   N1   FB   0    FC

** Wire segment for feeding (Label 10)
LA   10
BL   N1   N1H

** Translation of the geometry (To have 3 Patches)
TG   1    1    10   10   0                              #gnd_y
TG   1    1    10   20   0                              -#gnd_y

***************************************************************************
** End of Geometry inputs
EG   1    0    0    0    0
***************************************************************************


** GF Karte um die Substrat zu definieren
GF   10   1            0            1        1                    0
                      #h        #epsrSub  1              #tanSub

** Voltage source at the wire centre with impressed power
PW   1                  1.0
A1   0    10            1        0
A1   1    20            1        0
A1   1    30            1        0

** Frequency
FR   1                  76.5E9


** Near Field
**FE   3    1    19   72   2    15       0        0        0        5        5


** Far-field pattern
FF   1    181  9    1        -90      0        1        45


** Compute S11 at source
**SP                       70


** End
EN
```

6.2.7 Array 1x3 with amplitudes 0,5-1-0,5 and without phase

This is the ".pre" FEKO file defining the 1x3 array fed with the following configuration:

$$V_{y\uparrow} = 0.5\, V_{middle}$$
$$V_{y\downarrow} = 0.5\, V_{middle}$$

The results obtained with this file have been obtained with FEKO to determine if this configuration should be used or not with a superimposed lens.

After a careful examination of this file, the only difference between it and another files defining other amplitude distributions on the patches is the voltage source used to feed the circuit. The sources of voltage are simulated using the cards *"PW"* and *"A1"*, which establish respectively the power and the amplitude of the input.

Due to that, the rest of the simulated circuits (0,6-1-0,4; 0,75-1-0,25; 0,8-1-0,2; 0,9-1-0,1; 0,85-1-0,15) will be not included in this annex, as they only differ from these ones in the two lines of code which are enhanced in red in the following file.

```
** ACC 2 Antenne (Patche)
** Autor: ACC2 Gruppe
** Date created: **.**.****
** Modifified by: Julio Modrego Gil (Diplomand)
** Date last modified: 1.3.2005


#MAXNV = 9  ** Max number of connection points between surfaces and wires
** Scaling factor since all dimensions below in mm
SF   1                    0.001


** Dimensions of Patch
#patch_W = ***
#patch_L = ***

** Dimensions Feedline
#feed_W = ***    ** Breite Feedline
#feed_L = 0.522  ** Länge Feedline

** Dimensions Array
#d = 0

** Dimensions of the substrate
#gnd_x = 4 **4
#gnd_y = 2.31 **4
```

```
** Substrate parameters
#h = 0.127    ** Height
#epsrSub = 3.05 ** Relative permitivity
#tanSub = 0.0013


** Frequency (for the discretisation)
#freq = 76.5e9
#lam = 1000 * #c0 / #freq / sqrt(#epsrSub)    ** Wavelength in mm


** Segmentation parameters
**#tri_len = #lam /4
#fine_tri = min(#lam/2,#h)
#segl = #lam / 10
#segr = #lam/500
IP                        #segr     #fine_tri #segl    #fine_tri


** Berechnung der Punkte **********************************************

** Patche
** 1. Patch
#alpha = -45/180*#pi
#pa_x =  #patch_L/2*cos(#alpha)-#patch_W/2*sin(#alpha)
#pa_y = -#patch_L/2*sin(#alpha) - #patch_W/2*cos(#alpha)+  1/2*#d
#pb_x =  #patch_L/2*cos(#alpha)+ #patch_W/2*sin(#alpha)
#pb_y = -#patch_L/2*sin(#alpha) + #patch_W/2*cos(#alpha)+  1/2*#d
#pc_x = -#patch_L/2*cos(#alpha)+ #patch_W/2*sin(#alpha)
#pc_y =  #patch_L/2*sin(#alpha) + #patch_W/2*cos(#alpha)+  1/2*#d
#pd_x = -#patch_L/2*cos(#alpha)-#patch_W/2*sin(#alpha)
#pd_y =  #patch_L/2*sin(#alpha) - #patch_W/2*cos(#alpha)+  1/2*#d


** Feedline 1.Patch
#fa_x =  (#patch_L/2+#feed_L)*cos(#alpha)-#feed_W/2*sin(#alpha)
#fa_y = -(#patch_L/2+#feed_L)*sin(#alpha) - #feed_W/2*cos(#alpha)+  1/2*#d
#fb_x = (#patch_L/2+#feed_L)*cos(#alpha)+ #feed_W/2*sin(#alpha)
#fb_y = -(#patch_L/2+#feed_L)*sin(#alpha) + #feed_W/2*cos(#alpha)+  1/2*#d
#fc_x = -(#patch_L/2-#patch_L)*cos(#alpha)+ #feed_W/2*sin(#alpha)
#fc_y =  (#patch_L/2-#patch_L)*sin(#alpha) + #feed_W/2*cos(#alpha)+  1/2*#d
#fd_x = - (#patch_L/2-#patch_L)*cos(#alpha)-#feed_W/2*sin(#alpha)
#fd_y =   (#patch_L/2-#patch_L)*sin(#alpha) - #feed_W/2*cos(#alpha)+  1/2*#d
#n1_x =   (#patch_L/2+#feed_L)*cos(#alpha)
#n1_y =   -(#patch_L/2+#feed_L)*sin(#alpha)+  1/2*#d


*** Definition der Punkte ****************************************
```

```
** Definition of the points of the Patch
DP   PA                  #pa_x    #pa_y    0
DP   PB                  #pb_x    #pb_y    0
DP   PC                  #pc_x    #pc_y    0
DP   PD                  #pd_x    #pd_y    0

** Definition of the points of the Feedline
DP   FA                  #fa_x    #fa_y    0
DP   FB                  #fb_x    #fb_y    0
DP   FC                  #fc_x    #fc_y    0
DP   FD                  #fd_x    #fd_y    0
DP   N1                  #n1_x    #n1_y    0
DP   N1H                  #n1_x    #n1_y    -#h  ** Zum Speisen!!

** Definition Objekte ***********************************************
** Patch 1 (Label 1)
LA   1
PM   PA   FD   FC   PB   0    PC       PD

** Feedline (Label 2)
LA   2
PM   FD   FA   N1   FB   0    FC

** Wire segment for feeding (Label 10)
LA   10
BL   N1   N1H



** Translation of the geometry (To have 3 Patches)
TG   1    1    10   10   0                              #gnd_y
TG   1    1    10   20   0                              -#gnd_y

*****************************************************************************
** End of Geometry inputs
EG   1    0    0    0    0
*****************************************************************************

** GF Karte um die Substrat zu definieren
GF   10   1          0          1        1                    0
                    #h       #epsrSub  1              #tanSub

** Voltage source at the wire centre with impressed power
PW   1               1.0
A1   0    10         1        0          **Amplitude distributions of the patches!!!
A1   1    20         0.5      0
A1   1    30         0.5      0

** Frequency
```

```
FR   1                    76.5E9

** Near Field
**FE   3    1    19   72   2    15       0        0        0        5        5

** Far-field pattern
FF   1    181  9    1         -90       0        1        45

** Compute S11 at source
**SP                        70

** End
EN
```

6.2.8 Array 1x3 with amplitudes 0,5-1-0,5 and phases 12,5º-0-(-12,5º)

In this point is included the ".pre" FEKO file used to excite the lens. The chosen configuration is the following one:

$$V_{y\uparrow} = 0.5\,V_{middle} = V_{y\downarrow}$$
$$\Delta\varphi_{1-2} = 12.5^{o}$$
$$\Delta\varphi_{2-3} = -12.5^{o}$$

That means, assuming the central patch as reference for both amplitudes and phase shifts; that the voltage amplitude at the input of the extreme patches is one half of the amplitude at the central one, and that there is a shift of 12.5^{o} between the upper patch and the central one, and of -12.5^{o} between the central and the lower one.

Several configurations were tested to find the best solution, but they all only differ in the phase shift introduced at the input of the patches. In EditFEKO, it is indicated by the card *"A1"*. As the files are identical except in the numbers enhanced in red, only this file will be attached to the memory of the project.

```
** ACC 2 Antenne (Patche)
** Autor: ACC2 Gruppe
** Date created: **.**.****
** Modified by: Julio Modrego Gil (Diplomand)
** Date last modified: 8.3.2005


#MAXNV = 9  ** Max number of connection points between surfaces and wires
** Scaling factor since all dimensions below in mm
SF   1                    0.001


** Dimensions of Patch
#patch_W = ****
#patch_L = ****

** Dimensions Feedline
#feed_W = *****  ** Breite Feedline
#feed_L = 0.522  ** Länge Feedline

** Dimensions Array
#d = 0

** Dimensions of the substrate
#gnd_x = 4          ** 4
#gnd_y = 3.48       ** 2.31     **4
```

```
** Substrate parameters
#h = 0.127    ** Height
#epsrSub = 3.05 ** Relative permitivity
#tanSub = 0.0013



** Frequency (for the discretisation)
#freq = 76.5e9
#lam = 1000 * #c0 / #freq / sqrt(#epsrSub)    ** Wavelength in mm

** Segmentation parameters
**#tri_len = #lam /4
#fine_tri = min(#lam/2,#h)
#segl = #lam / 10
#segr = #lam/500
IP                      #segr     #fine_tri #segl    #fine_tri

** Berechnung der Punkte *********************************************
** Patche
** 1. Patch
#alpha = -45/180*#pi
#pa_x =  #patch_L/2*cos(#alpha)-#patch_W/2*sin(#alpha)
#pa_y = -#patch_L/2*sin(#alpha) - #patch_W/2*cos(#alpha)+  1/2*#d
#pb_x =  #patch_L/2*cos(#alpha)+ #patch_W/2*sin(#alpha)
#pb_y = -#patch_L/2*sin(#alpha) + #patch_W/2*cos(#alpha)+  1/2*#d
#pc_x = -#patch_L/2*cos(#alpha)+ #patch_W/2*sin(#alpha)
#pc_y =  #patch_L/2*sin(#alpha) + #patch_W/2*cos(#alpha)+  1/2*#d
#pd_x = -#patch_L/2*cos(#alpha)-#patch_W/2*sin(#alpha)
#pd_y =  #patch_L/2*sin(#alpha) - #patch_W/2*cos(#alpha)+  1/2*#d

** Feedline 1.Patch
#fa_x =  (#patch_L/2+#feed_L)*cos(#alpha)-#feed_W/2*sin(#alpha)
#fa_y = -(#patch_L/2+#feed_L)*sin(#alpha) - #feed_W/2*cos(#alpha)+  1/2*#d
#fb_x = (#patch_L/2+#feed_L)*cos(#alpha)+ #feed_W/2*sin(#alpha)
#fb_y = -(#patch_L/2+#feed_L)*sin(#alpha) + #feed_W/2*cos(#alpha)+  1/2*#d
#fc_x = -(#patch_L/2-#patch_L)*cos(#alpha)+ #feed_W/2*sin(#alpha)
#fc_y =  (#patch_L/2-#patch_L)*sin(#alpha) + #feed_W/2*cos(#alpha)+  1/2*#d
#fd_x = - (#patch_L/2-#patch_L)*cos(#alpha)-#feed_W/2*sin(#alpha)
#fd_y =   (#patch_L/2-#patch_L)*sin(#alpha) - #feed_W/2*cos(#alpha)+  1/2*#d
#n1_x =   (#patch_L/2+#feed_L)*cos(#alpha)
#n1_y =   -(#patch_L/2+#feed_L)*sin(#alpha)+  1/2*#d



*** Definition der Punkte ********************************************
** Definition of the points of the Patch
DP   PA                 #pa_x     #pa_y     0
DP   PB                 #pb_x     #pb_y     0
DP   PC                 #pc_x     #pc_y     0
```

```
DP   PD                #pd_x     #pd_y     0

** Definition of the points of the Feedline
DP   FA                #fa_x     #fa_y     0
DP   FB                #fb_x     #fb_y     0
DP   FC                #fc_x     #fc_y     0
DP   FD                #fd_x     #fd_y     0
DP   N1                #n1_x     #n1_y     0
DP   N1H                #n1_x     #n1_y     -#h  ** Zum Speisen!!

** Definition Objekte ************************************************
** Patch 1 (Label 1)
LA   1
PM   PA   FD   FC   PB   0    PC       PD

** Feedline (Label 2)
LA   2
PM   FD   FA   N1   FB   0    FC

** Wire segment for feeding (Label 10)
LA   10
BL   N1   N1H

** Translation of the geometry (To have 3 Patches)
TG   1    1    10   10   0                              #gnd_y
TG   1    1    10   20   0                              -#gnd_y


***************************************************************************
** End of Geometry inputs
EG   1    0    0    0    0
***************************************************************************

** We write the farfield data to a .ffe file:
DA   0    0    1    0    0    0


** GF Karte um die Substrat zu definieren
GF   10   1          0          1        1                  0
                    #h       #epsrSub  1              #tanSub


** Voltage source at the wire centre with impressed power
PW   1                1.0
A1   0    10          1        0          **Amplitudes & Phases of Power Supply
A1   1    20          0.5      12.5       **Phase in red, with respect to the center
A1   1    30          0.5      -12.5
```

```
** Frequency
FR   1                    76.5E9


** Near Field
**FE   3    1    19   72   2    15       0        0        0        5        5


** Far-field pattern
FF   1    181  9    1         -90       0        1        45


** Compute S11 at source
**SP                        70


** End
EN
```

6.2.9 Lissy definition of the cylindrical lens

This is the LISSY ".pre" file defining the geometry of the lens used above the 1x3 array (Patch_1x3 with Amplitudes=0,5-1-0,5 and Phase_Shifts= 12,5º-(-12,5º)). It defines the dielectric material of the lens, its dimensions and position referring to the array.

```
** ACC3 Linsen+Antenne(3 Patches)
** Autor: Julio Modrego Gil (Diplomand)
** Date crated: 7.03.2005
** Date last modified: 8.03.2005

** Charakteristik einer zylindrischen Linse für LRR3

** Alle Werte in mm
FK  0.001


** Definition Dielektrikum
MAT 1        1  3.00 1 0.000


** Geometriedaten
** Linse
KOE 1
APL     50     25     40     1


** Steuerkarten  ***********************************************
AB  0.1
** Es werden 181 Strahlen in Theta-Richtung erzeugt und 721 in Phi-Richtung (Auflösung 0,5°)
AU  91  721  0  45   0  360
DF  1
** Apertur 50.5 * 50.5 gross
AP
60.5  45  121 121

** Phasenquellpunkt im Nullpunkt
PQ  0  0  0

** Datei mit Fernfelddaten
AF  U:\Lissy\Patch_3x1_modif_GF.ffe

** Frequenz
FR  76.5E+9

** Fernfeldberechnung
FF  181  361  0  0  1  1
IN  0
```

6.2.10 Array 20x3

The following code defines the geometry of the array of 20x3 patches. That is, an array composed of 20 copies equally spaced along the x-axe of the 1x3 array of point 2.10 of this annex. The 1x3 array is fed with the following configuration:

$$V_{y\uparrow} = 0{,}5\, V_{middle} = V_{y\downarrow}$$
$$\Delta\varphi_{1-2} = 12{,}5^{o} = -\Delta\varphi_{2-3}$$

Thanks to this circuit, the ".ffe" file containing the results for the radiated far field is calculated by FEKO. This ".ffe" file is used by LISSY as input to obtain the far fields of the set array plus lens.

```
** ACC 2 Antenne (Patche)
** Autor: ACC2 Gruppe
** Date created: **.**.****
** Modifified by: Julio Modrego Gil (Diplomand)
** Date last modified: 21.3.2005


#MAXNV = 9  ** Max number of connection points between surfaces and wires
** Scaling factor since all dimensions below in mm
SF   1                    0.001


** Dimensions of Patch
#patch_W = ****
#patch_L = ****


** Dimensions Feedline
#feed_W = *****  ** Breite Feedline
#feed_L = 0.522  ** Länge Feedline


** Dimensions Array
#d = *****  ** Abstand zwischen Arrays Elementen


** Dimensions of the substrate
#gnd_x = 4          ** 4
#gnd_y = 3.48        ** 2.31     **4


** Substrate parameters
#h = 0.127    ** Height
```

```
#epsrSub = 3.05 ** Relative permitivity
#tanSub = 0.0013


** Frequency (for the discretisation)
#freq = 76.5e9
#lam = 1000 * #c0 / #freq / sqrt(#epsrSub)    ** Wavelength in mm

** Segmentation parameters
**#tri_len = #lam /4
#fine_tri = min(#lam/2,#h)
#segl = #lam / 10
#segr = #lam/500
IP                      #segr     #fine_tri #segl    #fine_tri


** Berechnung der Punkte ***********************************************
** Patche
** 1. Patch
#alpha = -45/180*#pi
#pa_x =  #patch_L/2*cos(#alpha)-#patch_W/2*sin(#alpha)
#pa_y = -#patch_L/2*sin(#alpha) - #patch_W/2*cos(#alpha)+  1/2*#d
#pb_x =  #patch_L/2*cos(#alpha)+ #patch_W/2*sin(#alpha)
#pb_y = -#patch_L/2*sin(#alpha) + #patch_W/2*cos(#alpha)+  1/2*#d
#pc_x = -#patch_L/2*cos(#alpha)+ #patch_W/2*sin(#alpha)
#pc_y =  #patch_L/2*sin(#alpha) + #patch_W/2*cos(#alpha)+  1/2*#d
#pd_x = -#patch_L/2*cos(#alpha)-#patch_W/2*sin(#alpha)
#pd_y =  #patch_L/2*sin(#alpha) - #patch_W/2*cos(#alpha)+  1/2*#d


** Feedline 1.Patch
#fa_x =  (#patch_L/2+#feed_L)*cos(#alpha)-#feed_W/2*sin(#alpha)
#fa_y = -(#patch_L/2+#feed_L)*sin(#alpha) - #feed_W/2*cos(#alpha)+  1/2*#d
#fb_x = (#patch_L/2+#feed_L)*cos(#alpha)+ #feed_W/2*sin(#alpha)
#fb_y = -(#patch_L/2+#feed_L)*sin(#alpha) + #feed_W/2*cos(#alpha)+  1/2*#d
#fc_x = -(#patch_L/2-#patch_L)*cos(#alpha)+ #feed_W/2*sin(#alpha)
#fc_y =  (#patch_L/2-#patch_L)*sin(#alpha) + #feed_W/2*cos(#alpha)+  1/2*#d
#fd_x = - (#patch_L/2-#patch_L)*cos(#alpha)-#feed_W/2*sin(#alpha)
#fd_y =   (#patch_L/2-#patch_L)*sin(#alpha) - #feed_W/2*cos(#alpha)+  1/2*#d
#n1_x =   (#patch_L/2+#feed_L)*cos(#alpha)
#n1_y =   -(#patch_L/2+#feed_L)*sin(#alpha)+  1/2*#d


*** Definition der Punkte *********************************************
** Definition of the points of the Patch
DP   PA                 #pa_x     #pa_y     0
DP   PB                 #pb_x     #pb_y     0
DP   PC                 #pc_x     #pc_y     0
DP   PD                 #pd_x     #pd_y     0
```

```
** Definition of the points of the Feedline
DP   FA                  #fa_x    #fa_y    0
DP   FB                  #fb_x    #fb_y    0
DP   FC                  #fc_x    #fc_y    0
DP   FD                  #fd_x    #fd_y    0
DP   N1                  #n1_x    #n1_y    0
DP   N1H                  #n1_x    #n1_y    -#h  ** Zum Speisen!!


** Definition Objekte ************************************************
** Patch 1 (Label 1)
LA   1
PM   PA   FD   FC   PB   0    PC       PD

** Feedline (Label 2)
LA   2
PM   FD   FA   N1   FB   0    FC
** Wire segment for feeding (Label 10)
LA   10
BL   N1   N1H


** Translation of the geometry (To have 3 Patches)
TG   1    1    10   10   0                              #gnd_y
TG   1    1    10   20   0                              -#gnd_y

** We copy this structure 9 times along the X-axe (to have 10 arrays of 3 patches)
TG   9    10 30 1000 0                          #d_x


** Use of the Simetry Card to have 20 arrays of 3 patches**************
SY   1    1    0    0    10000

***************************************************************************
** End of Geometry inputs
EG   1    0    0    0    0
***************************************************************************


** We write the farfield data to a .ffe file:
DA   0    0    1    0    0    0


** GF Karte um die Substrat zu definieren
GF   10   1            0            1        1                    0
                      #h        #epsrSub  1              #tanSub
```

```
** Voltage source at the wire centre with impressed power
PW   1                  1.0
** Array 1
A1   0   10             1        0
A1   1   20             0.5      12.5
A1   1   30             0.5      -12.5

** Array 2
A1   0   1010           1        0
A1   1   1020           0.5      12.5
A1   1   1030           0.5      -12.5

** Array 3
A1   0   2010           1        0
A1   1   2020           0.5      12.5
A1   1   2030           0.5      -12.5

** Array 4
A1   0   3010           1        0
A1   1   3020           0.5      12.5
A1   1   3030           0.5      -12.5

** Array 5
A1   0   4010           1        0
A1   1   4020           0.5      12.5
A1   1   4030           0.5      -12.5

** Array 6
A1   0   5010           1        0
A1   1   5020           0.5      12.5
A1   1   5030           0.5      -12.5

** Array 7
A1   0   6010           1        0
A1   1   6020           0.5      12.5
A1   1   6030           0.5      -12.5

** Array 8
A1   0   7010           1        0
A1   1   7020           0.5      12.5
A1   1   7030           0.5      -12.5

** Array 9
A1   0   8010           1        0
A1   1   8020           0.5      12.5
A1   1   8030           0.5      -12.5

** Array 10
```

```
A1   0   9010          1       0
A1   1   9020          0.5     12.5
A1   1   9030          0.5     -12.5

** Array 11 (y<0)
A1   0   10010         1       0
A1   1   10020         0.5     12.5
A1   1   10030         0.5     -12.5

** Array 12 (y<0)
A1   0   11010         1       0
A1   1   11020         0.5     12.5
A1   1   11030         0.5     -12.5

** Array 13 (y<0)
A1   0   12010         1       0
A1   1   12020         0.5     12.5
A1   1   12030         0.5     -12.5

** Array 14 (y<0)
A1   0   13010         1       0
A1   1   13020         0.5     12.5
A1   1   13030         0.5     -12.5

** Array 15 (y<0)
A1   0   14010         1       0
A1   1   14020         0.5     12.5
A1   1   14030         0.5     -12.5

** Array 16 (y<0)
A1   0   15010         1       0
A1   1   15020         0.5     12.5
A1   1   15030         0.5     -12.5

** Array 17 (y<0)
A1   0   16010         1       0
A1   1   16020         0.5     12.5
A1   1   16030         0.5     -12.5

** Array 18 (y<0)
A1   0   17010         1       0
A1   1   17020         0.5     12.5
A1   1   17030         0.5     -12.5

** Array 19 (y<0)
A1   0   18010         1       0
A1   1   18020         0.5     12.5
A1   1   18030         0.5     -12.5
```

```
** Array 20 (y<0)
A1   0    19010            1        0
A1   1    19020            0.5      12.5
A1   1    19030            0.5      -12.5


** Frequency
FR   1                  76.5E9


** Near Field
**FE   3    1    19   72   2    15       0        0        0        5        5


** Far-field pattern
FF   1    181  9    1        -90      0        1        45


** Compute S11 at source
**SP                       70


** End
EN
```

6.2.11 Array 24x3

This is the “*.pre” FEKO file defining the geometry and inputs of the circuit composed of 24 copies of “the 1x3 array”. This “1x3 array” has the following amplitudes and phases of the power supply signal at the input of the patches:

$$V_{y\uparrow} = 0{,}5\, V_{middle} = V_{y\downarrow}$$
$$\Delta\varphi_{1-2} = 12{,}5^{o} = -\Delta\varphi_{2-3}$$

Thanks to this circuit, the ".ffe" file containing the results for the radiated far field is calculated by FEKO. This ".ffe" file is used by LISSY as input to obtain the far fields of the set array plus lens.

```
** ACC 2 Antenne (Patche)
** Autor: ACC2 Gruppe
** Date created: **.**.****
** Modifified by: Julio Modrego Gil (Diplomand)
** Date last modified: 8.3.2005


#MAXNV = 9  ** Max number of connection points between surfaces and wires
** Scaling factor since all dimensions below in mm
SF   1                    0.001


** Dimensions of Patch
#patch_W = *****
#patch_L = ******


** Dimensions Feedline
#feed_W = ******  ** Breite Feedline
#feed_L = ******  ** Länge Feedline


** Dimensions Array
#d = *****  ** Abstand zwischen Arrays Elementen


** Dimensions of the substrate
#gnd_x = 4          ** 4
#gnd_y = 3.48       ** 2.31     **4


** Substrate parameters
#h = 0.127    ** Height
#epsrSub = 3.05 ** Relative permitivity
#tanSub = 0.0013
```

```
** Frequency (for the discretisation)
#freq = 76.5e9
#lam = 1000 * #c0 / #freq / sqrt(#epsrSub)    ** Wavelength in mm



** Segmentation parameters
**#tri_len = #lam /4
#fine_tri = min(#lam/2,#h)
#segl = #lam / 10
#segr = #lam/500
IP                      #segr     #fine_tri #segl    #fine_tri



** Berechnung der Punkte ***********************************************



** Patche
** 1. Patch
#alpha = -45/180*#pi
#pa_x =  #patch_L/2*cos(#alpha)-#patch_W/2*sin(#alpha)
#pa_y = -#patch_L/2*sin(#alpha) - #patch_W/2*cos(#alpha)+  1/2*#d
#pb_x =  #patch_L/2*cos(#alpha)+ #patch_W/2*sin(#alpha)
#pb_y = -#patch_L/2*sin(#alpha) + #patch_W/2*cos(#alpha)+  1/2*#d
#pc_x = -#patch_L/2*cos(#alpha)+ #patch_W/2*sin(#alpha)
#pc_y =  #patch_L/2*sin(#alpha) + #patch_W/2*cos(#alpha)+  1/2*#d
#pd_x = -#patch_L/2*cos(#alpha)-#patch_W/2*sin(#alpha)
#pd_y =  #patch_L/2*sin(#alpha) - #patch_W/2*cos(#alpha)+  1/2*#d



** Feedline 1.Patch

#fa_x =  (#patch_L/2+#feed_L)*cos(#alpha)-#feed_W/2*sin(#alpha)
#fa_y = -(#patch_L/2+#feed_L)*sin(#alpha) - #feed_W/2*cos(#alpha)+  1/2*#d
#fb_x = (#patch_L/2+#feed_L)*cos(#alpha)+ #feed_W/2*sin(#alpha)
#fb_y = -(#patch_L/2+#feed_L)*sin(#alpha) + #feed_W/2*cos(#alpha)+  1/2*#d
#fc_x = -(#patch_L/2-#patch_L)*cos(#alpha)+ #feed_W/2*sin(#alpha)
#fc_y =  (#patch_L/2-#patch_L)*sin(#alpha) + #feed_W/2*cos(#alpha)+  1/2*#d
#fd_x = - (#patch_L/2-#patch_L)*cos(#alpha)-#feed_W/2*sin(#alpha)
#fd_y =   (#patch_L/2-#patch_L)*sin(#alpha) - #feed_W/2*cos(#alpha)+  1/2*#d
#n1_x =   (#patch_L/2+#feed_L)*cos(#alpha)
#n1_y =   -(#patch_L/2+#feed_L)*sin(#alpha)+  1/2*#d



*** Definition der Punkte *********************************************



** Definition of the points of the Patch
DP   PA                  #pa_x    #pa_y    0
DP   PB                  #pb_x    #pb_y    0
DP   PC                  #pc_x    #pc_y    0
DP   PD                  #pd_x    #pd_y    0



** Definition of the points of the Feedline
```

```
DP   FA                #fa_x    #fa_y    0
DP   FB                #fb_x    #fb_y    0
DP   FC                #fc_x    #fc_y    0
DP   FD                #fd_x    #fd_y    0
DP   N1                #n1_x    #n1_y    0
DP   N1H                #n1_x    #n1_y    -#h  ** Zum Speisen!!


** Definition Objekte ************************************************


** Patch 1 (Label 1)
LA   1
PM   PA   FD   FC   PB   0    PC       PD


** Feedline (Label 2)
LA   2
PM   FD   FA   N1   FB   0    FC


** Wire segment for feeding (Label 10)
LA   10
BL   N1   N1H


** Translation of the geometry (To have 3 Patches)
TG   1    1    10   10   0                              #gnd_y
TG   1    1    10   20   0                              -#gnd_y

** We copy this structure 11 times along the X-axe (to have 12 arrays of 3 patches)
TG   11   10 30 1000 0                          #d_x


** Use of the Simetry Card to have 24 arrays of 3 patches**************

SY   1    1    0    0    10000

*****************************************************************************
** End of Geometry inputs
EG   1    0    0    0    0
*****************************************************************************


** We write the farfield data to a .ffe file:
DA   0    0    1    0    0    0


** GF Karte um die Substrat zu definieren
GF   10   1            0            1        1                    0
                      #h        #epsrSub  1              #tanSub
```

```
** Voltage source at the wire centre with impressed power
PW  1                1.0
** Array 1
A1  0   10           1       0
A1  1   20           0.5     12.5
A1  1   30           0.5     -12.5

** Array 2
A1  0   1010         1       0
A1  1   1020         0.5     12.5
A1  1   1030         0.5     -12.5

** Array 3
A1  0   2010         1       0
A1  1   2020         0.5     12.5
A1  1   2030         0.5     -12.5

** Array 4
A1  0   3010         1       0
A1  1   3020         0.5     12.5
A1  1   3030         0.5     -12.5

** Array 5
A1  0   4010         1       0
A1  1   4020         0.5     12.5
A1  1   4030         0.5     -12.5

** Array 6
A1  0   5010         1       0
A1  1   5020         0.5     12.5
A1  1   5030         0.5     -12.5

** Array 7
A1  0   6010         1       0
A1  1   6020         0.5     12.5
A1  1   6030         0.5     -12.5

** Array 8
A1  0   7010         1       0
A1  1   7020         0.5     12.5
A1  1   7030         0.5     -12.5

** Array 9
A1  0   8010         1       0
A1  1   8020         0.5     12.5
A1  1   8030         0.5     -12.5

** Array 10
A1  0   9010         1       0
A1  1   9020         0.5     12.5
A1  1   9030         0.5     -12.5

** Array 11
A1  0   10010        1       0
A1  1   10020        0.5     12.5
A1  1   10030        0.5     -12.5

** Array 12
A1  0   11010        1       0
A1  1   11020        0.5     12.5
A1  1   11030        0.5     -12.5
```

```
** Array 13 (y<0)
A1   0   12010          1       0
A1   1   12020          0.5      12.5
A1   1   12030          0.5     -12.5

** Array 14 (y<0)
A1   0   13010          1       0
A1   1   13020          0.5      12.5
A1   1   13030          0.5     -12.5

** Array 15 (y<0)
A1   0   14010          1       0
A1   1   14020          0.5      12.5
A1   1   14030          0.5     -12.5

** Array 16 (y<0)
A1   0   15010          1       0
A1   1   15020          0.5      12.5
A1   1   15030          0.5     -12.5

** Array 17 (y<0)
A1   0   16010          1       0
A1   1   16020          0.5      12.5
A1   1   16030          0.5     -12.5

** Array 18 (y<0)
A1   0   17010          1       0
A1   1   17020          0.5      12.5
A1   1   17030          0.5     -12.5

** Array 19 (y<0)
A1   0   18010          1       0
A1   1   18020          0.5      12.5
A1   1   18030          0.5     -12.5

** Array 20 (y<0)
A1   0   19010          1       0
A1   1   19020          0.5      12.5
A1   1   19030          0.5     -12.5


** Array 21 (y<0)
A1   0   20010          1       0
A1   1   20020          0.5      12.5
A1   1   20030          0.5     -12.5


** Array 22 (y<0)
A1   0   21010          1       0
A1   1   21020          0.5      12.5
A1   1   21030          0.5     -12.5


** Array 23 (y<0)
A1   0   22010          1       0
A1   1   22020          0.5      12.5
A1   1   22030          0.5     -12.5


** Array 24 (y<0)
A1   0   23010          1       0
A1   1   23020          0.5      12.5
```

```
A1   1    23030              0.5       -12.5

** Frequency
FR   1                    76.5E9



** Near Field
**FE   3    1    19   72   2    15        0         0         0         5         5



** Far-field pattern
FF   1    181  9    1         -90       0         1         45



** Compute S11 at source
**SP                         50



** End
EN
```

6.3 ANNEX 3: RECTANGULAR PATCH RADIATION THEORY

In 1953, the concept of microstrip radiators was first proposed by Deschamps. However, 20 years passed before the first practical antennas could be fabricated. They were developed by Howell and Munson, thanks to the availability of new substrates with low loss tangent and better thermal and mechanical properties. Since then, extensive research and development of microstrip antennas and arrays has been made.

Although radiation characteristics have been calculated for a large number of patch antennas, it has been proven that, despite the difference in geometrical shape, they have similar radiation properties. As consequence, rectangular and circular geometries have been widely used, as they are the easiest to analyze. In Figura 6-44 an arbitrary form patch antenna is presented. It consists of a radiating patch on one side of a dielectric substrate, which has a ground plane on the other side.

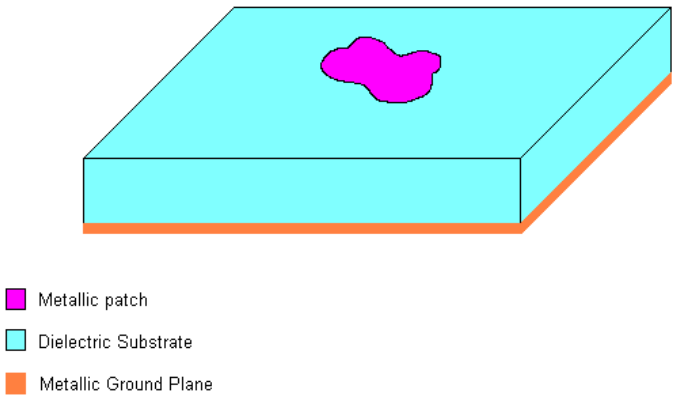

Figura 6-44 Arbitrary shape patch

It is known that the radiation from a microstrip line can be reduced considerably by the use of a thin substrate with a higher relative dielectric constant. And that a microstrip antenna is a quite similar structure, in which radiation will be encouraged for better radiation efficiency. Therefore, thick substrates with low permittivity are the preferred ones for the construction of microstrip antennas. In the following section, the basic radiation principle of a microstrip patch antenna will be introduced

6.3.1 Radiation's principle of a Microstrip Patch Antenna: Theory of the resonant cavity

To explain the radiation mechanism of a Microstrip Antenna, we make use of a rectangular patch antenna as the shown in the Figura 6-45. The basic antenna element is a strip conductor of dimensions ***L x W*** on a dielectric substrate of dielectric constant ***εr*** and thickness ***h*** backed by a ground conductor plane.

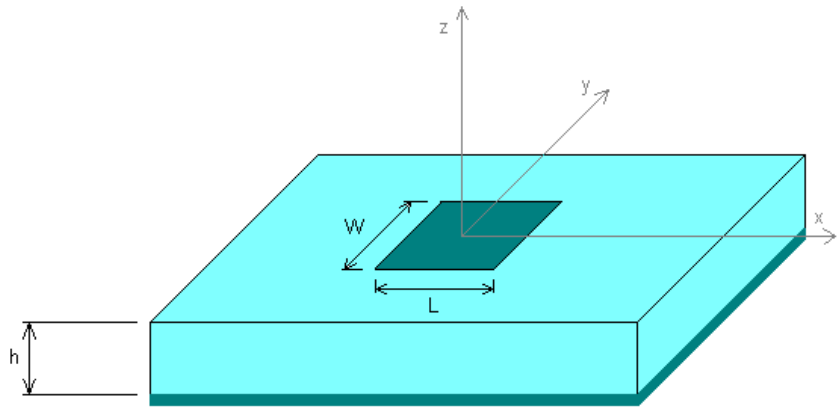

Figura 6-45 Geometry of a rectangular patch

When the patch is excited by a microwave feeding source, a charge distribution will be established on the upper and lower surfaces of the patch, as well as on the surface of the ground plane (Figura 6-46). The positive and negative nature of the charge distribution arises because the patch is about a half-wave long at the dominant mode. The repulsive force among positive charges on the surface of the patch pushes some of them toward the edges, resulting in large charge density at the edges. These charges are the source of fringing fields and the associated radiation.

This movement of charges creates corresponding current densities $\vec{J}_b$ and $\vec{J}_t$ at the bottom and top surfaces of the patch, as shown in Figura 6-46. Since the ratios *h/W* and *h/L* are small, the attractive force among charges is dominant and most of the charge remains underneath the patch. Nevertheless, a small quantity of charge flows around the edges, giving place to a weak magnetic field tangential to the edges. In the following, we will assume that this magnetic field is zero, and we will place four magnetic walls around the periphery of the patch. This assumption has greater validity for thin substrates with higher **εr**.

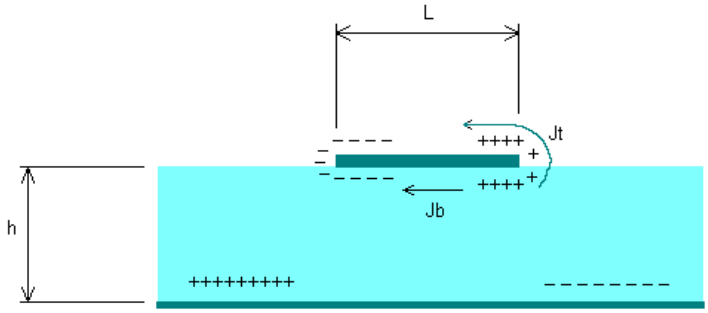

Figura 6-46 Charge distribution on a plane rectangular patch

As the height of the substrate is small compared with the wavelength (*h*<<*λ*), we can suppose that the electric field is constant and nearly normal to the patch surface. Thus we can place two electric walls: one over, and another one below, the surface of the patch.

As follows from these two assumptions, we can model our patch as a cavity with electric walls at top and below, and four magnetic walls along the edges of the patch. In this cavity only TM modes are possible. A sketch of the distribution of the electric field for the dominant TM100 mode of the cavity is presented in Figura 6-47.

The four magnetic walls surrounding the patch can be seen as four narrow apertures or slots, through which radiation occurs. The Huygens field equivalence principle let us represent the microstrip patch with an equivalent current density $\vec{J}_t$ at top surface, in order to take into account the presence of patch metallization. Besides, the four apertures are represented by the equivalent current densities $\vec{J}_{ap}$ and $\vec{M}_{ap}$, which are generated by the magnetic and electric fields at the cavity $\vec{H}_c$ and $\vec{E}_c$ respectively.

In Figura 6-48 the equivalent current densities are drawn. They have been obtained through the following expressions:

Ecuación 6-1 Expressions of the Current and Magnetic Density in the apertures

$$\vec{J}_{ap} = \hat{n} \times \vec{H}_c \qquad a)$$

$$\vec{M}_{ap} = -\hat{n} \times \vec{E}_c \qquad b)$$

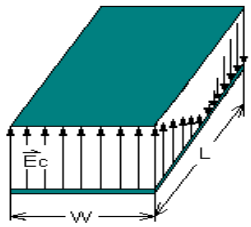

Figura 6-47 Electric field distribution for the TM100 mode in the microstrip cavity

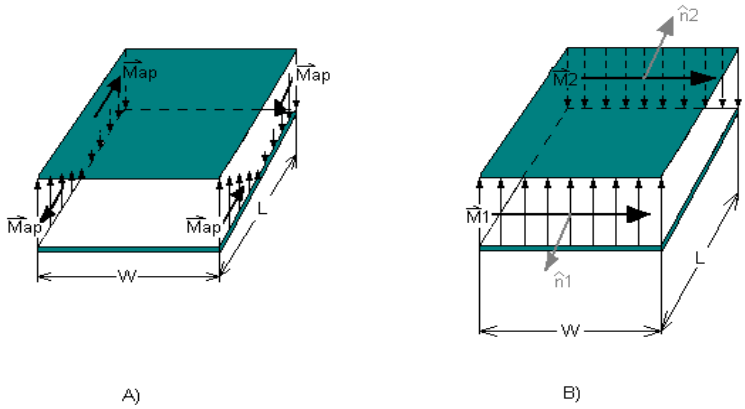

Figura 6-48 Distribution of the magnetic current density for the TM100 mode: A) Distribution on non radiating slots. B) Distribution on radiating slots

When the substrate is thin, the patch current at the top was much smaller than that at the lower part. Hence, we can set the current density at the top J_t to zero, as the radiation from the patch current is negligible. In a similar way, the tangential magnetic fields at the edges of the antenna and the corresponding current densities can be set to zero. According to this, the only nonzero current density is the equivalent magnetic current density M_{ap} (named $\vec{M}_1$ and $\vec{M}_2$ in Figura 6-48 B).

The presence of the ground plane will double the equivalent current density Map, as can be inferred from the image theory. The new current density is given by the Ecuación 6-2 Current density at the cavity:

Ecuación 6-2 Current density at the cavity

$$\vec{M}_s = -2\,\hat{n} \times \vec{E}_c$$

Ecuación 6-3 Electric field created by the cavity

$$\vec{E}_c = \hat{z}\, E_0 \qquad a)$$

$$\vec{E}_c = -\hat{z}\, E_0 \sin\left(\frac{\pi x}{L}\right) \qquad b)$$

The dominant mode of the electric field $\vec{E}_c$ for the slots of length *W* and height *h* is given by Ecuación 6-3 a). Similarly, the expression for the slots of length *L* and height *h* is presented in Ecuación 6-3 b). These equivalent magnetic current densities are shown in Figura 6-48.

The equivalence principle predicts that each aperture will radiate the same field as a magnetic dipole with current density $\vec{M}_{ap}$. But the radiation of the slots laying parallel to the x-axe (those with length *L* and height *h*) cancels to each other, because of the equal and opposite current distributions on them. According to this, the only remaining current densities that contribute to the radiation of the patch are those designed as ***M1*** and ***M2*** in Figura 6-48 B).

Thus, the radiation from a rectangular patch antenna can be seen as the radiation from two vertical apertures or slots separated by a distance L. Vertical slots in the inhomogeneous dielectric of the microstrip antenna are difficult to analyze. Hence, the vertical slots are replaced by two equivalent planar slots as shown in Figura 6-49.

This is the simplest approach to the radiation fields originated by a patch antenna, and it was first examined by Lewin. Its simplicity has made of it the basis for a number of theoretical models for microstrip antennas. Some of them are described in detail in ***[1]*** (Transmission line model, Transmission line model with mutual coupling, Generalized transmission line model, Cavity model, Generalized Cavity model, etc). “Although there is a more rigorous approach, in which radiation field has been calculated from the surface electric current on the conducting patch of the antenna; both methods have been found to be equivalent” ***[4].***

Next, vector potentials are used to determine the fields radiated by these equivalent density currents.

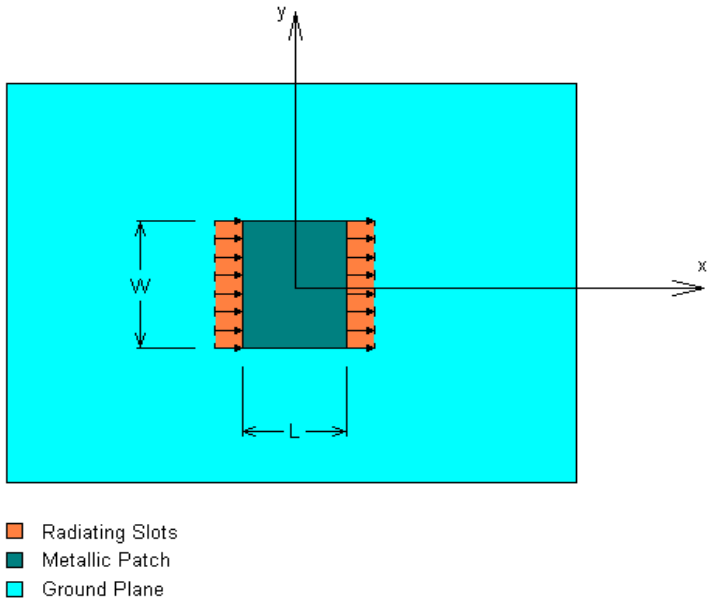

Figura 6-49 Equivalent horizontal radiating apertures of a rectangular microstrip antenna

6.3.2 Radiation Field Formulation

First of all, an explanation of the notation principles used should be made. From now on, the harmonic dependence of the fields with time will be assumed, and the phasorial notation (avoiding repeating every time the factor $e^{j\omega t}$) will be used. Besides, primed coordinates will be used to denote source point location and unprimed coordinates to denote field point location.

The electric and magnetic fields at any point $P(r,\theta,\phi)$ outside the microstrip antenna, created only by magnetic currents can be written as:

Ecuación 6-4 Electric and magnetic fields created only by magnetic density currents

$$\vec{E}^{\,m}(r) = -\frac{1}{\varepsilon}\nabla\times\vec{F} \qquad a)$$

$$\vec{H}^{\,m}(r) = \frac{1}{j\omega\mu\varepsilon}\nabla\left(\nabla\cdot\vec{F}\right) - j\omega\vec{F} \qquad b)$$

Where ε is the permittivity, μ is the permeability of the medium, and ω is the angular frequency. The superscript m indicates that the sources of these fields are only magnetic density currents. With these elements, the electric vector potential $\vec{F}$ is defined as:

Ecuación 6-5 Electric vector potential F

$$\vec{F} = \frac{\varepsilon}{4\pi}\iint_S \vec{M}(\vec{r}\,')\frac{e^{-jk_0|\vec{r}-\vec{r}\,'|}}{|\vec{r}-\vec{r}\,'|}dS'$$

Where $k_0 = {2\pi}/{\lambda_0}$ is the wave number in free space, and $\vec{M}(\vec{r}\,')$ is the surface magnetic current density at a point r' from the origin of coordinates.

Similarly, the fields due only to an electric current can be described by means of the following equations, using the vector magnetic potential $\vec{A}$:

Ecuación 6-6 Electric and magnetic fields created only by electric density currents

$$\vec{E}^{\,e}(r) = \frac{1}{j\omega\mu\varepsilon}\nabla(\nabla\cdot\vec{A}) - j\,\omega\,\vec{A} \qquad a)$$

$$\vec{H}^{\,e}(r) = \frac{1}{\mu}\nabla\times\vec{A} \qquad b)$$

Ecuación 6-7 Magnetic vector potential A

$$\vec{A} = \frac{\mu}{4\pi}\iint_S \vec{J}(\vec{r}\,')\frac{e^{-jk_0|\vec{r}-\vec{r}\,'|}}{|\vec{r}-\vec{r}\,'|}dS'$$

The total fields due to both the electric and magnetic currents sources are:

Ecuación 6-8 Total fields (addition of electric and magnetic)

$$\vec{E}(r) = \vec{E}^{\,e} + \vec{E}^{\,m} = \frac{1}{j\omega\mu\varepsilon}\nabla(\nabla\cdot\vec{A}) - j\,\omega\,\vec{A} - \frac{1}{\varepsilon}\nabla\times\vec{F} \qquad a)$$

$$\vec{H}(r) = \vec{H}^{\,e} + \vec{H}^{\,m} = \frac{1}{j\omega\mu\varepsilon}\nabla(\nabla\cdot\vec{F}) - j\,\omega\,\vec{F} + \frac{1}{\mu}\nabla\times\vec{A} \qquad b)$$

However, as it was said in the previous section and accordingly with the cavity model, magnetic current densities are the only sources of radiation in a microstrip patch antenna. In addition, the only significant field components in the far field are those transverse to the direction of propagation, that is, θ and ϕ components. From ***[5]*** we obtain:

Ecuación 6-9 Expression for the magnetic far fields generated with the cavities

$$H_\theta = -j\,\omega\,F_\theta \qquad a)$$

$$H_\phi = -j\,\omega\,F_\phi \qquad b)$$

And in free space, where the wave impedance $\eta_0 = 120\,\pi\ \ \Omega$, the components for the electric field are:

Ecuación 6-10 Electric far fields generated by the cavities

$$\vec{E} = -\eta_0 \, \hat{r} \times \vec{H} \quad \Rightarrow \quad E_\theta = -j \, \omega \, \eta_0 \, F_\phi \qquad a)$$
$$E_\phi = j \, \omega \, \eta_0 \, F_\theta \qquad b)$$

Far fields are delimitated by the condition that $r >> r'$ or likewise $r \geq 2 \, L^2 / \lambda_0$, where L is the largest dimension of the aperture. Hence we can make some approximations on Ecuación 6-5. With $\left| \vec{r} - \vec{r}' \right| = r - r' \cos\psi$ in the numerator, and $\left| \vec{r} - \vec{r}' \right| \approx r$ in the denominator, the following expression is obtained:

Ecuación 6-11 Electric potential vector for far field conditions

$$\vec{F} = \frac{\varepsilon}{4 \, \pi \, r} \, e^{-jk_0 r} \iint_S \vec{M}(r') \, e^{jk_0 r' \cos\psi} \, dS'$$

Where the meaning of the angle ψ is depicted in Figura 6-50.

Now, we apply the previous derivations to calculate the far fields generated by a rectangular patch antenna. A whole description of the problem and the coordinate systems involved is shown in Figura 6-50.

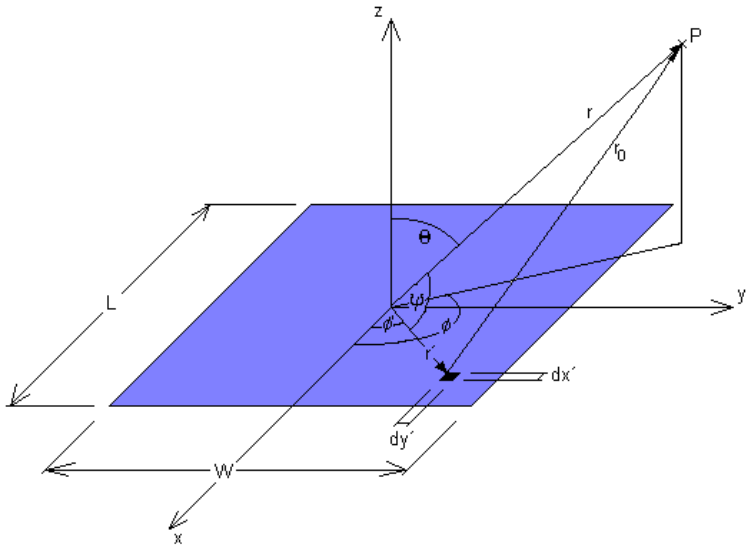

Figura 6-50 Far field calculation in a rectangular patch antenna

As it can be seen in Figura 6-50, $\theta' = 90^0$ for all the points of the patch, as it is located over the $z = 0$ plane. In addition, we can state that:

Ecuación 6-12 Geometric considerations for far field conditions

$$r' \cos\psi = x' \sin\theta \cos\phi + y' \sin\theta \sin\phi$$

Through the substitution of the Ecuación 6-12 in Ecuación 6-11, the far-zone vector potential can be expressed as:

Ecuación 6-13 Far field expression for the electric vector potential F

$$\vec{F} = \frac{\varepsilon_0}{4\pi r} e^{-jk_0 r} \int_{-W/2}^{W/2} \int_{-L/2}^{L/2} \vec{M}(x', y') \exp\left[j\, k_0 (x' \sin\theta \cos\phi + y' \sin\theta \sin\phi)\right] dx'\, dy'$$

The equivalent magnetic current density at the patch can be written as $\vec{M}(x', y') = M_x(x', y')\, \hat{x} + M_y(x', y')\, \hat{y}$. Separating the vector potential in its components, we reach the following result:

Ecuación 6-14 Electric vector potential in the far field in Cartesian coordinates

$$F_x = \frac{\varepsilon_0}{4\pi r} e^{-jk_0 r} \int_{-W/2}^{W/2} \int_{-L/2}^{L/2} M_x(x', y') \exp\left[j\, k_0 (x' \sin\theta \cos\phi + y' \sin\theta \sin\phi)\right] dx'\, dy' \qquad a)$$

$$F_y = \frac{\varepsilon_0}{4\pi r} e^{-jk_0 r} \int_{-W/2}^{W/2} \int_{-L/2}^{L/2} M_y(x', y') \exp\left[j\, k_0 (x' \sin\theta \cos\phi + y' \sin\theta \sin\phi)\right] dx'\, dy' \qquad b)$$

$$F_z = 0 \qquad c)$$

The transformation from Cartesian to spherical coordinates can be simply obtained using a transformation matrix, as given in most Literature. Therefore, the electric far field can be expressed in terms of F_x and F_y:

Ecuación 6-15 Electric far field in terms of F_x and F_y

$$E_\theta = j\, \omega\, \eta_0 (F_x \sin\phi - F_y \cos\phi) \qquad a)$$

$$E_\phi = j\, \omega\, \eta_0 (F_x \cos\theta \cos\phi + F_y \cos\theta \sin\phi) \qquad b)$$

6.3.3 Simulation Results with FEKO

A brief description of the abilities of this program can be consulted in point 6.2.1.1 of 6.2 “ANNEX 2: PROGRAMS AND CODE”.

First, we are going to calculate the far fields created by a single rectangular patch antenna lying over the $z = 0$ plane. The dimensions of the rectangular patch (length L and width W) were calculated to radiate efficiently at a frequency of 76,5 GHz.

The length L of the patch affects mainly to the input impedance Z_{in}, the $-3\,dB$ beam width BW_{-3dB} and the radiation efficiency η_{rad}. According to that, we want to design our patch with an $50\,\Omega$ input impedance, because the feeding lines of our system are thought to have this characteristic impedance ($Z_0 = 50\,\Omega$). In ***[1]***, an empirical expression which allows the calculation of L for $50\,\Omega$ input impedance is given as:

Ecuación 6-16 Calculation of the length L of the patch for an input impedance of $50\ \Omega$

$$L_{50\Omega} = \sqrt{h \cdot \lambda_d} \cdot \left[\ln\left(\frac{\lambda_d}{h} \right) - 1 \right]$$

$$with \quad \lambda_d = \frac{\lambda_0}{\sqrt{\varepsilon_r}}$$

Where h and ε_r are, respectively, the height and the relative permittivity of the dielectric medium. Finally, λ_d is the wavelength on the dielectric's surface.

On the other hand, another empirical expression for the width W of the patch can be found in ***[1]***, It's used to obtain resonant frequency at 76,5 GHz for the TM_{100} mode:

Ecuación 6-17 Calculation of the width W of the patch for an input impedance of $50\ \Omega$

$$W = \frac{c}{2\ f_r \sqrt{\varepsilon_{re}}} - 2 \cdot \Delta L$$

Where c is "celeritas" or the light velocity in vacuum and f_r is the resonant frequency (76,5 GHz). However, the expressions of ΔL and ε_{re} are tedious to calculate, as they involve a set of parameters that must be calculated separately. Consequently, to access to a more exhaustive explanation of the calculation of W, a complete working out of the solution is presented in ***[1]*** (page 265).

The reader may be astonished, as no numerical values have been given for the solutions, but the Bosch Group has made use of the privacy policy in order to preserve their publication. However, these expressions are only an approach to the actual solution. This is obtained trough simulation, and at the end, trough the fabrication of models with whom we essay different measures of L and W till we reach the best suited solution. For example, we have checked that, most times, the length of the endly constructed patch is a little bit greater than the obtained with Ecuación 6-16.

As we change the numerical solution according to the experimental results found, the behaviour of the patch experiments little variations in the input impedance. In fact, the variations in L and W have caused an increase in the input impedance of the patch. In order to manage a 50 Ω input impedance, a suitable transformator must be placed between the feeding point and the patch. The transformator is sketched in Figura 6-51:

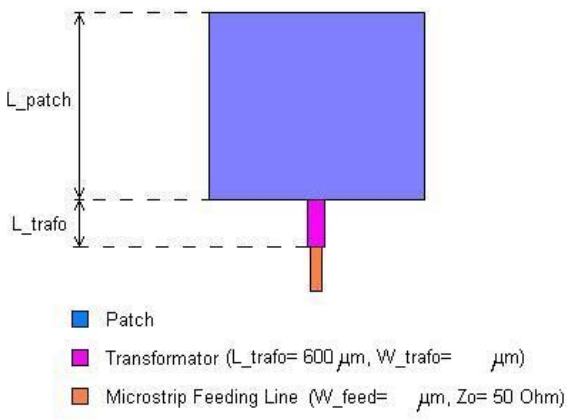

Figura 6-51 Dimensions of the input's impedance transformator

We introduce the geometry of the structure presented in Figura 6-51 in FEKO through the EditFEKO editor to obtain a simulation of its radiation properties. The EditFEKO file generated with this purpose can be consulted in point 6.2.2 of the annex 6.2 “ANNEX 2: PROGRAMS AND CODE”. Once the simulation end, the result for the antenna's gain obtained is presented in Figura 6-52. This figure is also included in point 6.1.1 of the annex 6.1 “ANNEX 1: GRAPHICS”.

As it can be seen in Figura 6-52, the gain of a single microstrip patch antenna is not high enough to accomplish the specifications of our system, as we only get an amount of approximately 6.5 dB. If we recall the specifications (presented in “Memory.pdf, chapter 0, Tabla 0-1), we can also check that the beam widths (elevation and azimuth) of our single patch are too wide (about 50º for the elevation beam width, and around 30º for the azimuth one).

To correct these two adversities, there are two possible solutions. The first one consists of making use of a set of patch antennas arranged in an array configuration. The second one consists of the utilization of aplanatic lenses to focalize the radiation of our patch, providing a narrower beam width.

Of course, a mixture of these two techniques would lead to a feasible solution too. This will be the final solution selected: array of rectangular patch antennas with a cylindrical lens.

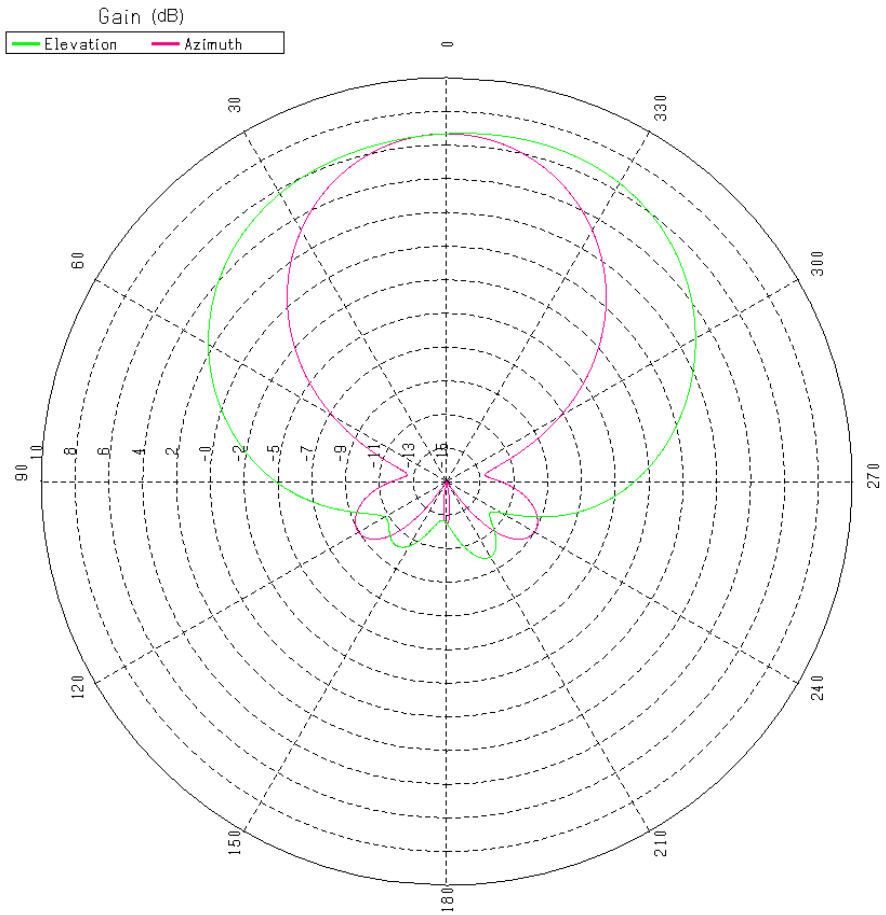

Figura 6-52 Gain in elevation and azimuth of a single patch antenna

6.4 ANNEX 4: MEMORY IN ENGLISH

In the following pages, a translation of the memory of the Project is included. The pictures, graphics and all the referred material shall not be included, as they can be seen in the original memory in Spanish.

6.4.1 Introduction

This project has been developed in the facilities of the multinational Robert Bosch Group GmbH situated in Leonberg (near Stuttgart, Germany) for the AE-DA area (Automotive Electronics-Driving Assistance Systems). This department focuses on the design, development and testing of various electronic devices related to road transport (such as ESP stability control, airbag systems, parking assistance, etc).

The point of departure of this work is the ACC 2 (Adaptive Cruise Control version 2), originally designed for driving on highways with high traffic density.

Under these conditions, the driver must step on the accelerator and brake continuously, also keeping a safe distance with the car right above. ACC was created to perform all these actions for us, making driving much more relaxed. To achieve this, ACC requires the user to set two input parameters:

- Minimum safety distance: User chooses among different levels of security, which distance wishes to keep with the car above.
- Cruising speed: The speed that the vehicle shall maintain while no cars ahead are found.

ACC has, therefore, two modes of operation. To illustrate them clearly enough, please observe the sample in Figura 0-1.

Of course, object detection and measurement of its speed and distance from us are made by a radar (an acronym for RAdio Detection And Range), located in front of our vehicle. The purpose of this project is the design and measurement of antennas for their use in transmit-receive subsystem of ACC.

The following section presents the main features and specifications of the system. The first is the starting point of this project, while the latter are the requirements to be met by any new design to be considered as a possible solution.

6.4.1.1 Characteristics of the ACC's Emitter-Receiver Subsystem

Like all radars, ACC is composed of several subsystems. However, the one that concerns us is the transmitter-receiver one. In the current version of ACC (his name is ACC 2 +, and can be purchased as optional equipment in the major automakers), four polyrod antennas overlapped by an aplanatic lens are used. The final aspect of the ACC system is illustrated in Figura 0-2.

The round part that can be seen in the center of the image (Figura 0-2) corresponds to the aplanatic lens used. Just below it, the four polyrod antennas lie forming a uniform array along the axis X. This achieves a better reduction of side lobes, thus avoiding unwanted reflections from vehicles on lanes adjacent to ours.

Polyrod antennas belong to the surface wave antennas. In these antennas, a two-dimensional wave driven by the supply travels through the dielectric rod antenna. Since a surface wave is radiated only in the discontinuities, the total radiation diagram is formed by interference between radiation due to the binding power supply-antenna, and due to the antenna surface interacting with the surrounding environment (air in our case).

Its radiation characteristics involve a number of limitations. The most important is due to the dependence between the diameter of the rod antenna and the dielectric constant. The diameter of the antenna affects the phase velocity, and therefore the frequency that can be transmitted. On the other hand, the higher the dielectric constant, the thinner can be the rod. Adding to these factors that shape and dielectric rod length affect the radiation pattern and the effectiveness of the antenna, a compromise must be met in order to optimize the dimensions of polyrod, obtaining the radiation pattern more appropriate to the frequency of interest.

This precludes a reduction of its dimensions, so we face the difficulty of integrating this type of RF antennas in a printed circuit.

6.4.1.2 Specifications of the ACC's Emitter-Receiver Subsystem

The requirements for the antennas of the ACC system to ensure proper obstacle detection by the radar are expressed in Tabla 0-1.

6.4.1.3 Proposed Solution

Since ACC is to be mounted in the frontal part of a vehicle, its size should be as small as possible in order to affect as little as possible to the aerodynamics of the car, engine cooling, aesthetics, etc. For these reasons we are faced with the task of reducing the size of the next generation of ACC (the ACC 3).

Due to their low weight, volume and manufacturing costs, and sponsored by its simple integration into a printed circuit board; Microstrip Patch Antennas (or simply Patch Antennas) are selected to carry out this mission.

A patch antenna consists of a patch conductor of any geometry (flat or not), placed on one side of a dielectric substrate. The opposite side of the substrate is occupied by a conducting plane, which acts as a reference. Figura 0-3 shows a patch of arbitrary geometry to illustrate this definition.

The radiation characteristics of patches of many different shapes have been determined in literature, but the most used are the circular and rectangular patches because they are the easiest to describe and study. In addition, both exhibit similar behavior and can be used for all types of applications, from the simplest ones to the most complicated we could imagine. For example, working with circular polarization, broad bandwidth, omnidirectional radiation, etc. is not any trouble with patches of these two types.

A theoretical analysis of the principles of radiation from microstrip patch antennas can be found in Annex 6.3 ANNEX 3: RECTANGULAR PATCH RADIATION THEORY This annex has been compiled from references [1], [2], [3] and [5] of the bibliography.

Although the circular patches are slightly smaller than the rectangular ones for the same radiation characteristics, the simplest configuration is a rectangular patch microstrip antenna. As a result, our efforts will be devoted to investigating the possibilities that this type of antennas can provide for compliance with the aforementioned requirements.

Of course, it would be impossible to meet the specifications of the transmitter-receiver subsystem with a single patch, so we use arrays of rectangular patches.

And to reduce the size of the resulting array, the use of lenses will be studied. These lenses focus the radiation from the array, reducing its size to achieve a certain -3dB beam width and a certain main to secondary lobe ratio. That is, we get the same results using an array with a smaller number of radiating elements.

Once the configuration to use is chosen, it is necessary to design the circuit to feed it. This is not a trivial task, since the circuit will be the responsible in providing the appropriate amplitudes and phases for each of the elements of the array, and thereby setting the final radiation pattern of the system.

Afterwards, the circuits that according to simulations provide more appropriate results will be manufactured and tested in laboratory. Thus, their actual radiation characteristics, consumption, power adaptation, etc will be verified. These results may not be identical to the simulation ones, which only serve as an approach and guidance in the design task. And finally, in sight of empirical data, a decision about which circuit should pass to the production process will be taken.

According to the paragraphs above, this Project is structured as expressed in Tabla 0-2.

Finally, the annexes are structured according to Tabla 0-3.

6.4.2 Proposed Solutions

Since a rectangular patch microstrip antenna has a typical gain of about 6 or 7 dB with a -3dB bandwidth around 56° in azimuth and 96° in elevation (approximate values consistent with the results obtained and presented in Figura 6-1 Gain (elevation and azimuth) of a single rectangular patch antenna from annex 6.1 ANNEX 1: GRAPHICS), the fulfillment of the specifications listed in Tabla 0-1 of the introduction requires the use of an array of antennas of this type.

6.4.2.1 Array without lens

Since the beam width in elevation of a patch antenna is wider than that in azimuth, this will be the first to be reduced. To do this, an array of rectangular patches distributed along the Y axis will be used.

Prior to the start of this project, development engineers of the Robert Bosch Group GmbH had already checked the behavior of an array of 16 rectangular patches (hereafter we refer to this array as the array 1x16) homogeneously distributed along the Y axis. This array is depicted in Figura 1-1. This figure contains no measures since the Bosch privacy policy prevents their publication.

All elements of the array are equidistant from each other. The distance should be within the range $d_y \in \left[\lambda_{eff}/2 , \lambda_0/2 \right]$, where λ_{eff} $\left(\lambda_{eff} = \lambda_0 / \sqrt{\varepsilon_{eff}} \right)$ is the effective wavelength on the surface of the patch, and refers to the effect that the dielectric substrate has in the charge distribution of the whole set. Also, note that λ_0 is the wavelength in vacuum, and its value is higher than λ_{eff}. A formula that allows us to calculate the value of ε_{eff} and a more detailed explanation of the physical significance of these and other constants can be found in [1]. The reason why the patches are placed to a distance of half the wavelength of propagation is to achieve a constructive interference of the fields radiated by each of them. The actual distance at which the patches are placed is obtained by simulation, using a technique of trial and error around the theoretical values calculated. This distance is protected by the privacy policy of the company and cannot be mentioned in this paper.

The array is fed in serial way by connecting power supply to patch 1 (located at the bottom of Figura 1-1). Among the different feeding techniques, the one chosen to feed the 1x16 array during the simulations with FEKO is the so-called "probe feed". More information about feeding techniques in microstrip antennas can be found in [5], but this issue will be discussed in depth in Chapter 2 of “Memory.pdf”.

Returning to Figura 1-1, there are two cuts at the 16th patch of the top of the array at both sides of the transmission line feeding it. These cuts have been made with a dual purpose: on the one hand, to provide an impedance match at the end of the transmission line to avoid current rebounds. On the other hand, easing the energy radiation of the set.

After careful observation of Figura 1-1, it can be observed that the transmission lines that connect one patch to the next in the array are slightly wider at the entrance of the patches. This is because the input impedance of a rectangular patch depends on its length L and width W, and the widest part of the line corresponds to an impedance transformer which adapts the input impedance of patch to a desired value of 50Ω.

A detailed explanation about the calculation of the input impedance of a patch type antenna can be found in [1] and [2]. The theory of impedance matching in transmission lines can be found in [3] and [5]. Finally, note that the in annex 6.3 "ANNEX 3: RECTANGULAR PATCH RADIATION THEORY" as well as in [1], [2], and [5] information about the early radiation of the patch type antennas can be found.

Our work starts with the simulation, with the FEKO program aforementioned, the behavior of the array of 1x16 patches drawn in Figure 1-1. The "*.pre" FEKO file created to carry out this simulation can be seen in section 6.2.3 of "ANNEX 2: PROGRAMS AND CODE".

With this circuit, very good results are managed in elevation, but not so much in azimuth. A picture with the gain in azimuth and elevation has been added in Figure 6 2 of section 6.1.2 "Theoretical results of the 1x16 array" of annex 6.1 "ANNEX 1: GRAPHICS". It can be seen that the maximum gain reaches 17.5 dB in both cases. However, while the beam width at -3 dB shows a suitable value in elevation of 8 degrees, the beam width in azimuth is 76 ° with the main lobe nearly flat. Its value should be around 5 degrees.

Going to adjust the azimuth half power beam width to more suitable values, the use of copies of this 1x16 array uniformly spaced along the x-axis is proposed. But first, the number of copies of the "1x16" array that will compound the flat array must be determined, as well as the distance between each of them.

On the one hand, to set the distance value, the same principle used to find the distance between patches of the 1x16 array will be followed. That is, this distance is a value close to half the wavelength in order to limit the visible range without the appearance of diffraction lobes in order to obtain constructive interference between the different arrays. The final value of distance is obtained by repeated simulations. It will be again comprised in the range from half the effective wavelength in the dielectric and half the wavelength in vacuum, as an important factor associated with coupling between near elements

On the other hand, the number of copies of the group to use emerges clearly. It is proposed to increase the number of elements along the X axis in a greater number than in the Y axis in order to reduce to a greater degree the half power beam width in azimuth. As a consequence different models were tested, and it was found that the most efficient were the arrays of 20x16 and 24x16 patches. The 20x16 array is shown in Figure 1 2 to give the reader an understanding of its dimensions.

The 24x16 array is completely analogous to that presented in Figure 1 2. Both use the feeding technique "probe feed" for the simulations with FEKO, with the same values of amplitude and power, creating a uniformly flat fed group. The distance between each cluster 1x16 is always the same and equal to d_x. The only difference between the two circuits is the number of copies used of the 1x16 array. The files created to define the geometry of these circuits can be found in Annex 6.2 "ANNEX 2: PROGRAMS AND CODE". Point 6.2.4 of Annex deals with the 20x16 array, while point 6.2.5 does with the 24x16 one.

The results obtained from simulations are included in Figure 1 3 and Figure 1 4, as well as in point 6.1.4 of Annex 6.1 "ANNEX 1: GRAPHICS". As can be seen in them, the behavior in azimuth has experienced a marked improvement, reaching a beam width of 5 degrees. As these groups meet the requirements requested in the "Table 0 1 Requirements transmitter-receiver set ACC2 system" in Section 0.2 "ACC: Specifications Transmitter-Receiver Subsystem" in the introduction, they can be considered as feasible solutions to our purpose.

However, the gain in elevation now presents worse characteristics than that for the 1x16 array, as can be seen in Figure 1 4. While the main beam width remains almost unchanged at a value of 8 degrees, the side lobes have higher levels of power, are wider

and almost flat. While still maintaining the relationship main to secondary lobes (value being about 11 dB), the absence of zeros of radiation in the elevation diagram in these side lobes is not recommended for our application. In fact, the radiation pattern could lead to erroneous results due to multipath reception after reflection on the floor. Because of all these factors, it would be advisable to seek a better solution before making a final decision. The reason why these results occur is that the power supply in the array is uniform and evenly spaced, instead of using a Dolph-Tschebyscheff power distribution type to reduce side lobes. This kind of distribution can be consulted in [5].

En el siguiente punto de este capítulo trataremos en detalle una solución alternativa, consistente en el uso de una lente aplanática colocada sobre una agrupación de parches rectangulares de manera que focalice la radiación total del conjunto. Tras estudiar ambas opciones se tomará una decisión acerca de qué circuito pasará a la siguiente fase: la fabricación de varios modelos de test.

Next point of this chapter discusses in detail an alternative solution consisting in the use of an aplanatic lens placed over an array of rectangular patches. This lens will focus the total radiation of the array. After considering both options, a decision about which circuit should pass to the test phase will be taken.

6.4.2.2 Array with cylindrical lens

The use of electromagnetic lenses is becoming an increasingly attractive practice, allowing the reduction of the effective size of the antennas or arrays maintaining its radiation characteristics.

Conceptually, an electromagnetic lens has few differences from an ordinary lens used in optics: both have a curvature and a focal length, shifting the radiation passing through to a particular focal point. Nevertheless, their look is quite different, since electromagnetic lens is not necessarily transparent. An electromagnetic lens is made of a dielectric material whose electromagnetic properties make the incident radiation with a frequency and angle of arrival converge towards a focal point. Reference [11] of the literature provides a detailed description of the theory of operation of electromagnetic lenses.

Thus, when a lens is placed over an antenna, it adjusts its radiation pattern resulting in a smaller half power beam width. Figure 6-6 in section 6.1.5 of Annex 6.1 "ANNEX 1: GRAPHICS" serves to illustrate and clarify the phenomenon. Since our application requires a fairly narrow beam width, the lenses can be of great help to achieve the requirements.

The present generation of ACC system on the market uses an aplanatic lens as shown in Figure 0 2 of the introduction. As a result, the first array to test as solution will be the one used in the previous system, ACC2 +, but with slight variations. While the former consisted of an array of three equally spaced polyrod antennas along the y-axis with a circular lens placed over them, the solution proposed here will make use of rectangular patch antennas with a cylindrical lens overlay. Figure 1 5 is a diagram of the proposed array.

Figure 1 5 shows that the patches have been rotated 90 degrees. This is because the feeding technique used for the simulations with FEKO. Each patch is fed individually instead of using a serial power distribution. The reason that motivates this change is none other than saving CPU work time during the simulations (in 20x16 and 24x16 arrays fed in serial, each simulation could last around 7 hours). On the other hand, this rotation of the patches will only affect the polarization of the emitted waves.

Although the concept of the array is totally different, the dimensions of the patches used are the same as in 1.1, "Array without lens" above. And like then, cannot be mentioned in this paper. By contrast, the distance d_y between adjacent patches experiences a very slight variation despite being back within the range $\left[\lambda_{eff}/2 , \lambda_0/2 \right]$.

Since FEKO does not have any option to calculate the effects of a lens superimposed to the problem to solve, the use of another simulation program shall be required. This program is called LISSY, created by the project director, Dr. Ing Thomas Binzer, for the Robert Bosch Group GmbH. LISSY uses as input the "*.ffe" extension files generated by FEKO. Thus it is able to calculate the effect of placing a lens over any structure simulated with FEKO. Because of this symbiosis between the two applications, LISSY's interface is completely analogous to that from EditFEKO.

LISSY uses different text commands to determine the position of the lens in relation to the radiating element, the characteristics of dielectric material with which it is built, etc.. These commands are entered in a text "*.pre" extension file (such as FEKO did) that will be read by LISSY. More details about the operation and management of this program can be found in Annex 6.5 "ANNEX 5: LISSY MANUALS (IN GERMAN)", and more succinctly

but in English version in section 6.2.1.3 of Annex 6.2 "ANNEX 2: PROGRAMS AND CODE".

With everything said in the two previous paragraphs, before using LISSY, the circuit having the best features of radiation must be found with FEKO. Consequently, the group of 1x3 patches is simulated with FEKO using different combinations of the input power.

First, the 3 patches are fed with currents having the same amplitude and phase, which is known as uniform feed. As a result we obtain the figures of point 6.1.6 of Annex 6.1 "ANNEX 1: GRAPHICS". In them, it can be seen that the radiation pattern in azimuth is virtually flat for all ϑ, while the elevation gain has a better appearance, due to the fact that the 3 patches are located along the Y-axis. As expected, the diagram has symmetry with respect to $\vartheta = 0^{o}$ in elevation, and the main to secondary lobe ratio is worth. "*.pre" FEKO file used to describe this assembly is attached in point 6.2.6 of Annex 6.2 "ANNEX 2: PROGRAMS AND CODE".

However, these results can be improved by introducing changes in both amplitude and phase with whom the patches are fed.

The task begins by changing the input's amplitude. Taking the central patch as reference, if the current amplitude at the entrance of the adjacent patches is reduced, the shape and level of side lobes can be adjusted. To achieve this, the three patches will be fed with the same signal, but multiplied by a factor of amplitude in the range $[0, 1]$. Or equivalently, they will be fed with different attenuations at their input. From now on, and for nomenclature easing purposes, the factors that affect each patch will be presented in descending order according to their position on the Y axis (i.e., the first factor will correspond to the patch located at the top with y > 0, the following to the central one with y = 0, and the last one to the lower one y <0).

In point 6.1.7 of Annex 6.1 "ANNEX 1: GRAPHICS" the radiation patterns in both azimuth and elevation are shown. Then, Figure 1 6 only shows the diagrams in elevation, as this is the pattern that is experiencing change. From Figure 1 6 is inferred that the configuration that provides more advantages is that with $V_{y\uparrow} = 0.5\, V_{middle} = V_{y\downarrow}$, and that power would correspond to a triangular pedestal distribution. This power configuration has lower side lobes of all tested. In return, the beam width increases slightly, as expected. But this effect is negligible compared with the attenuation achieved in the secondary lobes. In point 6.2.7 of Annex 6.2 "ANNEX 2: PROGRAMS AND CODE" appears the "*.pre" FEKO file used to define the configuration. With minor variations on that file, as explained in paragraph 6.2.7, all tested configurations are obtained. Likewise, in point 6.1.7 of Annex 6.1 "ANNEX 1: GRAPHICS" there is a brief explanation about the notation used in the pictures to designate the different tested configurations.

The next aspect to be modified to improve radiation pattern is the phase of the feeding reaching the patches. Again, the central patch is taken as the phase reference, and at the patches at the edges a phase difference with respect to it is introduced.

Figure 1 7 shows the changes introduced in the elevation's diagram of the array fed with amplitude factors 0,5-1-0,5 when patches are fed by introducing a certain phase difference between them. Again, with regard to nomenclature, the phase variations are set starting with the top patch, then the central one and ending with the lower one along the Y axis. Please consider also, that if the phase difference is positive, it means that the phase introduced in the signal is greater than at the central patch, and vice versa. In point 6.1.8 of Annex 6.1 "ANNEX 1: GRAPHICS" these diagrams are available for both azimuth and for elevation.

A larger number of phase differences was studied, but they have not been introduced in Figure 1 7 to preserve readability. As shown, a change in the phase of the input signal leads to a change in form and power levels of secondary lobes in response to displacement in the visible range. In fact, introducing a considerable gap we can eliminate one of the side lobes. However, this is not very advantageous because of the deviation introduced in the direction of maximum radiation with respect to $\vartheta = 0^{o}$.

Considering the deviation from $\vartheta = 0^{o}$, and the shape of the side lobes, the most appropriate configuration to be placed together with the cylindrical lens is:

$$V_{y\uparrow} = 0.5\, V_{middle} = V_{y\downarrow} \qquad \text{Ec. 6-1}$$

$$\Delta\varphi_{y\uparrow-middle} = 12.5^{o} = -\Delta\varphi_{middle-y\downarrow} \qquad \text{Ec. 6-2}$$

This configuration is known as "Patch_3x1_0-5_1_0-5_P12-5_-12-5" in Figure 1-7 and at point 6.1.8 of Annex 6.1 "ANNEX 1: GRAPHICS. The "*.pre " FEKO file necessary to obtain these results is included in section 6.2.8 of Annex 6.2 "ANNEX 2: PROGRAMS AND CODE".

Finally, once the feeding settings of the array are chosen, LISSY program is used to simulate the effects of superimposing a lens. The "*.pre" FEKO extension file which defines the geometry of the lens, its composition, its distance from the cluster, and the fields to calculate appears in point 6.2.9 of Annex 6.2. The results are shown in Figure 1 8 and Figure 1 9, as well as in point 6.1.9 of Annex 6.1.

In Figure 1 8 and Figure 1 9 a marked improvement in both azimuth and elevation diagrams is shown as the half power beam width is reduced while the gain level for the main lobe is increased. This increase in gain is due to the confinement effect of the lens inserted into the radiation of the whole. That is, there are a greater number of waves confined to a lower angle, which leads to an addition of contributions from fields that before the lens had different angles. Thus, at the exit of the lens these outgoing waves at the same angle are added, helping to achieve a higher level of radiated power.

However, while the elevation diagram shows a maximum gain of 20 dB and a half power beam width of 6 degrees, the azimuth pattern should be corrected in some way, because it has a beam width too large for our purposes.

The only possible correction is to again use copies of this array equally spaced along the X axis. That is, a flat two-dimensional or matrix array must be used as was the case in paragraph 1.1.

After testing several arrays, the most suitable ones proved to be the array of 20x1x3 patches (or simply 20x3 array) and the array of 24x1x3 patches (abbreviated 24x3). The fist one is composed of twenty copies of the group of 1x3 patches defined in Equation 1-1 and Equation 1-2. That is, twenty copies of the group with which the diagrams in Figure 1 8 and Figure 1 9 are obtained. The latter one is composed of twenty-four copies of the "1x3 array."

The distance between consecutive elements must be again calculated, but this time it will be within the range $\left[\lambda_{eff}, \lambda_{0}\right]$. This greater distance back to give the final set of constructive interference, as well as more space for the power supply to build, and that will be discussed in Chapter 2 of this work. The actual distance used is again obtained by simulation, and cannot be mentioned here because of the privacy policy of the Bosch group.

Figura 1-10 and Figura 1-11 contain the final results obtained in azimuth and elevation respectively, which have also been included in section 6.1.10 of Annex 6.1 "ANNEX 1: GRAPHICS". The "*.pre" FEKO files defining the geometry of clusters, and used later to run LISSY are attached in points 6.2.10 (20x3 array) and 6.2.11 (24x3 array) of Annex 6.2 "ANNEX 2: PROGRAMS AND CODE. " More specifically, the output "*.ffe" file extension generated by FEKO when modeling these arrays is used as input for LISSY.

As shown in Figure 1 10, the gain level in the direction of maximum radiation reaches an awesome value of $31{,}23\ dB$. Half power beam width is 4 degrees, a little bit less than that required in Tabla 0-1 from chapter 0 Introduction. Finally, note that the primary to secondary lobe ratio has a very appropriate value of $16{,}32\ dB$ in avoiding unwanted reflections from objects in side lanes.

Looking at the results in elevation shown in Figure 1 11 we can be well satisfied with a maximum gain of $32{,}35\ dB$ and a half power beam width of 6 degrees, which is slightly above the requirements of Tabla 0-1, where 5 degrees were called for. Nevertheless, this diagram still has a remarkable advantage, because the primary to secondary lobe ratio is so high ($36{,}92\ dB$) that we can almost guarantee that the value of the signals coming from reflections off the ground, even under the most adverse circumstances, as may be in the presence of ice, are practically negligible at the receiver input.

The results are virtually identical in the two arrays tested, 24x3 and 20x3. So we opted for the latter (20x3) as we did in section 1.1. This decision is based on power, space and money saving by using an array with a smaller number of patches.

6.4.2.3 Conclusion

As a result of detailed study of the proposed solutions in 1.1 and 1.2, it can be deduced that the array of 20x3 patches with cylindrical lens assembled is the best solution for the ACC system, because it meets all requirements set out in paragraph 0.2 of the introduction. In order to facilitate the verification of this statement, Figura 1-12 and Figura 1-13 are included, providing a comparison between the radiation patterns of the two configurations proposed throughout this chapter. These Figura 1 12 and Figura 1 13 are also included under Section 6.1.11 of annex 6.1 “ANNEX 1: GRAPHICS”.

As shown in Figura 1-12, the behavior of the two proposed solutions is very similar in azimuth, although the array of 20x3 patches with lens has higher gain. However it is in the behavior in elevation where differences arise. As shown in Figura 1-13, the array of 20x3 patches with lens has a radiation pattern in elevation very suitable for our purposes with low gain side lobes and a small half power beam width. In this overwhelmingly leads the array of 20x16 patches without lens, which has a diagram in elevation with oversized side lobes (both in width and amplitude).

These facts lead us to highlight the dramatic improvement provided by the lens that achieves higher levels of gain while reducing the number of patches of the array as much as 82%. This implies a significant reduction in the consumption of the circuit, which is very advantageous as the system shall be fed with the battery of the vehicle in which it is mounted.

For all these reasons, the decision to make is simple. The circuit to be manufactured and tested in anechoic chamber will be the array of 20x3 patches overlaid with a cylindrical lens.

6.4.3 Feeding Circuit

6.4.3.1 Introduction

Once the configuration that meets the system requirements of ACC2 has been found, the next task to tackle is the design of a circuit that feeds it and that would make this arrange a feasible solution.

As a result of the topics discussed in Chapter 1, the solution chosen is the array of 20x3 patches with superimposed cylindrical lens. That is, 20 copies of "1x3 array" which presented the peculiarities in their feeding referred to in Ec. 1-1 and Ec. 1-2. This equations are reproduced here for convenience:

$$V_{y\uparrow} = 0.5\, V_{middle} = V_{y\downarrow} \qquad \text{Ec. 6-3}$$

$$\Delta\varphi_{y\uparrow-middle} = 12.5^{o} = -\Delta\varphi_{middle-y\downarrow} \qquad \text{Ec. 6-4}$$

These 20 1x3 arrays are arranged equally spaced along the X axis, and the same signal power must reach all of them with equal amplitude and phase. Finally, the planar array is placed below a cylindrical lens made of a particular dielectric material.

During the modeling of the circuit, each patch of the final solution was fed individually to save CPU time during FEKO simulations. However, the patches will now be fed from a single point. So the power supply circuit will be in charge of providing the appropriate amplitudes and phases at the entrance to each and every one of the 60 patches that make up our 20x3 array.

The design of the network can therefore be divided into two stages. In the first one, we face the problem of feeding the group of 1x3 patches in series, but with different amplitude and phase for each patch. The second one deals with the power supply of the 20 arrays of 1x3 patches in a parallel scheme to ensure the same amplitude and phase at the entrance of them all.

According to aforementioned paragraphs, this chapter is divided into three sections. The first one is devoted to the choice of one of the available feeding techniques for microstrip circuits. The next two section focus on the design stages of the supply circuit above.

6.4.3.2 Feeding technique

Among the most widely known techniques for feeding a patch antenna, an election must be made. As the energy received by the antenna should be radiated with maximum efficiency, the antenna must be conveniently adapted to the power source. There are a variety of techniques easy to produce and with good matching properties, but the following four are the most commonly used:

- Microstrip line
- Probe Feed (or Coaxial Feed)
- Aperture Coupling
- Proximity Coupling

All of them are fully depicted in many texts of antennas, and a more generic description can be found in **[5]**. However, the two most interesting are the first two: Microstrip Line and Coaxial Feed. Figura 2-1 outlines their operation.

Throughout Chapter 1, each patch of the solution was fed separately during the simulations. **The technique used in FEKO to achieve this was the Probe Feed or Coaxial Feed**. This technique is a widely used feeding system and can be seen in Figura 2-1 b).

In addition to its own qualities (such as low spurious radiation, simple coupling to coaxial cables available in the market, ease for manufacturing, etc.), the use of this technique during the modeling process had 2 main reasons. The first is to save CPU time (always desirable). The second and main one is the facility provided by FEKO for its use. FEKO actually has a specific command to feed circuits defining a segment of current between two points. Once these points have been defined, the amplitude and phase voltage inserted through the cable segment can be adjusted at will. It is the command "A1" from EditFEKO, and is perfectly suited to our purposes.

However, having found the circuit more suitable for our solution, our work focuses on making it viable in practice. And a circuit coupled to 20x3 coaxial connectors on a printed circuit board is not feasible for the system ACC2 +. The way to overcome this limitation is to feed all the patches with a single connection to a source, along with a supply circuit providing proper voltage to every patch.

Returning to point 0.3 of the introduction, one of the main reasons for proposing the use of such microstrip patch antennas was their ability to be easily integrated into a printed circuit. Accordingly, our supply circuit will be composed of different sections of transmission lines of microstrip type for two reasons: the first is that its operating principle is the same as for patch antennas. The second one is their ease of printing on a silicon board. The only difference between them is that while the patch antenna favors radiation of energy, the microstrip line supports the conduction of that energy.

Consequently, the technique that will nourish our network will be the Microstrip Line one. It consists of connecting the patch to a strip of conductor, as shown in Figure 2 1 a). This strip is narrower than the patch, but both share the same dielectric substrate and the same plane conductor. That is, the height h and the dielectric permittivity of the substrate ε_r are the same for the antenna and the microstrip line.

To stimulate their radiation properties, the patch antenna requires a thicker substrate and a lower dielectric permittivity $\left(h \uparrow, \varepsilon_r \downarrow\right)$; while a microstrip transmission line needs just the opposite $\left(h \downarrow, \varepsilon_r \uparrow\right)$ to avoid transmission losses. As usual, a compromise between the two factors must be found in order to reach an optimal solution. According to [5], appropriate values for the thickness of dielectric substrate in a patch type antenna are within the range $0.003\,\lambda_0 \le h \le 0.05\,\lambda_0$, while the dielectric permittivity is usually in the range $2.2 \le \varepsilon_r \le 12$. **In our case, the values for the substrate used are the following: Height of dielectric** $h = 0.127\ mm = 0.0324\,\lambda_0$**, relative permittivity on it** $\varepsilon_r = 3.05$**, and its loss tangent** $\tan\phi = 0.0013$**.**

These values were chosen because the main goal of our system is to radiate through the patch antennas, even when the power supply circuit has more losses than it should and transmission lines are somewhat wider than usual for the different characteristic impedances used. These issues are discussed in more detail in references **[2]**, **[3]**, and **[5]** of the Bibliography.

6.4.3.3 Feeding of the 1x3 array

This section tackles the most complex aspect of the design of the power supply: The series circuit that feeds the array of 1x3 patches with different amplitudes and phases for each of them.

The rectangular patch used in our system as radiating element has been designed to present an input impedance of $Z_{in} = 50\,\Omega$ (actually does not reach this value, so a λ/4 transformer is placed at its entry to manage this). Consequently, the characteristic impedance of microstrip transmission lines will be $Z_0 = 50\,\Omega$, wherever possible. A detailed explanation about the theory of transmission lines and λ/4 transformers can be found in **[10]**.

From this statement, our first task is to provide the appropriate amplitudes at the entrance of each patch. Next, to adjust the phase shifts among them.

6.4.3.3.1 Providing the right amplitudes to each patch of the 1x3 array

Ec. 2-1 states that the amplitude in patches at the ends must be half the amplitude in the central patch. Drawing on the quadratic relationship between voltage and power (this relationship is still applicable to our circuit, even for frequency range of microwaves on microstrip transmission lines), the powers at the entrance of each of the patches can be expressed as follows:

$$P_{middle} = 4P_{y\uparrow} = 4P_{y\downarrow} \qquad \text{Ec. 6-5}$$

From Ec. 6-5, the relationship among the S parameters of the various ports of the circuit can be deduced. But before going further, it would be reasonable to present an outline of the circuit being dealt, detailing its ports and the powers that should be raised in each node of it. According to this, Figura 2-2 is included.

As shown in Figura 2-2, the circuit has four ports. Port 1 is the point of connection to the parallel power circuit reaching the 20 arrays 1x3, and ports 2, 3 and 4 are the rectangular patches, as they are the load impedances connected to these ports. Please note the different widths of the microstrip lines shown in Figura 2-2. This variety of widths is due to the different characteristic impedances of the transmission lines used, and they will be widely discussed throughout the chapter. Finally, Figura 2-2 describes the powers present in each branch of the circuit and they will be used in subsequent developments. In fact, Ec. 6-5 can be reformulated using the notation of Figura 2-2 as shown in Ec. 6-6.

$$P_3 = 4P_2 = 4P_4 \qquad \text{Ec. 6-6}$$

Looking at Figura 2-2 and making use of Ec. 6-6, a simple system of equations can be posed, in which unknowns are P2, P3 and P4:

$$\left.\begin{aligned} P_1 &= P_2 + P_3 + P_4 \\ P_2 &= \tfrac{1}{4} P_3 \\ P_4 &= P_2 \end{aligned}\right\} \qquad \text{Ec. 6-7}$$

Solving Ec. 6-7 by the method of substitution and expressing the solutions as a function of input power P1 the following results are obtained:

$$P_2 = P_4 = \frac{1}{6} P_1 \qquad \text{Ec. 6-8}$$

$$P_3 = \frac{4}{6} P_1 \qquad \text{Ec. 6-9}$$

However, the power that arrives at a port is not a very usual magnitude in microwave circuits, while it is very common to use S. Parameters S parameters, or scattering, are a set of values that describe the transmission and reflection of waves traveling through a circuit for a given frequency. Commonly used to characterize high-frequency circuits or networks, where the simpler models used at lower frequencies are no longer valid. Reference **[9]** of the literature provides a much more detailed study of these parameters.

A network of N ports is completely defined in their behavior at a fixed frequency by the NxN matrix of all their S parameters. In our case, as the 1x3 array has 4 ports, a 4x4 matrix will be needed to work out the indices of reflected and transmitted power at each port. However, the main aspects of our network are twofold:

i. Have a good impedance matching between our loads and the feeding circuit
ii. Have a good impedance matching between the input of our 1x3 array and the supply circuit

The first key is that there must be no reflection of power at the input of our rectangular patches, because they are the load of the circuit, and as radiating elements of the system should receive the maximum power available, without reflecting anything. While the importance of the second is that our circuit will be connected to a source (or to other circuit itself connected to a source) and an input impedance, when placing the patches on their respective ports, equal to the generator impedance is essential so that the entire power output will be exploited without any reflections.

According to all the expositions made in the two previous paragraphs, from the 16 S parameters that exist in our supply network of the 1x3 array, the most important ones are included in Tabla 2-1.

Typically, the magnitude of S parameters is not usually expressed as linear but logarithmic or dB units. The relationship between both is expressed in Ec. 6-10.

$$\begin{aligned} S_{xy}\big|_{dB} &= 20 \log_{10} S_{xy} \\ &= 20 \log_{10}\left(\frac{Power\ delivered\ to\ a\ Z_0\ load\ at\ port\ x}{Power\ available\ from\ Z_0\ source\ at\ port\ y} \right)^{1/2} \\ &= 10 \log_{10}\left(\frac{Power\ delivered\ to\ a\ Z_0\ load\ at\ port\ x}{Power\ available\ from\ Z_0\ source\ at\ port\ y} \right) \end{aligned} \qquad \text{Ec. 6-10}$$

Regarding the value of S_{11}, the lower amount, the better the performance of the network. This means that almost all the energy arriving to the circuit is used in it, as the insertion losses are very low. The achievement of this goal requires a good impedance matching between the source and the input of the circuit. Once managed this adjustment, S_{11} could be set to a value as low as desired, so it will be necessary to establish a threshold criterion. Thus, any solution will be deemed as acceptable when it provides values such that the return loss meet $S_{11}\big|_{dB} \leq -12\ dB$. That is, any solution in which the power delivered from the source is 16 times greater than that reflected at their input will be accepted.

For the remaining S-parameters of interest given in Tabla 2-1, the values to be accomplished are calculated according to Ec. 6-10, and they are expressed in Ec. 6-11.

$$S_{21}\big|_{dB} = -7.78\ dB \qquad a)$$
$$S_{31}\big|_{dB} = -1.76\ dB \qquad b) \qquad \text{Ec. 6-11}$$
$$S_{41}\big|_{dB} = -7.78\ dB \qquad c)$$

Once the values to be achieved for the S parameters at each port are known, next step is to calculate the impedance of the circuit transmission lines that will achieve these results. These calculations are simple, as they are comparable to the calculation of voltages and currents in a passive circuit for small signal. The results are shown in Figura 2-3, and the steps taken to obtain them are described in Equation 6-12 a) and b).

$$P = V \cdot I = \frac{V^2}{Z} \Rightarrow \begin{cases} P_{\text{int}} = 5 \cdot P_2 \Rightarrow Z_{\text{int}} = \frac{1}{5} \cdot Z_2 = 10\ \Omega & a) \\ P_4 = \frac{1}{4} \cdot P_3 \Rightarrow Z_4 = 4 \cdot Z_3 = 200\ \Omega & b) \end{cases} \qquad \text{Ec. 6-12}$$

The results shown in Ec. 6-12 a) and b) only take into account the powers that flow through each branch of the circuit, and start from the assumption that $Z_2 = Z_3 = 50\ \Omega$, due to the fact that $Z_L = 50\ \Omega$ is the input impedance presented by the patches. Once the final loads of the array are known, a characteristic impedance of $Z_0 = 50\Omega$ will be used in the transmission lines of the circuit, wherever possible, to avoid line-end reflections.

This last "wherever possible" in the preceding paragraph refers to the fact that in a microwave circuit, it is not possible to pass directly from one transmission line section with a characteristic impedance Z_0 to other with a different characteristic impedance Z_0', as this would produce reflections of current on the line that would reduce its conduction efficiency. Nevertheless, this reflections can be avoided when the step from Z_0 to Z_0' is done properly, by means of the use of a λ/4 transformer.

To move from a section of line with a characteristic impedance to another with a different impedance without causing reflections, we have to "adapt" both impedances. This is done using so-called λ/4 transformers. These are sections of transmission lines with a length of one quarter of the length of the wave that travels through them at the center frequency, with a characteristic impedance such that adjusts the impedance present at its input to that present at its output. The equation governing this type of transformer is expressed in Ec. 6-13.

$$Z_0^2 = Z_{in} \cdot Z_L \qquad \text{Ec. 6-13}$$

Where Z_0 is the characteristic impedance of the section with length λ/4 (the transformer). And Z_{in} and Z_L are the impedances we want to adapt at the entry and the exit, respectively, of the λ/4 transformer. A more comprehensive description of the impedance transformation in transmission lines can be found in **[10].**

Figura 2-3 shows the impedances that must be present in each branch of the circuit to have the desired power distribution in each of them. After a careful observation of it, the following: can be inferred:

i. At the junction among the branches 1, 2 and intermediate ("int" in Figura 2-3) there is the connection of the branch 1 with two parallel lines (2 and intermediate). The parallel of Z_{int} and Z_2 results in $Z_{2//\text{int}}^{eq} = 8{,}33\Omega$ [1]. A λ/4 transformer will be needed to adapt Z_0 (=50 Ω) with $Z_{2//\text{int}}^{eq}$. This transformer will be called T1

ii. In the intermediate branch, a matching is needed between $Z_{\text{int}} = 10\Omega$ and $Z_0 = 50\Omega$ of the transmission line, as a transmission line with a 10Ω characteristic impedance is just too wide and would be difficult to integrate into our circuit. This transformer will be called T2.

iii. At the junction among the branches, 3, 4 and intermediate there is again a line parallel connected to two transmission lines (branches 3 and 4). In this case the equivalent impedance of parallel between Z_3 and Z_4 will be $Z_{3//4}^{eq} = 40\Omega$. A transformer T3 will be needed between Z_0 and $Z_{3//4}^{eq}$.

iv. At branch 4, a transformer T4 will be needed to adapt the passage from $Z_4 = 200\Omega$ to $Z_0 = Z_L = 50\Omega$.

All these transformers have been included in Figura 2-4, indicating for each its input impedance, its output impedance, and its characteristic impedance.

In view of Figura 2-4, it might consider to join impedance transformations undertaken by the transformers T2 and T3 in a single step from $Z_{in} = 10\Omega$ up to $Z_L = 40\Omega$. However, it is preferable to use two transformers in what is known as a gradual transition to multi-hop impedance, because this solution offers better performance, especially with regard to possible use of wider bandwidth in the frequency domain.

Moreover, the appearance of real circuit manufactured will differ a little from the scheme shown in Figura 2-4, as at the intersections between branches there will be a T-connection in which each branch will present a certain width corresponding to the characteristic impedance of the transformer or transmission line to which it is connected. Figura 2-5 presents a more accurate final appearance of the circuit before the patches will be added in their ports.

Furthermore, while calculating the width of a transmission line for certain characteristic impedance Z_0, we found that there will be some width limits within which we can move depending on the type of dielectric substrate used.

$$\frac{\lambda_0}{4} \geq W_{Z_0} \geq W_{100\Omega} \qquad \text{Ec. 6-14}$$

Where $W_{100\Omega} = 0{,}09mm$ at our central frequency. This indicates that the width of the transmission line to be added cannot be greater than its length, as this would give rise to harmonics of our operating frequency, which are also known as transverse propagation modes. Besides, Ec. 6-14 imposes a minimum width limit, under which the circuit would present more losses than acceptable for the substrate used.

---

[1] The equivalent impedance of the parallel of n impedances is calculated with the following expression:

$$1/Z_{1//2..//n}^{eq} = \sum_{i=1}^{n} 1/Z_i$$

To calculate the width of each transmission line section, the expressions contained in Ec. 6-15 will be used conveniently. A more in-depth explanation of its justification can be found in **[3]**.

$$If\ \frac{W}{h}\rangle 2 \Rightarrow \frac{W}{h}=\frac{2}{\pi}\left\{B-1-\ln(2B-1)+\frac{\varepsilon_r-1}{2\varepsilon_r}\left[\ln(B-1)+0{,}39-\frac{0{,}61}{\varepsilon_r}\right]\right\};$$

$$with\quad B=\frac{377\pi}{2Z_0\sqrt{\varepsilon_r}} \qquad Ec.2-13\ a)$$

$$If\ \frac{W}{h}\langle 2 \Rightarrow \frac{W}{h}=\frac{8e^A}{e^{2A}-2};$$

$$with\quad A=\frac{Z_0}{60}\sqrt{\frac{\varepsilon_r+1}{2}}+\frac{\varepsilon_r-1}{\varepsilon_r+1}\left(0{,}23+\frac{0{,}11}{\varepsilon_r}\right)$$

Ec. 6-15 b)

Where W is the width of the section with characteristic impedance Z_0 we want to calculate, h is the height of the dielectric (0.127 mm in our case), and ε_r is the relative electrical permittivity of the dielectric (3.05 in response to the dielectric chosen). Only practice will enable us to properly choose the appropriate formula from the two available. Until then, we must calculate both, and stay with one that meets the requirement of departure. $If\ \frac{W}{h}\langle 2\ or\ If\ \frac{W}{h}>2$. In the case of equality to 2, both calculations coincide.

Once the calculations of the widths of the lines involved in our supply circuit have been finished, and in view of Ec. 6-14, it is inferred that some changes must be made in T1 and T2 transformers, since:

1. $W_{21\Omega}=1{,}0625\ mm\rangle \lambda_0/4 \Rightarrow T1\ Not\ OK$
2. $W_{22\Omega}=1{,}0065\ mm\rangle \lambda_0/4 \Rightarrow T2\ Not\ OK$
3. $W_{45\Omega}=0{,}406\ mm\leq \lambda_0/4 \Rightarrow T3\ OK$
4. $W_{100\Omega}=0{,}090\ mm\leq \lambda_0/4 \Rightarrow T4\ OK$

These changes will consist of the introduction of two transformers λ/4 to replace T1, and two more to replace T2. In this way it is avoided the use of characteristic impedances wider than those established in Ec. 6-14. There are endless possibilities for the replacement of T1 by two transformers and the same is true for T2. However, it is common to make an intermediate step by the geometric mean of the impedances to adapt between the extremes. As in this case the geometric mean turned out to be very low, which involved an excessive width not according to Ec. 6-14, various options were tested during the modeling of the circuit.

Calculations of the widths of each transmission line for the desired characteristic impedance from Ec. 6-15 are theoretical. Subsequently, they must be validated via simulation. With this aim the program ADS (Advanced Design System) is used. Through a friendly graphical interface, ADS allows you to define sections of transmission lines configurable in length and width, height, relative dielectric permittivity and dielectric loss tangent, etc. Also offers the ability to feed these sections with a certain source impedance and placing a load on its output, making it ideal for designing λ/4 transformers. Finally, note that also facilitates the calculation of S parameters that are of greatest interest,

showing graphs with respect to frequency, and even Smith charts. All information on this program can be found in **[8]** and more briefly in section 6.2.1.2 of Annex 6.2 "ANNEX 2: PROGRAMS AND CODE".

With the help of ADS, width values obtained were checked section by section. They differ minimally with respect to the theoretical values. Once all sections have been simulated, we start to join them. Starting with port 1 on the branch 1 in Figura 2-4, the different transmission lines are added to the circuit, making the changes needed to obtain good results for S parameters specified in Tabla 2-1. This process lasted about a week of work.

ADS also allows you to enter as loads other circuit user-defined sections, characterized by their S parameters through a file with extension "*.s1p", such as those generated by FEKO in their calculations. In this way, the patches of the "1x3 array" can be entered as loads. However, before doing so, simulations were carried out with loads of 50 Ω replacing the patches, in order to estimate the parameters S_{21}, S_{31} and S_{41} at the frequencies of interest. Only after the results were acceptable, the patches were located in their place.

The feeding circuit of the array of 1x3 patches that allowed us to provide the correct amplitude to each patch has the configuration shown in Figura 2-7.

The results obtained are shown in Figura 2-6. There can be seen the value of $S_{11} = -25{,}336\ dB$, an extraordinary income, and well above the -12 dB required in principle. Values S_{21} and S_{41} are close to the desired theoretical values. While S_{31} differs in 0.9 dB from the ideal value. The difference being less than 1 dB, it is considered that we are within a range sufficient to achieve good results.

On the other hand, Figura 2-6 also shows an evolution of the S_{11} parameter with the frequency in the Smith Chart. As we are near the center of the diagram, we conclude that the adaptation of our circuit to the source is correct.

Figura 2-6 and Figura 2-7 are also available at the point 6.1.12 of Annex 6.1 "ANNEX 1: GRAPHICS".

Once the proper amplitude is managed at the input of each patch of the 1x3 array, we focus on obtaining the necessary phase shifts among them.

6.4.3.3.2 Feeding circuit of the 1x3 array with different amplitudes and phase shifts

The following task consists of introduce a phase shift in the input signal so as to fulfill Ec. 6-1, that is again included here for convenience as Ec. 6-14, since the phases arriving to the patches influence the shape of the radiation pattern obtained with the set.

$$\Delta\varphi_{y\uparrow-middle} = 12.5^{o} = -\Delta\varphi_{middle-y\downarrow} \qquad \text{Ec. 6-16}$$

The signal phase shift varies with the movement of the wave in z-direction following a law of $e^{jz(\omega t-\beta)}$ type, and at every point of the circuit will be different. In fact, the phase accumulated by a wave traveling along a transmission line of length l follows Ec. 6-17, which is treated in more detail in **[3]**.

$$\phi = \beta \cdot l = \sqrt{\varepsilon_e} \cdot k_0 \cdot l = \sqrt{\varepsilon_e} \cdot \frac{2\pi}{\lambda_0} \cdot l$$

Ec. 6-17

$$con \quad \varepsilon_e = \frac{\varepsilon_r + 1}{2} + \frac{\varepsilon_r - 1}{2} \frac{1}{\sqrt{1 + 12\frac{h}{W}}}$$

Where ε_e is the effective electric permittivity on the substrate, λ_0 the wavelength in vacuum, ε_r the relative dielectric permittivity of the dielectric, h is the height of the dielectric between conductors, and W is the width of the transmission line.

From Equation 2-15 can be inferred the value of the wavelength in the substrate λ_s. It can be seen as the length that a transmission line with certain characteristic impedance and width must have to make that a wave traveling through it at the central working frequency accumulates a phase shift of 2π radians. Its value is shown in Ec. 6-18.

$$\lambda_S = \frac{\lambda_0}{\sqrt{\varepsilon_e}} \qquad \text{Ec. 6-18}$$

With these data, and starting from the circuit obtained in section 2.2.1, the phase difference between the S parameters at each port is observed, as they will give us an idea of the phase gap between the signals arriving at each of the patches of the 1x3 array. These data have been included in Figura 2-8.

As shown in Figura 2-8, the phase gaps among patches are close to the desired, but inaccurate. As we saw in section 1.2 of the previous chapter, a minimum phase variation severely affects the results. Due to this, the length of the path traveled by the radio signals must be modified to reach the desired phase shift of 12.5 º.

The change in the length traveled by the signal to radiate must not alter the distance d_y between patches, or the distance d_x between 1x3 arrays, which remain fixed. To achieve this, bends or meanders must be introduced in our power circuit, involving only electrical lengths. After conducting several tests, it appears that the best results were obtained by introducing sets of curves in the branches 2 and 3 in Figura 2-7.

The final circuit which gives a better fulfillment of the requirements is shown in Figura 2-6. As can be seen, it introduces two sets of four curves, one set in the branch 2 and the other one on the branch 3. This curves change the phase shifts to the desired values.

The results obtained for phase shifts and the relevant S parameters are shown in Figura 2-10. The results are very adequate, although some improvements could be introduced to the value of $S_{31} = -2{,}89\ dB$ (the desired theoretical value was -1.8 dB). However, due to time constraints we have to go ahead with the next challenge: to design the circuit carrying the same amplitude and phase to the 20 arrays 1x3 that make up the radiating system.

Finally, only comment that the point 6.1.13 of Annex 6.1 "ANNEX 1: GRAPHICS" shows Figura 2-9 and Figura 2-10.

6.4.3.4 Feeding circuit of the 20X3 array

Next task to afford seems, a priori, simpler. It consists on designing the circuit in charge of providing the same amplitude and phase to each and every one of the 20 arrays 1x3 of the system. And along with the circuit obtained in Section 2.3, it will constitute the complete power circuit of the 20x3 patches radiant set.

This circuit will consist of 21 ports: one for power supply, and 20 where the 1x3 arrays will be connected. The fact of receiving all the arrays the same amplitude implies a balanced distribution of power in all branches. And the requirement of accumulating all of them the same phase shift will mean that the path length must be the same for all of them.

Figura 2-11 outlines the optimal solution that responds to the two previous rules, along with other possible solutions.

The reason why option a) of Figura 2-11 is chosen among the others is that the path to the four groups of 5 1x3 arrays (painted in orange in Figura 2-11) is the same. This will greatly facilitate our design, which will focus on the design of a circuit that feeds with equal amplitude and phase the 5 arrays 1x3 comprising each group.

Therefore, the task can be divided into two phases. The first and easiest one is to design the common path to each group of 5 arrays 1x3, marked in blue in Figura 2-11. The second one will focus on the design of the circuit with 5 arrays 1x3 itself, in orange in Figura 2-11, where despite the different paths, all the 1x3 arrays must be fed with equal amplitude and phase.

6.4.3.4.1 Feeding circuit from power supply to the 4 groups of 5 arrays 1x3

The task is simple, and consists of designing the paths in black in Figura 2-12 arriving to the 4 groups of 5 arrays 1x3 displayed in red in the same figure.

Since the connection between the circuits in red and black in Figura 2-12 is between transmission lines with a characteristic impedance of $Z_0 = 50\Omega$, it does not require any λ/4 transformer

Figura 2-12 shows the main design variables:

- d_x is the horizontal distance between groups of patches, as discussed in chapter 1.2.
- λ_s is the wavelength in the substrate for a line with characteristic impedance of $Z_0 = 50\ \Omega$ at the central frequency. This distance has been selected for convenience for the vertical sections, as it saves computing time in the simulation programs, and is suitable to the dimensions of the circuit to build.
- All sections drawn in black correspond to a microstrip type transmission line with characteristic impedance $Z_0 = 50\ \Omega$.
- The 3 sections drawn in blue correspond to respective λ/4 transformers. Each of them is used to adjust the line impedance of $50\ \Omega$ with the parallel of the two branches to which it connects: $Z^{eq}_{50\,//\,50} = 25\ \Omega$

With these data, the expected results of $S_{i,5}^{i\in[1,4]} = -6\ dB$ are obtained for each one of the ports shown in Figura 2-12, where ports 1 to 4 correspond to the upper terminals of the circuit, and port 5 to the power supply. The phase shifts are also identical for all of them. These results are available at the point 6.1.14 of annex 6.1 "ANNEX 1: GRAPHICS".

6.4.3.4.2 Feeding circuit for the group of 5 arrays 1x3

Now we approach to a more difficult task, since a circuit of 5 branches in parallel must be fed with the same amplitude and phase. It is a very similar task to that already discussed in point 2.2 of this chapter, and as it was done there, it could be divided into two phases: obtaining the appropriate amplitudes, then the extent of the phase shifts needed.

To obtain the appropriate amplitudes for each of the 5 branches where the 1x3 arrays will be placed it is necessary to make use of the λ/4 transformers expressed in Figura 2-13, and that are detailed below:

i. At the junction between branches 1 and 2 there is a connection in parallel of two lines with characteristic impedance $Z_0 = 50\Omega$. This fact justifies the presence of a λ/4 transformer, called T1, which adapts between $Z_{1//2}^{eq} = 25\ \Omega$ and $Z_0 = 50\Omega$ of the section reaching from branch 3 to branch 2. The characteristic impedance of the transformer T1 is $Z_{T1} = 35\ \Omega$.

ii. At branch 3 an input impedance of 100 Ω is required for an adequate distribution of power, in which all branches receive the same power. We therefore need a λ/4 transformer to adapt the input impedance of this branch $Z_{in3} = 100\ \Omega$ to the load impedance of the same branch $Z_{L3} = 50\ \Omega$. This transformer is called T2 and has a characteristic impedance of $Z_{T2} = 71\ \Omega$.

iii. At the junction between the branches 4 and 5 there is again a connection in parallel of the two branches above with the characteristic impedance of the circuit $Z_0 = 50\Omega$. Therefore, a new λ/4 transformer is needed. This transformer is called T3 and has the same value as T1.

iv. At branch 6 there are two branches in parallel with $Z_0 = 50\Omega$ (one is the one leading to branches 1 and 2, and the other one leads towards branches 4 and 5) connected in parallel to branch 3 with $Z_{in3} = 100\ \Omega$. The resulting equivalent impedance of this parallel scheme is $Z_{1y2//3//4y5}^{eq} = 20\ \Omega$. Thus, it is necessary to use a transformer T4 for adapting this 20 Ω to the characteristic impedance of the circuit $Z_0 = 50\Omega$. The impedance of this transformer T4 will be $Z_{T4} = 32\ \Omega$

To manage the phase shift to be the same in all branches of the circuit, the introduction of curves or bends in the area between branches 1 and 2 and also between branches 2 and 3 is required. As the circuit is symmetrical respecting branch 3, the same bends will be introduced between branches 4 and 5, and 3 and 4.

The circuit providing the best results to our problem is shown in Figura 2.15, and in point 6.1.15 of Annex 6.1 "ANNEX 1: GRAPHICS". And the results obtained with it are shown in Figura 2-14, as well as in the aforementioned annex.

The results are excellent, but misleading. The results of Figura 2-14 have been obtained using the tool "Schematic" from ADS program. "Schematic" is intended to give the designer a first idea about the goodness of microstrip circuit design. When the circuit design is optimal with “Schematic”, it is then simulated with the tool "Momentum", also within the ADS program. “Momentum” is more powerful than "Schematic", so their calculations are much closer to reality, and are also more expensive (respecting to CPU time consuming).

While using "Momentum" the simulations of the circuit shown in Figura 2-15 produced not very good results. This is normal, since it requires some adjustments in the circuit until the best results are obtained. However, in this case, many attempts were made without getting better results. The reason is in the piece "MCROSO" located in the center of Figura 2-15. It is the cross-shaped piece that connects the power port with the central array of the group of 5, and the remaining arrays. ADS offers the possibility of using this piece, but with margins of Use.

Junction "MCROSO" can only be used if the following proportions are met:

$$0{,}4 \leq {}^{w_i}\!/_{h} \leq 2{,}5, \; con \; i \in [1{,}4] \qquad \text{Ec. 6-19}$$

In our case, only branch 3 complies with the requirement in Ec. 6-19. For this reason it was decided to test its performance in isolation with "MOMENTUM" to go then adding the other elements till completing the final circuit. The partial results were encouraging, but in the end, when included with other components of each branch, it was impossible to reach a reliable result. Nevertheless, we decided to build a model from the best results obtained with "Schematic" to check their actual behavior.

However, we cannot be sure that these good results achieved are real, so another solution must be found. It will be discussed in the next section.

6.4.3.5 Feeding circuit of the 24X3 array

In Chapter 1 was determined that the optimal solution was the circuit of 20 copies of the 1x3 array. But now we have to change our decision because of the factual problems seen in section 2.4.2.

As happened with the 20x16 and 24x16 arrays in Section 1.1, we can assume that the behavior of the array of 24x3 patches will not differ much from the 20x3. The only variation will be in the diagram in azimuth, which will be a bit narrower for the set of 24x3 patches, as the number of copies of the 1x3 array along the X axis has been increased.

To validate this assumption, the array of 24x3 patches was simulated with FEKO. The "*. pre" FEKO file defined for this purpose can be found in Section 6.2.11 of Annex 6.2 "ANNEX 2: PROGRAMS AND CODE". With the results obtained with FEKO, and using the cylindrical lens as defined in Section 6.2.9 of the same Annex along with the program LISSY yielded the results shown in Section 6.1.10 of Annex 6.1 "ANNEX 1: GRAPHICS". As can be seen, the behavior of this circuit is very similar to the circuit 20x3, and is a valid solution to our design as it meets all the requirements specified in the Tabla 0-1 of the introduction" .

24x3 circuit will consist of 25 ports: one for power supply, and 24 where the 1x3 arrays that will be our load will be connected. Receiving all the same amplitude implies a balanced distribution of power in all branches. And the requirement to accumulate all the same phase shift will mean that the path length must be the same.

Figura 2-16 outlines the optimal solution that responds to the two previous rules. Moreover, this solution, as consists of the use of 6 groups of 1x3 arrays (in red in Figura 2-16), does not need to use the piece "MCROSO" with all its limitations.

And just as we did in Section 2.4, we divide the task into two parts. In the first part we will carry the same amplitude and phase to the four groups of 6 arrays 1x3 (black-circuits in Figura 2-16). And in the second part, to provide the same amplitude and phase to the 6 1x3 arrays in each group (in red in Figura 2-16).

6.4.3.5.1 Feeding circuit from power supply to the 4 groups of 6 arrays 1x3

Figura 2-16 shows the main design variables, which are completely analogous to those seen in paragraph 2.4.1 above. The only change, as shown in Figura 2-16, is the length of the connecting sections, due to the fact that now we have 4 more 1x3 arrays than we had before. So the resting dimensions of the circuit do not require further explanations.

Since the connection between the circuits in red and black of Figura 2-16 is between transmission lines with a characteristic impedance of $Z_0 = 50\Omega$ no λ/4 transformers are needed.

With these data, the expected results, $S_{i,5}^{i\in[1,4]} = -6\,dB$, are obtained for each of the ports shown in Figura 2-16, where ports 1 to 4 correspond to the upper terminals of the circuit, and port 5 to the power supply. The phase shifts are also identical for all of them.

The circuit used and the results with it obtained can be found in Section 6.1.16 of Annex 6.1 "ANNEX 1: GRAPHICS".

6.4.3.5.2 Feeding circuit for the group of 6 arrays 1x3

Is now addressed the task of feeding 6 branches in parallel with the same amplitude and phase. It is a task very similar to that already dealt with in paragraphs 2.3 and 2.4.2 of this chapter, and like in them, it will be divided into two phases: obtaining the appropriate amplitudes, then the extent of the phase shifts needed.

To obtain the appropriate amplitudes for each of the 6 branches where the 1x3 arrays will be placed, the use of the transformers expressed in Figura 2-17 will be needed. This transformers are detailed below:

i. At the junction between branches 1 and 2 there is a parallel connection of two lines with characteristic impedance $Z_0 = 50\Omega$. It is necessary the presence of a λ/4 transformer, called T1, which adapts between $Z_{1//2}^{eq} = 25\,\Omega$ and $Z_0 = 50\Omega$ of the section reaching branch 2 from branch 3. The characteristic impedance of the transformer T1 is $Z_{T1} = 35\,\Omega$.

ii. At the junction of the central zone with branch 3 is again needed a new λ/4 transformer to adapt the parallel equivalent impedance $Z_{1y2//3}^{eq} = 25\,\Omega$ of two branches with the characteristic impedance of the transmission line circuit $Z_0 = 50\Omega$. This transformer is identical to T1 and will be called T2 ($Z_{T2} = 35\,\Omega$).

iii. At the confluence of branch 7 with central part of the circuit, the same situation of points i) and ii) happens again. This λ/4 transformer is called T3 and its matching values are identical to those of T1 and T2 ($Z_{T3} = 35\,\Omega$).

iv. At the junction of the branch 4 to the central part of the circuit, we face again the same situation as in ii) due to the symmetry of the circuit. This λ/4 transformer, called T4, is entirely identical to T2.

v. Finally, at the junction of branches 5 and 6 there is again the parallel connection seen in i) due to the symmetry of the circuit. That is why the λ/4 transformer T5 is placed, and it is identical in values and matching properties to T1.

To manage that the phase shifts are the same in all branches of the circuit, the introduction of curves or bends in the area between branches 1 and 2 and also between branches 2 and 3 is required. As the circuit is symmetrical respecting branch 7, this bends should also be introduced between the branches 5 and 6, and 4 and 5.

The circuit providing the same amplitude and phase at the input of the 6 arrays with the best conditions is shown in Figura 2-18.

And the results, this time obtained with MOMENTUM, are shown in Figura 2-19. It can be seen that the phase is almost the same in the six ports where the 6 arrays will be placed. With regard to the amplitudes, the S parameters show a fairly behavior consistent with expectations, being $S_{i,7}^{i\in[1,6]} \approx -9{,}2\,dB$ in all of the 6 ports (1 to 6) with respect to the power supply port number 7. The theoretical value expected to obtain was $S_{i,7}^{i\in[1,6]} = -7{,}78\,dB$, so that reality is not too far. The only objection we could put would be in the value reached for $S_{7,7} = -15{,}17\,dB$. It is beyond the requirements, but it could be adjusted to a lower level in view of its chart against frequency seen in the lower left of

Figura 2-19, where it is seen with respect to the return loss a shift in the behavior of the structure towards lower frequencies.

6.4.3.6 Conclusions

The final circuit with the best results we have achieved is that which contains 24 copies of the 1x3 array, fed according to Ec.1-1 and Ec. 1-2, and repeated again in Ec. 6-20 per comfort.

$$V_{y\uparrow} = 0.5\,V_{middle} = V_{y\downarrow} \qquad a)$$
$$\Delta\varphi_{y\uparrow-middle} = 12.5^{o} = -\Delta\varphi_{middle-y\downarrow} \qquad b)$$

Ec. 6-20

And this with a superimposed cylindrical lens.

Therefore, this circuit will be produced to measure its real characteristics in the laboratory. However, there won't be the unique, because also a few others will be built to check the goodness of the different phases and elements of design.

Circuits to be manufactured are referred in Tabla 2-2.

The following chapter discusses in detail the measures undertaken and results achieved with each of them.

6.4.4 Experimental Results

Following the comments in paragraph 2.6 of the previous chapter, a series of realistic models of our designs will be produced to be measured in laboratory. These measurements will allow us determine whether they meet the requirements of Tabla 0-1 from Chapter 0.

Of each circuit from those in Tabla 2-2, 2 variants will be produced, and from each variant 2 copies will be made, in principle identical, to avoid potential manufacturing defects. Each version of the circuits has a definite purpose:

- One is for measuring the S parameters of the circuit.
- The other to obtain the radiation parameters of the circuit (basically its gain and directivity).

The reason for constructing two versions of each circuit is the fact that the feeding technique used will be different depending on the parameters to be measured.

In case of measuring the S parameters of the circuit, the technique "Coplanar Waveguide" will be used by adding CPW structure "CPW_77_Uebergang" from ADS libraries to the feeding point of our circuits. Development in detail about these transmission lines can be found in **[10]**.

When measuring the parameters of radiation, the technique used is the “microstrip line" already mentioned in Chapter 2, as well as in **[5]** and **[10]** of the bibliography. To insert the signal from a generator in the circuit, dielectric and conducting plane, on which our circuit lines are placed, are removed. With a especial conducting glue, a special connector conductor is attached to the circuit. Through this connector, the input signal will feed the circuit. To carry out this operation, the line of $50\ \Omega$ where the connector is to be placed is enlarged 20 mm, to allow the removing of the dielectric and to paste the coupling element without affecting the characteristics of our circuit. Exactly, the elongation is 7 times the wavelength of a line of characteristic impedance $50\ \Omega$.

The two feeding techniques described in the previous two paragraphs can be seen from Figura 6-32 to Figura 6-35 of point 6.1.18 of Annex 6.1 "ANNEX 1: GRAPHICS”. In all these figures, the characteristic details of each technique and a more generous description of each can be seen.

Thus, from the four circuits to produce two versions are made, and also 1 copy of each version. This makes a total of 16 circuits to be manufactured. They will be manufactured on a single sheet of dielectric with conductive plane at the base of 236mm wide by 427 mm long. These measures are preset by the manufacturer of printed circuit boards and do not accept change.

For the design of the aforementioned layout or dielectric sheet and the positioning of the various circuits on it, Agilent's ADS program is again used, as it lets you create a layout from schematic and circuits simulated with it. In this layout, we distinguish different layers for greater readability by the manufacturer. They are expressed in Tabla 3-1.

The layers corresponding to the plane and the dielectric substrate are not specified due to their obviousness.

Once the layout is designed, with the GERBER tool from ADS those data are translated into four files with extension ".gbr". These files will be used by the manufacturer for the preparation of the test plate.

Upon receipt of all circuits, we proceed to paste manually and with the help of an electronic microscope the connectors in the circuits for measuring the parameters of radiation or antenna. The power supply connector is a rectangular waveguide, which sticks to the circuit. The connector aligns with our microstrip feeding line, so that the microstrip acts as line probe into the waveguide. This process takes a full day of work, as it requires some familiarity with the process and some manual dexterity.

With all the circuits prepared to be measured, we turn to the laboratory. The measures should be conducted in an anechoic chamber duly approved. However, by the time when this project was done, it was under construction, so the results are far from being considered ideal.

The assembly used in the laboratory to perform measurements of radiation parameters is shown in Figura 3-1. A horn radiating element with 3 dBi gain is used, set on a pedestal and pointing to the center of the circuit to be measured. The pointing was done with the help of a laser pointer, so it can be considered fairly accurate. On the opposite side, and about 4 meter away will stack consecutively all circuits to be characterized. These are based on a precision rotor, which will sweep over the azimuth extent with $\vartheta \in \left[-90^0, 90^0\right]$.

Through a GPIB bus, all the elements involved in the measure will be connected, as detailed in Tabla 6-2:

Equipment	Function
PC	Controls the whole measurement process, and stores the results.
SWEEPER	Generates signals with frequency and power established from PC. It is not needed to use any modulation pulse for the measurements to be done.
SPECTRUM ANALYZER	It measures the power and frequency of the received signal in the circuits to characterize.
ROTOR POSITION CONTROLLER	From PC, the angle to sweep and the velocity of the movement will be indicated to it. In our case, the angle to sweep will be of 180º in 540 seconds, in steps of 0,3º. This controller translates this settings to the rotor via an internal protocol not intended in this project.

Tabla 6-3 Measurement equipments connected via GPIB bus

It is important to note that the sweeper cannot directly generate the circuit operating frequency (76.5 GHz), as it is too high for current technology available in commercial equipment. However, if at the output of the signal generator a multiplier head is placed, double and triple frequencies than those at its input can be managed. These devices are nonlinear, and introduce intermodulation noise. However, with an appropriate band pass filter at their output, this noise can be, if not eliminated, at least greatly mitigated. Therefore, selecting a frequency sweeper in half (38.25 GHz), and attacking with it a frequency multiplier head the frequency of work sought is obtained. This frequency of 38.25 GHz is called IF or Intermediate Frequency, and its use is nourished by an increased ability to generate, amplify, filter, and ultimately operate with these frequencies. Once the FI has been adequately addressed, comes the "Up Conversion" to the working frequency, usually called RF or Radio Frequency. Typically, the IF is usually much lower (about tens of GHz), but in our case, the RF has a so high frequency that causes this.

For this reason, the IF signal is amplified and filtered before it is converted into RF signal. Once the signal leaves the multiplier head, it will be again filtered and transmitted, hopefully with enough power to support the propagation losses in free space between transmitter and the circuit to be characterized.

According to the statements of the two preceding paragraphs, the module labeled as "Amplifier" in Figura 3-1, located between the "sweeper" and the transmitter horn actually consists of the elements mentioned in Figura 3-3.

In this case the order of the factors affects the product itself. The order shown in Figura 3-3 must be followed, as this order is imposed by the fact that the amplifiers are inherently noisy systems. As amplifiers are connected to voltage sources, they can introduce much background noise to our signal. As signal is amplified, the noise increase will not be too serious, but greatly affects the multiplier head, because that noise will be amplified and mixed in frequency, resulting in the extension of this noise across the frequency spectrum. Because of this, and to eliminate it if possible, the amplifier is placed after a band pass filter centered at the IF frequency (38.25 GHz). This will remove all the noise except that of our frequency band, which inevitably will slip with the signal. Finally, to avoid the emitter horn getting a signal with noise in all bands, the signal is filtered again, now around the RF frequency, to eliminate all possible harmonics generated in the multiplier head (or "CUADRADOR" in Figura 3-3, as it squares input signal, which in frequency domain results in a doubling of the frequency).

The ideal measurement conditions would require the use of a certified anechoic chamber where the emitter horn antenna with its "amplifier" would be placed (we refer to the whole set explained in the preceding paragraph) with the circuit to characterize. The remaining items would remain outside to avoid unwanted reflections, which lead to inaccurate measurements of the radiation pattern.

The actual appearance of the environment of measure is shown in Figura 3-2, and as can be seen, it is far from ideal, so the results will present some loss of accuracy.

The control PC will store all the data received from the spectrum analyzer for further analysis.

On the other hand, for the measurement of S parameters of the various circuits, a vector analyzer will be used. It directly obtains all required data at different frequencies.

The following sections present the data obtained in each of the circuits under study.

6.4.4.1 1x3 Array without Phase Shifts among Patches

Figura 3-4 shows the return loss (S_{11}) at the input to the array. Above in the figure the magnitude, and below the phase.

The magnitude value reached at our frequency ("Marker 3" in Figura 3-4) is -13.517 dB, so it can be considered adequate. Yet we see that does not match a minimum. As shown, the resonance frequency has been shifted to lower frequencies, so a decrease in the dimensions of the lengths of the circuits would re tune the circuit. The phase value is not relevant to this application, so it will not be analyzed.

The conclusion is that the matching of impedances at the input could be better by making a prototype in which to obtain a lower value of the S_{11} parameter would be easy. However, the actual value is not inappropriate for our purposes.

Figura 3-5 and Figura 3-6 show the measured radiation pattern in azimuth and elevation respectively.

Azimuth diagram shows very poor results as the array receives equally in any angle. This is because there is only one array of 3 Patches over X axis, when our optimal solution consists of 24 copies of that array, providing much higher directivity in this plane.

The ripple present in the signal is due to noise in the measure (remember the conditions stated at the beginning of this chapter), as the measure should be much more flat and uniform. This ripple will be a constant in all measurements and no doubt is related to unwanted reflections in the measurement system.

Respecting the elevation diagram shown in Figura 3-6, the results are much better and closer to the expected values after simulation. The main lobe is still wider than we would like, because its value is 30 degrees, but remember that the measurement is made without the cylindrical lens used to improve the directivity of the whole.

Also of note in Figura 3-6 that the main lobe is slightly deviated from $\vartheta = 0^{o}$, as it is centered on $\vartheta \approx 4^{o}$, which was not wanted in our simulations. This is because the proper phase shifts among patches has not been introduced yet, and should be resolved in the next circuit to be measured.

The fabricated circuits with whom these measures are obtained can be found in Section 6.1.18.1 of Annex 6.1 "ANNEX 1: GRAPHICS".

6.4.4.2 1x3 Array with Phase Shifts among Patches

Figura 3-7 shows the return loss (S_{11}) at the input to the array. Above in the figure the magnitude, and below the phase.

The value of magnitude reached at our working frequency is -8.455 dB, which is too high for our purposes. However, we see that even it is not placed on a matching minimum, it could be easily moved to one, by shortening the length of the circuit elements.

It can be concluded therefore that although the value is too high, the margin of improvement for impedance matching to the input of our circuit is very broad and viable, because we could easily reduce its value by designing a new prototype with smaller dimensions of length.

Figura 3-8 and Figura 3-9 show the measured radiation pattern in azimuth and elevation respectively.

As in the previous point, the azimuth diagram shows very poor results because there is only one array of 3 patches over the X-axis, instead of 24. Hence the low directivity.

Again appears the ripple due to imperfections in the measurement system, which causes the appearance of multiple reflections. And now is also seen that the diagram is no longer centered as in the previous point, since a radiation zero appears at -90 degrees, and not at 90 degrees. This loss of symmetry in the azimuth diagram may be due to improper placement of the circuit to characterize over the rotating pedestal. This could have prevented the reception in the initial sweep angles.

In elevation, however, the behavior is again much better. According to Figura 3-9, the half power beam width is, as in the previous section, near 30 degrees, and the main lobe is again slightly moved off the center (it is at 2° instead of 0°). The application of the phase shifts has improved this deviation from the main lobe with respect to that seen in 3.1, but it should still be refined. However, on the left side of Figura 3-9 an anomalous peak amplitude between -90º and -84º can be seen. This peak is surprising for its placement, but can be filtered by placing absorbent around our circuit, thus avoiding their influence.

In view of these results, especially for elevation, it can be concluded that very appropriate values are obtained, and they will be enhanced with the implementation of the cylindrical lens superimposed on the whole.

The fabricated circuits with whom these measures are obtained can be found in Section 6.1.18.2 of Annex 6.1 "ANNEX 1: GRAPHICS".

6.4.4.3 20X3 Array

After checking in POINTS 3.1 and 3.2 that our simulations were not misguided, and simulation programs used are very useful, it is time to analyze the behavior of our final circuits.

First we dedicate to the 20x3 array. This was our first solution, but the problems encountered during the simulation of line section "MCROSO" forced us to consider other possibilities. Although it is not the optimal solution, it was manufactured to check how is its actual behavior like.

Figura 3-10 shows the return loss (S_{11}) at the input to the array. Above in the figure the magnitude, and below the phase.

The value of magnitude reached at our working frequency is -24.760 dB, an extraordinary result that indicates a perfect impedance matching with the source.

Figura 3-11 and Figura 3-12 show the measured radiation pattern in azimuth and elevation respectively.

Azimuth diagram presents a sharp directivity now compared with the results of 3.1 and 3.2, as at last we have a sufficient number of repetitions of the 1x3 array to achieve a radiation pattern with a narrow main lobe and adequate to the purpose of the project.

In fact, the half power beam width is only of 3.8° as shown in Figura 3-11. But the problem arises as it is slightly deviated from 0 °, since the maximum radiation is obtained at -2.1 º. This can lead to errors of about 3.6 meters at distances of 100 meters away, which would lead us to detect obstacles from adjacent lanes. This should be corrected by changing the distribution of power or phase in the array. Besides a secondary lobe with only 5 dB less power than the main lobe appears. This main to secondary lobe ratio is not big enough compared with the theoretical calculations, in which differences of around 15-20 dB were foreseen. The presence of this so powerful secondary lobe, very close to the main lobe is of concern, and its origin should be studied, in order to try to eliminate it. But its apparition is many likely to be due to an unwanted reflection in the measurement environment.

In elevation, Figura 3-12, the behavior is again similar to that seen in points 3.1 and 3.2, as there is no variation in the number of elements along the X-axis (we continue with 3

patches along this axis). Half power beam width has a value of 27 degrees, but now the main beam is fully centered on 0º. Therefore, the designed supply network has improved the deviations that worried us while checking the 1x3 arrays isolated.

The results will be improved with the implementation of the cylindrical lens superimposed on the whole set. It would be desirable to be able to test the full set, so as to dictate the final design quality, but the lens had not been produced at the end of this work.

In light of the results, it can be concluded that the design seems close to the initial objectives. But it cannot be considered as a feasible solution, and should still go through a redesign to correct the deficiencies noted in the azimuth diagram of Figura 3-11. Should be reviewed specifically the power distribution and phase, that caused the deviation in the main lobe. This deviation may well be due to the use of MCROSO piece at the junction of the 5 arrays 1x3 with the rest of the circuit. This piece was impossible to simulate with the method of moments (MoM) and led to this circuit would no longer be the optimal solution to the requirements of departure. On the other hand, say that the origin of such a high secondary lobe is surely the unwanted reflection caused by the measurement conditions, so it does not really matter.

The fabricated circuits with whom these measures are obtained can be found in Section 6.1.18.3 of Annex 6.1 "ANNEX 1: GRAPHICS".

6.4.4.4 24X3 array

And finally we come to the considered optimal solution. Figura 3-13 shows the return loss (S_{11}) at the input to the 24x3 array. Above in the figure the magnitude, and below the phase.

The value of magnitude reached at our working frequency is -19.453 dB. This is a good result, but in view of Figura 3-13, it is clear that the impedance matching could be improved a lot by shortening the length of the transformers of the circuit, and a value around -27 dB could be reached.

Figura 3-14 and Figura 3-15 show the measured radiation pattern in azimuth and elevation respectively.

Azimuth diagram now presents a sharp directivity now compared with the results of 3.1 and 3.2, as at last we have a sufficient number of repetitions of the 1x3 array to achieve a radiation pattern with a narrow main lobe and adequate to the purpose of the project.

In fact, as seen in Figura 3-14, the half power beam width has a value of only 2.7º. But the problem arises as it is slightly deviated from 0°, since the maximum radiation is obtained at -3º. This deviation can lead to errors of about 5.75 meters at a distance of 100 meters away, which would produce the detection of obstacles from adjacent lanes. This should be corrected by changing the distribution of power or phase in the set, or by using a slightly tilted lens to compensate the deviation.

Again, just as happened in section 3.3, reappears in azimuth a side lobe (Figura 3-14) with approximately 5 dB less power than the main lobe. However, now this side lobe is located in $\vartheta = 72^{o}$, which is much less harmful than that found in the previous section with the 20x3 array. As happened then, this peak is motivated by unwanted reflections in the measuring environment.

In elevation (Figura 3-15) the behavior is again similar to the previous points, as there is no variation in the number of elements along the Y-axis (we continue having 3 patches along this axis). In fact, the beam width at -3 dB is 27 degrees, and the main beam is fully centered on 0º. The only problem is the presence of some ripple in the main lobe, which is due to unwanted reflections prompted by the inadequate measurement environment.

We again see in Figura 3-15 the anomalous peak between -90° and -84° that we saw in the point 3.2 with the 1x3 array with phase shifts among patches. This peak owes its origin to unwanted reflections in the measurement environment, and would be eliminated by measuring in an anechoic chamber duly approved.

Therefore, the azimuth values obtained are suitable. However, they still have to be confined by the cylindrical lens, which will provide greater directivity to meet the requirements of Tabla 0-1 of the introduction.

And in view of the results shown both in azimuth and elevation, can be concluded that this circuit meets the requirements prescribed in section 0.2 "ACC: Specifications Transmitter-Receiver Subsystem" from the introduction (remember that in elevation they will be met with the superimposed cylindrical lens). And even this minor incidents:

- deviation of the main lobe in azimuth
- presence of a very strong secondary lobe in azimuth centered in $\vartheta = 72^{o}$
- abnormal elevation diagram between -84º and -90º

Only the main lobe deviation in azimuth should worry us. As the other two incidents outlined are caused by the conditions under which measurements were made.

To address the deviation of the main lobe in azimuth 2 options would be possible: either to redesign the power circuit of the 24 arrays 1x3, and that would be recommended. Or, place the circuit on an inclined plane to correct the deviation (being so small, only -3.3º, this option is not preposterous, as it saves time.) After correcting this detail, the solution can be considered successful, before checking the results achieved with the cylindrical lens overlay.

The fabricated circuits with whom these measures are obtained can be found in Section 6.1.18.4 of Annex 6.1 "ANNEX 1: GRAPHICS".

6.4.5 Final Conclusions

On completion of this work, which has expanded greatly over time, we can be satisfied with the work performed. The circuit proposed as a solution, **the array of 24x3 patches with superimposed cylindrical lens** fulfills all the requirements of departure under chapter 0, Tabla 0-1. Although it is true that some improvements can be made that will lead to better compliance with the initial requirements.

In view of all work performed and displayed, the following conclusions can be established:

1. The main aspect of the solution to be corrected is the deviation of -3.3º present in the 24x3 circuit in azimuth.

   This is most likely due to poor distribution of power or poor distribution of phase differences among elements of the supply circuit, at the locations shown in Figura 4-1. Despite its simplicity, a small imbalance in the distribution of power at these points (their design is identical in all three elements in Figura 4-1) has serious consequences for the rest of the circuit.

   As a result, more time should have been devoted to the simulation and measurement of these parts of the circuit. In fact, once we had simulated the feeding circuit for 6 arrays 1x3 (in red in Figura 4-1), more of these groups should have been added gradually up to complete the path to power supply. Thus, it would have been able to detect defects of distribution that may have been masked in the full circuit

   However, due to time constraints, what was done was to join all groups of 6 arrays 1x3 with the power supply circuit (in black in Figura 4-1) to test the full circuit at once. This was what might motivate these mismatches, which must be corrected before moving to mass production of the circuit.

2. Another possibility to correct the defect referred to in the preceding paragraph, as well as in Section 3.4, would consist of placing the array 24x3 on an incline of 3.3° as shown in Figura 4-2. Or even tilt the cylindrical lens, leaving the circuit in the horizontal.

   Although this solution seems less suitable than in point 1, it could be used as a desperate measure in case there is no more room for maneuver, such as in this case, since there was no more time to develop new designs.

3. It would have been very convenient to measure the parameters $S_{i,j}$ in the different ports of the circuits, both in amplitude and phase. This would have allowed confirming beyond any doubt if the phase and power distributions were appropriate for each item.

   However, this is very costly, both financially and in time. As for each parameter to measure, a different circuit is needed, in which the port to be characterized must be replaced by a connection "Coplanar Waveguide" while the other ports maintain their load patches.

4. The cylindrical lens has not been tested. Lack of time has meant that has not come to perform any test with it superimposed on our circuit. The lens itself was already designed, and was not subject to this project. But could not come into production, nor developed a plastic housing to place it next to our circuit. Consequently, it was not possible to validate the designs definitely made.

At least, the results agree even better than expected by the circuits without using the lens. But this work cannot be considered complete without checking the behavior of the solution with the lens. This leaves a bitter taste as being so close to the goal.

This step would have corrected the deviation aforementioned in paragraph 1.

The works in this field continued, solving all the problems exposed here through new designs. And by year 2009 (four years after the completion of this work) came out the latest generation of ACC. It makes use of patch antennas with a superimposed aplanatic lens working at the same frequency of 76.5 GHz, however the transmitter-receiver set was extensively modified, now being formed by a flat array 4x3.

The use of the aplanatic lens explains the reduction in the number of arrays used in the X axis. While the cylindrical lens did not affect this axis, aplanatic lens confined radiation both X axis and Y axis In addition, the lens can finally be regulated in its opening, expanding or reducing the angular range in both azimuth and elevation, covered by the receiving system.

It is therefore a proud to have been involved in this project, since these first steps in developing the new system have paid off, if used the same basic idea: patch antennas and electromagnetic lens overlay. This has led to a considerable reduction in the size of the system.

5. The use of an anechoic chamber duly authorized is essential for this type of measurements. However, the high cost of hiring one, and the fact that the one intended to be constructed by the Robert Bosch Group GmbH was not yet completed, has caused that the laboratory measurements have been influenced by the presence of unwanted reflections in the measurement system. These reflections give rise to false side lobes and ripple in the results.

   An estimation of their amount is difficult to define, but it can influence the value of maximum radiation and the half power beam width. In our case, the more pernicious effect was to "smear" the azimuth directivity diagram of the set of 20x3 in Figura 3-11, as well as azimuth and elevation diagrams of the 24x3 array displayed in Figura 3-14 and Figura 3-15 of section 3.4 in the previous chapter.

6. This project was conducted from February 7th until July 31st 2005, at the premises of Robert Bosch Group GmbH in Leonberg (Baden Württemberg - Germany). At the end of the contract, there was no possibility of continuing the work to completion, as an extension of it was not raised. This is the event causing that some aspects of the project were not continued, as expressed in above.

   At the end of that period, I returned to Spain and started working as engineer for systems integration and testing in Defense Electronics department of the Spanish company Indra in Madrid. This has led to the 6-year delay in the delivery of this work, because although at first I tried to reconcile work and project, it was not possible, as I had to travel continuously. Then I settled in and left it parked for several years. But not forgotten, so it is time to finish it, because only the writing of this report kept me away from the title of engineer.

7. The practical or experimental project lasted 5 months and 24 calendar days. Of these, 120 were working days, with an average of 8 hours a day, and including some weekends. This makes a total of 960 hours.

   In the preparation of this report with all attachments an enormous amount of time has been dedicated, distributed unevenly in the past 6 years. Give an accurate estimate of the amount is difficult, but surely exceed 600 hours.

Because of this, perhaps the most important conclusion to be drawn from this work is that we must never give up. That every project involves a period of uncertainty, but with perseverance and hard work can be carried forward. Therein lies the work of an engineer: To finish projects with the highest possible quality.

8. Finally, but not less important, my thanks to everyone who made this work possible, from those who gave me the opportunity to do so, through the help provided me during it, without forgetting those who encouraged me to continue in the worst moments.

   Among them I would like to thank Dr. Ing Thomas Binzer, who oversaw the project in Germany, and contributed with not a little help and wisdom in it.

   And also, why not, to my partner, Paula. A source of constant inspiration, and a stunning companion. Thanks.

   Thank you all.

Torrejón de Ardoz, on April the 3rd, 2011

6.5 ANNEX 5: LISSY MANUALS (IN GERMAN)